5-1-2013

Discontinuous Galerkin Finite Element Methods for Maxwell's Equations in Dispersive and Metamaterials Media

Jiajia Waters
University of Nevada, Las Vegas, wangj16@unlv.nevada.edu

DISCONTINUOUS GALERKIN FINITE ELEMENT METHODS FOR MAXWELL'S EQUATIONS IN DISPERSIVE AND METAMATERIALS MEDIA

by

Jiajia Waters

Bachelor of Science
Chongqing University of Posts and Telecommunications, Chongqing China
2007

A dissertation submitted in partial fulfillment
of the requirements for the

Doctor of Philoshophy in Mathematical Science

Department of Mathematical Sciences
College of Science
The Graduate College

University of Nevada, Las Vegas
May 2013

THE GRADUATE COLLEGE

We recommend the dissertation prepared under our supervision by

Jiajia Waters

entitled

Discontinuous Galerkin Finite Element Methods for Maxwell's Equations in Dispersive and Metamaterials Media

be accepted in partial fulfillment of the requirements for the degree of

Doctor of Philosophy in Mathematical Science
Department of Mathematical Sciences

Jichun Li, Ph.D., Committee Chair

Hongtao Yang, Ph.D., Committee Member

Monika Neda, Ph.D., Committee Member

Yi-Tung Chen, Ph.D., Graduate College Representative

Tom Piechota, Ph.D., Interim Vice President for Research &
Dean of the Graduate College

May 2013

ABSTRACT

Discontinuous Galerkin Finite Element Method (DG-FEM) has been further developed in this dissertation. We give a complete proof of stability and error estimante for the DG-FEM combined with Runge Kutta which is commonly used in different fields. The proved error estimate matches those numerical results seen in technical papers. Numerical simulations of metamaterials play a very important role in the design of invisibility cloak, and sub-wavelength imaging. We propose a leap-frog discontinuous Galerkin Finite Element Method to solve the time-dependent Maxwell's equations in metamaterials. The stability and error estimate are proved for this scheme. The proposed algorithm is implemented and numerical results supporting the analysis are provided. The wave propagation simulation in the double negative index metamaterials supplemented with perfectly matched layer(PML) boundary is given with one discontinuous galerkin time difference method(DGTD), of which the stability and error estimate are proved as well in this dissertation. To illustrate the effectiveness of this DGTD, we present some numerical result tables which show the consistent convergence rate and the simulation of PML in metamaterials is tested in this dissertation as well. Also the wave propagation simulation in metamaterals by this DGTD scheme is consistent with those seen in other papers. Several techniques have appeared for solving the time-dependent Maxwell's equations with periodically varying coefficients. For the first time, I apply the discontinuous Galerkin (DG) method to this homogenization problem in dispersive media. For simplicity, my focus is on obtaining a solution in two-dimensions (2D) using 2D corrector equations. my numerical results show the DG method to be both convergent and efficient. Furthermore, the solution is consistent with previous treatments and theoretical expectations.

ACKNOWLEDGMENTS

I would like to thank my advisor Dr. Jichun Li, for giving me the opportunity to do this degree, for being patient with my learning curve, and for making sure I did not feign understanding. I would also like to thank the members of my committee: Dr. Hongtao Yang, Dr. Monika Neda and Dr. Yi-Tung Chen.

This thesis is dedicated to my mother Defeng Qiu, my father Ping Wang, and my husband Tim without whose love, help and support I could not have gotten this far.

TABLE OF CONTENTS

LIST OF TABLES

LIST OF FIGURES

Figure Page

Chapter 1

INTRODUCTION AND OUTLINE

1.1 INTRODUCTION

The modern theory of electromagnetism was founded in 1873 with the publication of Maxwell's treatise on Electricity and Magnetism. Maxwell's equations consist of two pairs of coupled partial differential equations relating six fields, two of which model sources of electromagnetism. These equations are not sufficient to uniquely determine the electromagnetic field in matter. However, additional relations, known as constitutive equations are needed to model the way in which the fields interact with matter. There is considerable flexibility in the constitutive equations. In general, we can distinguish three cases:

- Vacuum or free space

  In free space the fields are related by the equations

$$\hat{\boldsymbol{D}} = \epsilon_0 \hat{\boldsymbol{E}} \quad and \quad \hat{\boldsymbol{B}} = \mu_0 \hat{\boldsymbol{H}} \tag{1.1}$$

  where the constants ϵ_0 and μ_0 are called, respectively, the electric permittivity and magnetic permeability. The values of ϵ_0 and μ_0 depend on the system of units used. In the standard SI or MKS units

$$\mu_0 = 4\pi \times 10^{-7} Hm^{-1}$$

$$\epsilon_0 \approx 8.854 \times 10^{-12} Fm^{-1}.$$

  Furthermore the speed of light in a vacuum, denoted by c_0, is given by $c_0 = \frac{1}{\sqrt{\epsilon_0 \mu_0}}$ ($c_0 \approx 2.998 \times 10^8 ms^{-1}$).

- Inhomogeneous, isotropic materials

  The most commonly occurring case in practice is that various different materials (e.g.

copper, air, etc.) occupy the domain of the electromagnetic field. The medium is called inhomogeneous if the material properties do not depend on the direction of the field and the material is linear. Then we have

$$\hat{\boldsymbol{D}} = \epsilon \hat{\boldsymbol{E}} \quad and \quad \hat{\boldsymbol{B}} = \mu \hat{\boldsymbol{H}} \tag{1.2}$$

where ϵ and μ are positive, bounded, scalar functions of position.

- Inhomogeneous, anisotropic materials

  In some materials the electric or magnetic properties of the constituent materials depends on the direction of the field(e.g. in the macroscopic description of a finely layered medium). In such cases ϵ and μ are 3 positive-definite matrix functions of positive-definite matrix functions of position. Usually, the finite element method is equally applicable to isotropic or anisotropic materials in that programs can be written from the onset for the anisotropic case. The theoretical justification of the convergence of the method is more difficult in these cases.

These are the classic media discussed in introductory graduate level textbooks. However, there are more appropriate categories that can be used to classify the topics encountered in this dissertation.

- dispersive media

  In reality, the properties of most electromagnetic materials are wavelength dependent. Such materials are generally called dispersive media, and examples include human tissue, water, soil, snow, ice, plasma, optical fibers, and radar-absorbing materials.

- metamatrials

  In recent years, double-negative (DNG) materials, in which both permittivity and permeability are negative have become the subset of intense investigation. In this case, the constitutive relations are given by

$$\boldsymbol{D} = \epsilon_0 \boldsymbol{E} + \boldsymbol{P} \equiv \epsilon \boldsymbol{E}, \ \boldsymbol{B} = \mu_0 \boldsymbol{H} + \boldsymbol{M} \equiv \mu \boldsymbol{H}, \tag{1.3}$$

  where $\boldsymbol{P}$ and $\boldsymbol{M}$ are the induced electric and magnetic polarizations, respectively. As

in [21, 61], lossy Drude polarization and magnetization models are used to simulate the DNG medium. In the frequency domain, the permittivity and permeability are described as [61, Eq. (7)]:

$$\epsilon(\omega) = \epsilon_0(1 - \frac{\omega_{pe}^2}{\omega(\omega + i\Gamma_e)}), \tag{1.4}$$

$$\mu(\omega) = \mu_0(1 - \frac{\omega_{pm}^2}{\omega(\omega + i\Gamma_m)}), \tag{1.5}$$

where ω_{pe} and ω_{pm} are the electric and magnetic plasma frequencies, and Γ_e and Γ_m are the electric and magnetic damping frequencies.(we shall give a more careful description of Maxwell's equations in metamaterials in Chapter (3))

Finite element methods (FEM) represent a very general set of techniques to approximate solu- tions of partial differential equations. Their main advantage lies in their ability to handle arbitrary geometries via unstructured meshes of the domain of interest: The discretization of oblique geometric edges is natively built in. FEMs have been adopted by engineers in the areas of structural mechanics and fuild dynamics for decades, but until the early 1980's, two major drawbacks prevented them from being used in electro-magnetic problems. First, the nodal element basis used did not satisfy the physical(dis)continuity of the vector fields components and led to spurious solutions [10]. Second, there was no proper way to truncate unbounded regions in open wave problems. The first limitations was overcome with the vector elements developed by Nedelec [52], while the second with the discovery of Perfectly Matched Layers (PMLs), discovered by Berenger [9]. Since then, it has been shown that PMLs could be described in the general framework of transformation optics [1, 16, 56, 60].

We also consider, with the introduction of Discontinuous Galerkin finite element methods(DG-FEM), the discontinuity problem that comes with the nodal element basis. It has been established that DG-FEM is an overall better method for solving a partial differential equation computationally [28, 29]. The Discontinuous Galerkin (DG) method more generally can be traced back to the paper of Reed and Hill (1973). It is important to note that it is not a single method but rather an approach that uses approximating functions that have no continuity constraints imposed on interelement boundaries. In recent years the DG method

is widely applicable for solving any types of PDEs, which explains its ever increasing popularity. It is especially advantageous for modeling extremely complex physics phenomena, such as convection dominated flows (Cockburn, 1997; Cockburn and Shu, 1998) and wave propagation through different materials (i.e. metamaterials), the latter being one of the major focuses of this dissertation. The absence of continuity constraints on the interelement boundaries implies that one has a great deal of flexibility to the method, at the cost of increasing the number of degrees of freedom. This flexibility is the source of many but not all of the advantages of the DG method over the Continuous Galerkin (CG) method, which uses spaces of continuous piecewise polynomial functions and other less standard methods such as nonconforming methods. One great advantage lies in the fact that one is able to easily refine or coarsen the mesh locally or to vary the degree of the piecewise polynomials across the mesh.

In 2008, Jan S. Hesthaven and Tim Warburton proposed an extensive introduction to Discontinuous Galerkin Methods for the solution of partial differential equations in [29], during which they gave a number of examples on how to implement these methods for a variety of problems.

1.2 OUTLINE

This dissertation can be divided into four parts. In the first part, Chapter 2, we provide a brief review of the DG method by specifically applying it to partial differential equations written in conservation form.

Section 2.2 combines DG-FEM with a Runge Kutta algorithm for integrating in time. The resulting RK-DG scheme is the most commonly used method for solving time-dependent equations using DG-FEM. We conclude the second part by providing a detailed proof of both the stability and error estimate of our RK-DG scheme.

The third part presents the use of DG-FEM to solve Maxwell's equations in metamaterials. After explaining the essential concepts underlying metamaterials in Section 3.1, Section 3.2 introduces a leap-frog discontinuous Galerkin method for solving the time domain Maxwell's equations in metamaterials. A complete proof of the stability and error

estimate follows, as well as numerical results supporting our analysis. In Section 3.3 another DG time difference method for Maxwell's equations in metamaterials is proposed and similar proofs are given. The numerical results for this DGTD method utilize boundary conditions known as perfectly matched layers (PML) to simulate wave propagation in metamaterials.

The last part, Chapter 4, deals with what is known as a homogenization problem, which involves an application of DG-FEM to Maxwell's Equations in Dispersive Media with periodically varying coefficients. We introduce the governing equation in dispersive media and the general homogenization problem in Section 4.1. The fully discrete DG scheme is given in Section 4.2, and examples are provided in Section 4.3 to support this scheme.

We conclude this dissertation in Chapter 5.

Chapter 2

DG FINITE ELEMENT METHOD

2.1 INTRODUCTION TO THE DG FINITE ELEMENT METHOD

One of the most appealing aspects of finite difference method are their simplicity; the discretization of general problems and operators is often intuitive and can lead to very efficient schemes. Furthermore, the explicit semidiscrete form gives flexibility in the choice of time-stepping methods if needed. However, it is ill-suited to deal with complex geometries.

A method closely related to the finite difference method, but with added geometric flexibility, is the finite volume method. However, the need for a high-order reconstruction reintroduces the need for a particular grid structure and thus destroys the geometric flexibility of the finite volume method in higher dimensions. The main limitation of finite volume methods is found in its inability to extend to higher-order accuracy on general unstructured grids.

With the classic continuous finite element, one can have different orders of approximation in each element, thereby enabling local changes in both size and order, known as hp-adaptivity. However, the schemes result in the introduction of computationally expensive matrices (the globally defined mass matrix and stiffness matrix), and because the semidiscrete scheme is implicit, the mass matrix must be inverted. For time-dependent problems, this is a clear disadvantage compared to finite difference and finite volume methods.

An intelligent combination of the finite element and the finite volume methods, utilizing a space of basis and test functions that mimics the finite volume method, appears to offer many of the desired properties. This combination is exactly what leads to the discontinuous Galerkin finite element method (DG-FEM). In [29], there is a table (Table 2.1) that summarized generic properties of the most widely used methods for discretizing partial differential equations [i.e., finite difference methods(FDM), finite volume methods(FVM), and the finite element methods(FEM), as compared with the discontinuous Galerkin finite ele-

ment methods(DG-FEM)]. A ✓ represents success, while × indicates a short-coming in the method. Finally, a (✓) reflects that the method, with modifications, is capable of solving such problems but remains a less natural choice.

Table 2.1: Comparison of different methods for discretizing partial differential equations

	Complex geometries	High-order accuracy and hp-adaptivity	Explicit semi-discrete form	Conservation laws	Elliptic problems
FDM	×	✓	✓	✓	✓
FVM	✓	×	✓	✓	✓
FEM	✓	✓	×	(✓)	✓
DG-FEM	✓	✓	✓	✓	(✓)

In DG-FEM, the information used to calculate the solution on each element only involves communication with directly neighboring elements and not all elements in the mesh, unlike classic continuous finite element methods. Each element shares flux information across the connecting edge. This flux is continuous and can be extended to a continuous flux on the entire domain. The great advantage of this approach is that with the proper choice of flux, it is possible to arrive at a computationally inexpensive and easily parallelizable (i.e. local) mass matrix. The following discussion closely parallels [29].

In order to understand the DG method, we consider the conservation laws.

$$\frac{\partial u(\boldsymbol{x},t)}{\partial t} + \nabla \cdot \boldsymbol{f}(u(\boldsymbol{x}),\boldsymbol{x},t) = 0, \quad \boldsymbol{x} \in \Omega \in \boldsymbol{R}^2 \tag{2.1}$$

$$u(\boldsymbol{x},t) = g(\boldsymbol{x},t), \quad \boldsymbol{x} \in \partial\Omega \tag{2.2}$$

$$u(\boldsymbol{x},0) = f(\boldsymbol{x}). \tag{2.3}$$

We assume that Ω can be triangulated using K elements,

$$\Omega \approx \Omega_h = \bigcup_{k=1}^{K} D^k$$

where D^k is a straight-sided triangle and the triangulation is assumed to be geometrically

conforming. We can approximate $u(\boldsymbol{x}, t)$ using

$$u(\boldsymbol{x}, t) \approx u_h(\boldsymbol{x}, t) = \oplus_{k=1}^{K} u_h^k(\boldsymbol{x}, t) \in \boldsymbol{V}_h = \oplus_{k=1}^{K} u_h^k \psi_n(D^k)_{n=1}^{N_p}$$

Here $\psi_n(D^k)$ is a two-dimensional polynomial basis defined on element D^k and $\oplus$ denotes adding all elements together. The local function,

$$u_h^k(\boldsymbol{x}, t) = \sum_{i=1}^{N_p} u_h^k(\boldsymbol{x}_i^k, t) l_i^k(\boldsymbol{x}),$$

where $l_i(\boldsymbol{x})$ is the multidimensional Lagrange polynomial defined by some grid points, $\boldsymbol{x}_i$, on the element D^k.

Introducing the test function, $\psi_h \in \boldsymbol{V}_h$, we get the local conditions

$$\int_{D^k} [\frac{\partial u_h^k}{\partial t} l_i^k(\boldsymbol{x}) - \boldsymbol{f}_h^k \cdot \nabla l_i^k(\boldsymbol{x})] dx = -\int_{\partial D^k} \hat{\boldsymbol{n}} \cdot \boldsymbol{f}^* l_i^k(\boldsymbol{x}) dx \tag{2.4}$$

and

$$\int_{D^k} [\frac{\partial u_h^k}{\partial t} + \nabla \cdot \boldsymbol{f}_h^k] l_i^k(\boldsymbol{x}) dx = \int_{\partial D^k} \hat{\boldsymbol{n}} \cdot [\boldsymbol{f}_h^k - \boldsymbol{f}^*] l_i^k(\boldsymbol{x}) dx \tag{2.5}$$

as the weak and strong form, respectively, of the nodal Discontinuous Galerkin method in two spatial dimensions. We primarily consider the local Lax-Friedrich's flux

$$\boldsymbol{f}^*(a, b) = \frac{\boldsymbol{f}(a) + \boldsymbol{f}(b)}{2} + \frac{C}{2} \hat{\boldsymbol{n}}(a - b),$$

where (a, b) are the interior and exterior solution value, respectively and C is the local maximum of the directional flux Jacobian; that is,

$$C = max_{u \in [a,b]} \left| \hat{n}_x \frac{\partial f_1}{\partial u} + \hat{n}_y \frac{\partial f_2}{\partial u} \right|,$$

where $\boldsymbol{f} = (f_1, f_2)$.

We define the following matrices:

- Mass matrix:

$$\mathrm{M}_{ij}^{k} = \int_{\boldsymbol{D}} l_i^k(\boldsymbol{x}) l_j^k(\boldsymbol{x}) d\boldsymbol{x} = \boldsymbol{J}^k \int_{\boldsymbol{I}} l_i(\boldsymbol{r}) l_j(\boldsymbol{r}) d\boldsymbol{r}, \tag{2.6}$$

  where $\boldsymbol{J}^k$ is the transformation Jacobian;

- Differentiation matrix D_r:

$$\mathrm{D}_{r,(i,j)} = \frac{dl_j}{dr}|_{r_i},$$

  where $r \in \boldsymbol{I}$ is the reference variable;

- Stiffness matrices:

$$\mathrm{S}_r = \mathrm{M}^{-1}\mathrm{D}_r, \quad \mathrm{S}_s = \mathrm{M}^{-1}\mathrm{D}_s; \tag{2.7}$$

- Edge-mass matrices:

$$\mathrm{M}_{ij}^{k,e} = \int_{edge} l_j^k(\boldsymbol{x}) l_i^k(\boldsymbol{x}) d\boldsymbol{x}.$$

The two Maxwell's equations relevant are Ampere's law and Faraday's law:

$$\begin{aligned} \epsilon_0 \frac{\partial \boldsymbol{E}}{\partial t} &= \nabla \times \boldsymbol{H}, \quad \text{in } \ \Omega \times (0,T), \\ \mu_0 \frac{\partial \boldsymbol{H}}{\partial t} &= -\nabla \times \boldsymbol{E}, \quad \text{in } \ \Omega \times (0,T), . \end{aligned} \tag{2.8}$$

We can express Maxwell's equations in conservation form:

$$\boldsymbol{Q}\frac{\partial \boldsymbol{q}}{\partial t} + \nabla \cdot \boldsymbol{F}(\boldsymbol{q}) = \boldsymbol{S}, \tag{2.9}$$

where $\boldsymbol{S} = [\boldsymbol{S^E}, \boldsymbol{S^H}]$ represents body forces and the material matrix, $\boldsymbol{Q}(\boldsymbol{x})$, the state vector, $\boldsymbol{q}$, and the flux, $\boldsymbol{F}(\boldsymbol{q}) = [F_1(\boldsymbol{q}), F_2(\boldsymbol{q}), F_3(\boldsymbol{q})]^T$, are

$$\boldsymbol{Q}(\boldsymbol{x}) = \begin{bmatrix} \epsilon_r(\boldsymbol{x}) & 0 \\ 0 & \mu_r(\boldsymbol{x}) \end{bmatrix}, \boldsymbol{q} = \begin{bmatrix} \boldsymbol{E} \\ \boldsymbol{H} \end{bmatrix}, \boldsymbol{F}_i(\boldsymbol{q}) = \begin{bmatrix} -\boldsymbol{e}_i \times \boldsymbol{H} \\ \boldsymbol{e}_i \times \boldsymbol{E} \end{bmatrix}.$$

Here e_i signifies the three Cartesian unit vectors.

Before we go any further, we will show how equation(2.9) is equivalent to equations(2.8) in

the case that $\boldsymbol{S} = \mathbf{0}$. Note that

$$\boldsymbol{e}_1 \times \boldsymbol{H} = \begin{vmatrix} \vec{i} & \vec{j} & \vec{k} \\ 1 & 0 & 0 \\ \boldsymbol{H}_x & \boldsymbol{H}_y & \boldsymbol{H}_z \end{vmatrix} = -\boldsymbol{H}_z\vec{j} + \boldsymbol{H}_y\vec{k}.$$

Similarly, we can show that

$$\boldsymbol{e}_2 \times \boldsymbol{H} = \boldsymbol{H}_z\vec{i} - \boldsymbol{H}_x\vec{k}, \quad \boldsymbol{e}_3 \times \boldsymbol{H} = \boldsymbol{H}_y\vec{i} - \boldsymbol{H}_y\vec{j}.$$

Hence the first component of $\nabla \cdot \boldsymbol{F}$ equals to

$$\begin{aligned} &\frac{\partial F_1}{\partial x} + \frac{\partial F_2}{\partial y} + \frac{\partial F_3}{\partial z} \\ =&\frac{\partial}{\partial x}(\boldsymbol{e}_1 \times \boldsymbol{H}) + \frac{\partial}{\partial y}(\boldsymbol{e}_2 \times \boldsymbol{H}) + \frac{\partial}{\partial x}(\boldsymbol{e}_3 \times \boldsymbol{H}) \\ =&\frac{\partial}{\partial x}(\boldsymbol{H}_z\vec{j} - \boldsymbol{H}_y\vec{k}) + \frac{\partial}{\partial y}(-\boldsymbol{H}_z\vec{i} + \boldsymbol{H}_x\vec{k}) + \frac{\partial}{\partial z}(\boldsymbol{H}_y\vec{i} - \boldsymbol{H}_x\vec{j}) \\ =&(\frac{\partial H_y}{\partial z} - \frac{\partial H_z}{\partial y})\vec{i} + (\frac{\partial H_z}{\partial x} - \frac{\partial H_x}{\partial z})\vec{j} + (\frac{\partial H_x}{\partial y} - \frac{\partial H_y}{\partial x})\vec{k} \\ =&\nabla \times \boldsymbol{H}. \end{aligned}$$

In the same fashion, we can prove that the second component of $\nabla \cdot \boldsymbol{F}$ equals to $-\nabla \times \boldsymbol{E}$. Therefore, we can conclude that (2.9) is equivalent to (2.8), with $\boldsymbol{Q}(\boldsymbol{x}) = diag(\epsilon_0, \mu_0)$, and no body forces.

To derive the DG-FEM scheme, we assume that Ω is decomposed into tetrahedral mesh elements T_h, i.e. $\Omega = \bigcap_{k \in T_h} \boldsymbol{K}$. According to (2.5),the DG scheme of (2.9) should satisfy element-wise the strong form

$$\int_K (\boldsymbol{Q}\frac{\partial \boldsymbol{q}_h}{\partial t} + \nabla \cdot \boldsymbol{F}_h - \boldsymbol{S}_h)\phi(\boldsymbol{x})dx = \int_{\partial K} \psi(\boldsymbol{x})\hat{\boldsymbol{n}} \cdot (\boldsymbol{F}_h - \boldsymbol{F}_h^*]dx, \tag{2.10}$$

here ϕ and ψ are test functions while $\hat{\mathbf{n}}$ is an outward normal vector, $\boldsymbol{F}_h^*$ is a numerical flux and the DG solution $\boldsymbol{q}_h$ on each element K is represented as

$$q_h(\boldsymbol{x}, t) = \sum_{j=0}^{N} q(\boldsymbol{x}_j, t)L_j(\boldsymbol{x}) = \sum_{j=0}^{N} q_j(t)L_j(\boldsymbol{x}).$$

While there are many possibilities for the numerical flux, $\boldsymbol{F}_h^*$, the linearity of the problem suggests that unwinding is a natural choice. To understand the form of this, it is helpful to recall that

$$\hat{\boldsymbol{n}} \cdot \boldsymbol{F}_h = \begin{bmatrix} -\hat{\boldsymbol{n}} \times \boldsymbol{H}_h \\ \hat{\boldsymbol{n}} \times \boldsymbol{E}_h \end{bmatrix}.$$

Then the explicit form of the upwinded penalizing boundary term is

$$\hat{\boldsymbol{n}} \cdot (\boldsymbol{F}_h - \boldsymbol{F}_h^*) = \{ \begin{array}{c} \hat{Z}^{-1}\hat{\mathbf{n}} \times (Z^+[\boldsymbol{H}_h] - \hat{n} \times [\boldsymbol{E}_h]) \\ \hat{Y}^{-1}\hat{\mathbf{n}} \times (-\hat{n} \times [\boldsymbol{H}_h] - Y^+[\boldsymbol{E}_h]) \end{array},$$

where

$$[\boldsymbol{E}_h] = \boldsymbol{E}_h^+ - \boldsymbol{E}_h^-, \, [\boldsymbol{H}_h] = \boldsymbol{H}_h^+ - \boldsymbol{H}_h^-,$$

measures the jump across an interface, and

$$Z^{\pm} = 1/Y^{\pm} = \sqrt{\frac{\mu^{\pm}}{\epsilon^{\pm}}},$$

$$\hat{Z} = Z^+ + Z^-, \, \hat{Y} = Y^+ + Y^-.$$

Here, superscript "+" refers to field values from the neighbor element while superscript "−" refers to field values inside the element. Now we get the nodal DG semi-discrete scheme of (2.10) with the following element-wise expressions for the electric field components

$$\sum_{j=0}^{N} \left(\boldsymbol{M}_{ij}^{\epsilon} \frac{d\boldsymbol{E}_j}{dt} - \boldsymbol{S}_{ij} \times \boldsymbol{H}_j - \boldsymbol{M}_{ij} \boldsymbol{S}_j^{\boldsymbol{E}} \right) = \sum_l \boldsymbol{F}_{il} \left(\hat{n}_l \times \frac{Z_l^+[\boldsymbol{H}_l] - \hat{\boldsymbol{n}}_l \times [\boldsymbol{E}]}{Z_l^+ + Z_l^-} \right), \quad (2.11)$$

and magnetic field components

$$\sum_{j=0}^{N} \left(\boldsymbol{M}_{ij}^{\mu} \frac{d\boldsymbol{H}_j}{dt} + \boldsymbol{S}_{ij} \times \boldsymbol{E}_j - \boldsymbol{M}_{ij} \boldsymbol{S}_j^{\boldsymbol{H}} \right) = \sum_l \boldsymbol{F}_{il} \left(\hat{n}_l \times \frac{-\hat{\boldsymbol{n}}_l \times [\boldsymbol{H}_l] - Y_l^+[\boldsymbol{E}]}{Y_l^+ + Y_l^-} \right). \quad (2.12)$$

Here we have mass matrices

$$\boldsymbol{M}_{ij}^{\epsilon} = \int_K L_i(\boldsymbol{x}) \epsilon(\boldsymbol{x}) L_j(\boldsymbol{x}) d\boldsymbol{x},$$

$$\boldsymbol{M}_{ij}^{\mu} = \int_K L_i(\boldsymbol{x})\mu(\boldsymbol{x})L_j(\boldsymbol{x})d\boldsymbol{x},$$

and the face mass matrix

$$\boldsymbol{F}_{ij} = \oint_{\partial K} L_i(\boldsymbol{x})L_j(\boldsymbol{x})ds.$$

Expressing Eqs.(2.11) and (2.12) in semi-discrete explicit form yields

$$\begin{aligned}
\frac{d\boldsymbol{E}_h}{dt} &= (\boldsymbol{M}^{\epsilon})^{-1}\boldsymbol{S}\times\boldsymbol{H}_h + (\boldsymbol{M}^{\epsilon})^{-1}\boldsymbol{M}\boldsymbol{S}^{\boldsymbol{E}} + (\boldsymbol{M}^{\epsilon})^{-1}\boldsymbol{F}(\hat{n}\times\frac{Z^+[\boldsymbol{H}_h]-\hat{\boldsymbol{n}}\times[\boldsymbol{E}_h]}{Z_l^+ + Z_l^-})|_{\partial K} \\
\frac{d\boldsymbol{H}_h}{dt} &= -(\boldsymbol{M}^{\mu})^{-1}\boldsymbol{S}\times\boldsymbol{E}_h + (\boldsymbol{M}^{\mu})^{-1}\boldsymbol{M}\boldsymbol{S}^{\boldsymbol{H}} - (\boldsymbol{M}^{\mu})^{-1}\boldsymbol{F}(\hat{n}\times\frac{\hat{\boldsymbol{n}}\times[\boldsymbol{H}_h]+Y^+[\boldsymbol{E}_h]}{Y_l^+ + Y_l^-})|_{\partial K}.
\end{aligned} \tag{2.13}$$

So far we have been only talking about the spatial dimension, and notice that (2.13) is in the form of ordinary differential equations

$$\frac{d\boldsymbol{u}_h}{dt} = \mathrm{L}_h(\boldsymbol{u}_h, t).$$

Therefore, we can just use some standard time discretization technique to arrive at the fully time-dependent solutions. We will discuss the Runge-Kutta method in the next section.

2.2 DG FINITE ELEMENT METHOD COMBINED WITH RUNGE KUTTA FOR MAXWELL'S EQUATIONS

In this section, we shall show how to treat the temporal aspect as solving PDEs. First we consider the explicit Runge-Kutta(RK) methods for integration in the time dimension. Since (2.13) is in the form of the ordinary differential equations

$$\frac{d\boldsymbol{u}_h}{dt} = \mathrm{L}_h(\boldsymbol{u}_h, t),$$

we can use the standard fourth-order explicit RK method

$$
\begin{aligned}
u_h^{n,1} &= \mathrm{L}_h(u_h^n) \\
u_h^{n,2} &= \mathrm{L}_h(u_h^n + \frac{1}{2}\Delta t u_h^{n,1}), \\
u_h^{n,3} &= \mathrm{L}_h(u_h^n + \frac{1}{2}\Delta t u_h^{n,2}), \\
u_h^{n,4} &= \mathrm{L}_h(u_h^n + \frac{1}{2}\Delta t u_h^{n,1}), \\
u_h^{n+1} &= u_h^n + \frac{1}{6}\Delta t[u_h^{n,1} + 2u_h^{n,2} + 2u_h^{n,3} + u_h^{n,4}].
\end{aligned}
$$

to advance one time step Δt from u_h^n to u_h^{n+1}.

Now we will give the proofs of stability and error estimate for the fully discrete Runge Kutta Discontinuous Galerkin method for Maxwell's equations

2.2.1 THE STABILITY OF FULLY RK DISCRETIZATION OF DG SCHEME

Recall that the Maxwell's equations are

$$\epsilon_0 \frac{\partial \boldsymbol{E}}{\partial t} = \nabla \times \boldsymbol{H}, \quad \text{in } \ \Omega \times (0,T), \tag{2.14}$$

$$\mu_0 \frac{\partial \boldsymbol{H}}{\partial t} = -\nabla \times \boldsymbol{E}, \quad \text{in } \ \Omega \times (0,T). \tag{2.15}$$

For simplicity, we assume that Ω is a bounded polyhedral domain of R^3 (note that our analysis holds true for R^2 also) and the system (2.14)–(2.15) is supplemented with the metallic boundary condition (referring to a perfectly conducting surface)

$$\boldsymbol{n} \times \boldsymbol{E} = 0 \quad on \quad \partial\Gamma_m$$

and initial conditions

$$\boldsymbol{E}(\boldsymbol{x},0) = \boldsymbol{E}_0(\boldsymbol{x}), \qquad \boldsymbol{H}(\boldsymbol{x},0) = \boldsymbol{H}_0(\boldsymbol{x}), \tag{2.16}$$

where $\boldsymbol{n}$ denotes the unit outward normal to $\partial\Omega$, and $\boldsymbol{E}_0$, $\boldsymbol{H}_0$ are some given functions.

We assume that the domain Ω is partitioned into disjoint tetrahedral elements T_i such

that $\bar{\Omega} = \bigcap_i T_i$. For each internal face $a_{ik} = T_i \bigcap T_k$, we denote $\mathbf{n}_{ik}$ the unitary normal, oriented from T_i towards T_k. We denote by ν_i the set of indices of the neighboring elements of the T_i, and F_h the union of faces.

Furthermore, square brackets are used to signify the jump terms

$$[\boldsymbol{E}_i] = \boldsymbol{E}_i^+ - \boldsymbol{E}_i^-, \qquad [\boldsymbol{H}_i] = \boldsymbol{H}_i^+ - \boldsymbol{H}_i^-,$$

where superscripts " $+$ " and " $-$ " refer to field values from the neighbor element and the local element, respectively.

We introduce the discontinuous finite element space:

$$\mathrm{V}_h = \{v_h \in L^2(\Omega)^3 : \quad v_h|T_i \in (\mathrm{P}_k(T_i))^3, \quad for \quad \forall T_i \in \bar{\Omega}\}. \tag{2.17}$$

i.e. the basis function of discontinuous polynomial of degree k over each element.

To define a fully discrete scheme,we divide the time interval $[0, T]$ into M uniform subintervals by points $0 = t_0 < t_1 < ... < t_M = T$, where $t_k = k\Delta t$ and Δt is the time step size. Moreover, we define $\boldsymbol{E}_i^n = \boldsymbol{E}(\cdot, t_n)$ as the approximate field on element T_i, and $\boldsymbol{E}_h$ as the global approximate field, i.e. $\boldsymbol{E}_{h|T_i} = \boldsymbol{E}_i$.

With the above preparation, now we can construct the semi-discrete Discontinuous Galerkin scheme. One seeks the semi-discrete solution $\boldsymbol{U}_h = (\boldsymbol{H}_h, \boldsymbol{E}_h) \in C^1([0, T], \mathrm{V}_h^2)$ as a solution of the following weak formulation, $\forall (u_h, v_h) \in \mathrm{V}_h^2$, $\forall t \in [0, T]$:

$$\int_{T_i} \epsilon_0 \frac{\partial \boldsymbol{E}_i}{\partial t} \cdot u_i \quad = \quad \int_{T_i} \nabla \times \boldsymbol{H}_i \cdot u_i + \sum_{k \in \nu_i} \int_{a_{ik}} u_i \cdot \frac{1}{2} \mathbf{n}_{ik} \times ([\boldsymbol{H}_i] - \mathbf{n}_{ik} \times [\boldsymbol{E}_i]) \tag{2.18}$$

$$\int_{T_i} \mu_0 \frac{\partial \boldsymbol{H}_i}{\partial t} \cdot v_i \quad = \quad - \int_{T_i} \nabla \times \boldsymbol{E}_i \cdot v_i - \sum_{k \in \nu_i} \int_{a_{ik}} v_i \cdot \frac{1}{2} \mathbf{n}_{ik} \times (\mathbf{n}_{ik} \times [\boldsymbol{H}_i] + [\boldsymbol{E}_i]) \tag{2.19}$$

Letting $u_h = \boldsymbol{E}_h$ and $v_h = \boldsymbol{H}_h$, we get

$$\begin{aligned}\int_\Omega \epsilon_0 \frac{\partial}{\partial t}||\boldsymbol{E}_h||^2 + \int_\Omega \mu_0 \frac{\partial}{\partial t}||\boldsymbol{H}_h||^2 = &-\frac{1}{2}\sum_{f_i \in F_h}\int_{f_i}(\mathbf{n}_{ik}\times[\boldsymbol{E}_i])\cdot(\mathbf{n}_{ik}\times[\boldsymbol{E}_i]) \\ &-\frac{1}{2}\sum_{f_i \in F_h}\int_{f_i}(\mathbf{n}_{ik}\times[\boldsymbol{H}_i])\cdot(\mathbf{n}_{ik}\times[\boldsymbol{H}_i])\end{aligned} \tag{2.20}$$

Since $\frac{d}{dt}||\boldsymbol{U}_h||^2 < 0$, it follows that (2.18) to (2.19) is a well-posed problem in the continuous time.

On elements T_k, the numerical solution can be written as

$$\boldsymbol{u}_h(\boldsymbol{x},t) = \sum_{i=1}^{N_p} u_h(\boldsymbol{x}_i,t) l_i(\boldsymbol{x}) = \sum_{i=1}^{N_p} u_i(t) l_i(\boldsymbol{x}), \quad \boldsymbol{x} \in T_k \tag{2.21}$$

where $l_i(\boldsymbol{x})$ is the multivariate Lagrange interpolation polynomial of degree n. The local mass, stiffness and face-based mass matrices are given respectively by

$$M_{ij} = (l_i(\boldsymbol{x}), l_j(\boldsymbol{x}))_{T_k}, \quad S_{i,j} = (l_i(\boldsymbol{x}), \nabla l_j(\boldsymbol{x}))_{T_k}, \quad F_{ij} = (l_i(\boldsymbol{x}), l_j(\boldsymbol{x}))_{\partial T_k}. \tag{2.22}$$

Letting $\boldsymbol{u}_N = [u_1, u_2, \cdots, u_{N_p}]$, we realize that

$$M\boldsymbol{u}_N \cdot \boldsymbol{u}_N = \int_{T_k} \sum_{i=1}^{N_p} u_h(\boldsymbol{x}_i) l_i(\boldsymbol{x}) \sum_{i=1}^{N_p} u_h(\boldsymbol{x}_i) l_i(\boldsymbol{x}) d\boldsymbol{x} = ||\boldsymbol{u}_h||^2_{T_k}, \tag{2.23}$$

which leads the semi-discrete Discontinuous Galerkin scheme:

$$\begin{aligned}\epsilon_0 \frac{d\boldsymbol{E}_N}{dt} =& M^{-1} S \times \boldsymbol{H}_N + \frac{1}{2} M^{-1} F(\boldsymbol{n} \times ([\boldsymbol{H}_i] - \mathbf{n} \times [\boldsymbol{E}_i]))|_{\partial T_k} \\ \mu_0 \frac{d\boldsymbol{H}_N}{dt} =& - M^{-1} S \times \boldsymbol{H}_N - \frac{1}{2} M^{-1} F(\boldsymbol{n} \times (\mathbf{n} \times [\boldsymbol{H}_i] + [\boldsymbol{E}_i]))|_{\partial T_k}\end{aligned} \tag{2.24}$$

where

$$\boldsymbol{E}_N = [\boldsymbol{E}_1, \boldsymbol{E}_2, \cdots, \boldsymbol{E}_{N_p}]^T, \quad \boldsymbol{H}_N = [\boldsymbol{H}_1, \boldsymbol{H}_2, \cdots, \boldsymbol{H}_{N_p}]^T. \tag{2.25}$$

Here, $\boldsymbol{E}_i = \boldsymbol{E}_h(\boldsymbol{x}_i)$ and $\boldsymbol{H}_i = \boldsymbol{H}_h(\boldsymbol{x}_i)$.

We can recover the local energy

$$||\boldsymbol{E}_h||^2_{T_k} = \int_{T_k} \sum_{i=1}^{N_p} \boldsymbol{E}_h(\boldsymbol{x}_i) l_i(\boldsymbol{x}) \sum_{i=1}^{N_p} \boldsymbol{E}_h(\boldsymbol{x}_i) l_i(\boldsymbol{x}) d\boldsymbol{x} = M\boldsymbol{E}_N \cdot \boldsymbol{E}_N$$

$$||\boldsymbol{H}_h||^2_{T_k} = \int_{T_k} \sum_{i=1}^{N_p} \boldsymbol{H}_h(\boldsymbol{x}_i) l_i(\boldsymbol{x}) \sum_{i=1}^{N_p} \boldsymbol{H}_h(\boldsymbol{x}_i) l_i(\boldsymbol{x}) d\boldsymbol{x} = M\boldsymbol{H}_N \cdot \boldsymbol{E}_N$$

$$||\boldsymbol{E}_h||^2_{T_k} + ||\boldsymbol{H}_h||^2_{T_k} = M\boldsymbol{E}_N \cdot \boldsymbol{E}_N + M\boldsymbol{H}_N \cdot \boldsymbol{H}_N \tag{2.26}$$

We need to prove the following theorem.

Theorem 2.2.1. *Under the CFL condition*

$$\frac{\Delta t}{\sqrt{\epsilon_0 \mu_0}} \leq C_s h, \tag{2.27}$$

where $C_s > 0$ is the constant depending on the s-order RK discretization and the constant from the inverse inequality

$$|u|_{0,\partial T} \leq C_{inv} h_T^{-\frac{1}{2}} \|u\|_0^T, \quad |u|_{1,T} \leq C_{inv} h_T^{-1} \|u\|_{0,T}, \quad \forall u \in V_h, \tag{2.28}$$

the RK discretization of the DG scheme (2.18)-(2.19) (or (2.24)) is stable,

$$\epsilon_0 \left\|\boldsymbol{E}_h^m\right\|_0^2 + \mu_0 \left\|\boldsymbol{H}_h^m\right\|_0^2 \leq \epsilon_0 \left\|\boldsymbol{E}_h^0\right\|_0^2 + \mu_0 \left\|\boldsymbol{H}_h^0\right\|_0^2.$$

Before we prove the stability, we need some preparation.

We will consider the normalized system of equations form of (2.14)-(2.15)

$$\frac{\partial \boldsymbol{E}}{\partial t} = \nabla \times \boldsymbol{H}, \quad \text{in } \Omega \times (0,T), \tag{2.29}$$

$$\frac{\partial \boldsymbol{H}}{\partial t} = -\nabla \times \boldsymbol{E}, \quad \text{in } \Omega \times (0,T), \tag{2.30}$$

where the dimensionless variables are defined as

$$t = \frac{c_0 \widetilde{t}}{L}, \quad \boldsymbol{x} = \frac{\widetilde{\boldsymbol{x}}}{L}, \quad \boldsymbol{H} = \frac{\widetilde{\boldsymbol{H}}}{H_0}, \quad \boldsymbol{E} = (Z_0)^{-1} \frac{\widetilde{\boldsymbol{E}}}{H_0}. \tag{2.31}$$

Here, H_0 is a unit magnetic filed strength, Z_0 is the vacuum impedance, c_0 is the speed of

light, and L is some reference length, on the scale of the phenomena if interest.

We again apply the semidiscrete DG scheme of (2.18) and (2.19),

$$\int_{T_i} \frac{\partial \boldsymbol{E}_i}{\partial t} \cdot u_i = \int_{T_i} \nabla \times \boldsymbol{H}_i \cdot u_i + \sum_{k \in \nu_i} \int_{a_{ik}} u_i \cdot \frac{1}{2} \mathbf{n}_{ik} \times ([\boldsymbol{H}_i] - \mathbf{n}_{ik} \times [\boldsymbol{E}_i]) \tag{2.32}$$

$$\int_{T_i} \frac{\partial \boldsymbol{H}_i}{\partial t} \cdot v_i = -\int_{T_i} \nabla \times \boldsymbol{E}_i \cdot v_i - \sum_{k \in \nu_i} \int_{a_{ik}} v_i \cdot \frac{1}{2} \mathbf{n}_{ik} \times (\mathbf{n}_{ik} \times [\boldsymbol{H}_i] + [\boldsymbol{E}_i]) \tag{2.33}$$

In matrix form, the semidiscrete DG scheme is analogous to (2.24),

$$\begin{aligned} \frac{d\boldsymbol{E}_N}{dt} =& M^{-1} S \times \boldsymbol{H}_N + \frac{1}{2} M^{-1} F(\boldsymbol{n} \times ([\boldsymbol{H}_i] - \mathbf{n} \times [\boldsymbol{E}_i]))|_{\partial T_k} \\ \frac{d\boldsymbol{H}_N}{dt} =& - M^{-1} S \times \boldsymbol{E}_N - \frac{1}{2} M^{-1} F(\boldsymbol{n} \times (\mathbf{n} \times [\boldsymbol{H}_i] + [\boldsymbol{E}_i]))|_{\partial T_k} \end{aligned} \tag{2.34}$$

Letting $\boldsymbol{U}_N = (\boldsymbol{E}_N, \boldsymbol{H}_N)$, we can write the semidiscrete DG scheme as

$$\frac{\partial \boldsymbol{U}_N}{\partial t} = L_N \boldsymbol{U}_N. \tag{2.35}$$

Furthermore, we define

$$||\boldsymbol{U}_N||^2 = ||\boldsymbol{E}_h||^2 + ||\boldsymbol{H}_h||^2$$

and

$$\begin{aligned} R(L_N \boldsymbol{U}_N, \boldsymbol{U}_N) =& S \times \boldsymbol{H}_N \cdot \boldsymbol{E}_N + \frac{1}{2} F(\boldsymbol{n} \times ([\boldsymbol{H}_i] - \mathbf{n} \times [\boldsymbol{E}_i]))|_{\partial T_k} \cdot \boldsymbol{E}_N \\ & - S \times \boldsymbol{E}_N \cdot \boldsymbol{H}_N - \frac{1}{2} F(\boldsymbol{n} \times (\mathbf{n} \times [\boldsymbol{H}_i] + [\boldsymbol{E}_i]))|_{\partial T_k} \cdot \boldsymbol{H}_N \\ =& \int_\Omega \nabla \times \boldsymbol{H}_h \cdot \boldsymbol{E}_h + \sum_{T_i} \sum_{k \in \nu_i} \int_{a_{ik}} \boldsymbol{E}_i \cdot \frac{1}{2} \mathbf{n}_{ik} \times ([\boldsymbol{H}_i] - \mathbf{n}_{ik} \times [\boldsymbol{E}_i]) \\ & - \int_\Omega \nabla \times \boldsymbol{E}_h \cdot \boldsymbol{H}_h - \sum_{T_i} \sum_{k \in \nu_i} \int_{a_{ik}} \boldsymbol{H}_i \cdot \frac{1}{2} \mathbf{n}_{ik} \times (\mathbf{n}_{ik} \times [\boldsymbol{H}_i] + [\boldsymbol{E}_i]) \\ =& -\frac{1}{2} \sum_{f_i \in F_h} \int_{f_i} |\mathbf{n}_{ik} \times [\boldsymbol{E}_i]|^2 - \frac{1}{2} \sum_{f_i \in F_h} \int_{f_i} |\mathbf{n}_{ik} \times [\boldsymbol{H}_i]|^2. \end{aligned}$$

Thus

$$|R(L_N \boldsymbol{U}_N, \boldsymbol{U}_N)| = \frac{1}{4}\sum_{T_i}\int_{\partial T_i} |\mathbf{n}_{ik} \times [\boldsymbol{E}_i]|^2 + \frac{1}{4}\sum_{T_i}\int_{\partial T_i} |\mathbf{n}_{ik} \times [\boldsymbol{H}_i]|^2 \tag{2.36}$$

The following two lemmas are needed to prove the Theorem 2.2.1.

Lemma 2.2.1. *Given that* $\sum_{k\in\nu_i}\int_{a_{ik}} u_i \cdot \mathbf{n}_{ik} \times [\boldsymbol{H}_i] \neq 0$ *and* $\sum_{k\in\nu_i}\int_{a_{ik}} u_i \cdot \mathbf{n}_{ik} \times [\boldsymbol{E}_i] \neq 0$ *for any* $u_i \in V_h$*, we obtain*

$$|\mathrm{R}(L_N \boldsymbol{U}_N, \boldsymbol{U}_N)| \geq \frac{C}{h}||\boldsymbol{U}_N||^2 \tag{2.37}$$

where $h = \max_{T_i} h_i$.

Proof. Since all norms are equivalent in the finite dimensional, the following must hold on the reference element $\widehat{T}$, for any $\widehat{v_i} \in \mathrm{V}_h$, where $||\widehat{\mathbf{n}} \times \widehat{v_i}||_{\partial\widehat{T}} \neq 0$:

$$||\widehat{\mathbf{n}} \times \widehat{v_i}||_{\partial\widehat{T}} \geq C||\widehat{v_i}||_{\widehat{T}}, \tag{2.38}$$

where C is a positive constant. Letting $F : \widehat{T} \to T_i$

$$\begin{aligned}
&\int_{\partial\widehat{T}} |(\mathbf{n_i} \circ \mathbf{F}) \times (\mathbf{v_i} \circ \mathbf{F})|^{\mathbf{2}} \frac{\mathbf{d\hat{s}}}{\mathbf{ds_i}} \mathbf{ds_i} \geq \mathbf{C}\int_{\widehat{\mathbf{T}}} |\mathbf{v_i} \circ \mathbf{F}|^{\mathbf{2}} \frac{\mathbf{d\widehat{T}}}{\mathbf{dT_i}} \mathbf{dT_i} \\
&\int_{\partial T_i} |v_i|^2 \frac{1}{h_i} ds_i \geq C\int_{T_i} |v_i|^2 \frac{1}{A_i} dT_i
\end{aligned} \tag{2.39}$$

where h_i is the side for 2D and the area for 3D, while A_i is the area for 2D and the volume for 3D. Making the approximation that $\frac{h_i}{A_i} \approx \frac{1}{h_i}$, (2.39) becomes

$$||\boldsymbol{n}_i \times v_i||^2_{\partial T_i} \geq \frac{C}{h_i}||v_i||^2_{T_i}$$

for any $v_i \in \mathrm{V}_h$.

Therefore

$$\int_{\partial T_i} |\mathbf{n}_{ik} \times [\boldsymbol{E}_i]|^2 + \int_{\partial T_i} |\mathbf{n}_{ik} \times [\boldsymbol{H}_i]|^2 \geq \frac{C}{h_i}(|||[\boldsymbol{H}_i]|||^2_{T_i} + |||[\boldsymbol{E}_i]|||^2_{T_i}).$$

Adding all elements together for (2.36), we get

$$|R(L_N \boldsymbol{U}_N, \boldsymbol{U}_N)| \geq \frac{C}{h}||\boldsymbol{U}_N||^2, \tag{2.40}$$

which concludes the proof. □

Lemma 2.2.2. *Given that*

$$\begin{aligned}||L_N \boldsymbol{U}_N||^2 =& M(M^{-1}S \times \boldsymbol{H}_N + \frac{1}{2}F(\boldsymbol{n} \times ([\boldsymbol{H}_i] - \mathbf{n} \times [\boldsymbol{E}_i]))|_{\partial T_k}) \cdot \\ & (M^{-1}S \times \boldsymbol{H}_N + \frac{1}{2}M^{-1}F(\boldsymbol{n} \times ([\boldsymbol{H}_i] - \mathbf{n} \times [\boldsymbol{E}_i]))|_{\partial T_k}) \\ & + M(-M^{-1}S \times \boldsymbol{E}_N - \frac{1}{2}F(\boldsymbol{n} \times (\mathbf{n} \times [\boldsymbol{H}_i] + [\boldsymbol{E}_i]))|_{\partial T_k}) \cdot \\ & (-M^{-1}S \times \boldsymbol{E}_N - \frac{1}{2}M^{-1}F(\boldsymbol{n} \times (\mathbf{n} \times [\boldsymbol{H}_i] + [\boldsymbol{E}_i]))|_{\partial T_k}),\end{aligned}$$

it follows that

$$||L_N \boldsymbol{U}_N||^2 \leq \frac{C_h}{h^2}||\boldsymbol{U}_h||^2, \tag{2.41}$$

where C_h is a constant.

Proof. We have

$$\begin{aligned}&||L_N \boldsymbol{U}_N||^2 = (S \times \boldsymbol{H}_N + \frac{1}{2}F(\boldsymbol{n} \times ([\boldsymbol{H}_i] - \mathbf{n} \times [\boldsymbol{E}_i]))|_{\partial T_k}) \cdot \\ &(M^{-1}S \times \boldsymbol{H}_N + \frac{1}{2}M^{-1}F(\boldsymbol{n} \times ([\boldsymbol{H}_i] - \mathbf{n} \times [\boldsymbol{E}_i]))|_{\partial T_k}) \\ &+ (-S \times \boldsymbol{E}_N - \frac{1}{2}F(\boldsymbol{n} \times (\mathbf{n} \times [\boldsymbol{H}_i] + [\boldsymbol{E}_i]))|_{\partial T_k}) \cdot \\ &(-M^{-1}S \times \boldsymbol{E}_N - \frac{1}{2}M^{-1}F(\boldsymbol{n} \times (\mathbf{n} \times [\boldsymbol{H}_i] + [\boldsymbol{E}_i]))|_{\partial T_k}) \\ =& S \times \boldsymbol{H}_N \cdot M^{-1}S \times \boldsymbol{H}_N + \frac{1}{2}F(\boldsymbol{n} \times ([\boldsymbol{H}_i] - \mathbf{n} \times [\boldsymbol{E}_i]))|_{\partial T_k} \cdot M^{-1}S \times \boldsymbol{H}_N \\ &+ S \times \boldsymbol{H}_N \cdot \frac{1}{2}M^{-1}F(\boldsymbol{n} \times ([\boldsymbol{H}_i] - \mathbf{n} \times [\boldsymbol{E}_i]))|_{\partial T_k} \\ &+ \frac{1}{4}F(\boldsymbol{n} \times ([\boldsymbol{H}_i] - \mathbf{n} \times [\boldsymbol{E}_i]))|_{\partial T_k} \cdot M^{-1}F(\boldsymbol{n} \times ([\boldsymbol{H}_i] - \mathbf{n} \times [\boldsymbol{E}_i]))|_{\partial T_k} \\ &+ S \times \boldsymbol{E}_N \cdot M^{-1}S \times \boldsymbol{E}_N + \frac{1}{2}F(\boldsymbol{n} \times (\mathbf{n} \times [\boldsymbol{H}_i] + [\boldsymbol{E}_i]))|_{\partial T_k} \cdot M^{-1}S \times \boldsymbol{E}_N \\ &+ S \times \boldsymbol{E}_N \cdot \frac{1}{2}M^{-1}F(\boldsymbol{n} \times (\mathbf{n} \times [\boldsymbol{H}_i] + [\boldsymbol{E}_i]))|_{\partial T_k} \\ &+ \frac{1}{4}F(\boldsymbol{n} \times (\mathbf{n} \times [\boldsymbol{H}_i] + [\boldsymbol{E}_i]))|_{\partial T_k} \cdot M^{-1}F(\boldsymbol{n} \times (\mathbf{n} \times [\boldsymbol{H}_i] + [\boldsymbol{E}_i]))|_{\partial T_k}\end{aligned} \tag{2.42}$$

Based on (2.22), we can arrive at a simple inequality:

$$
\begin{aligned}
&|\frac{1}{2}F(\boldsymbol{n}\times([\boldsymbol{H}_i]-\mathbf{n}\times[\boldsymbol{E}_i]))|_{\partial T_k}\cdot M^{-1}S\times\boldsymbol{H}_N| \qquad (2.43)\\
\leq&\frac{1}{4\delta}||\frac{1}{2}F(\boldsymbol{n}\times([\boldsymbol{H}_i]-\mathbf{n}\times[\boldsymbol{E}_i]))|_{\partial T_k}||^2+\delta||M^{-1}S\times\boldsymbol{H}_N||^2\\
\leq&\frac{1}{4\delta}\sum_{T_i}\sum_{j=1}^{N_p}|\sum_{k\in\nu_i}\int_{a_{ik}}\mathbf{n}_{ik}\times([\boldsymbol{H}_i]-\mathbf{n}_{ik}\times[\boldsymbol{E}_i])\cdot l_j(\boldsymbol{x})|^2\\
&+\delta C\sum_{T_i}\sum_{j=1}^{N_p}|\int_{T_i}\nabla\times[\boldsymbol{H}_i]\cdot l_j(\boldsymbol{x})|^2\\
\leq&\frac{C_1}{h^2}(||\boldsymbol{H}_h||^2+||\boldsymbol{E}_h||^2) \qquad (2.44)
\end{aligned}
$$

Similarly,

$$
\begin{aligned}
&|S\times\boldsymbol{H}_N\cdot\frac{1}{2}M^{-1}F(\boldsymbol{n}\times([\boldsymbol{H}_i]-\mathbf{n}\times[\boldsymbol{E}_i]))|_{\partial T_k}|\\
\leq&\frac{C}{4\delta}\sum_{T_i}\sum_{j=1}^{N_p}|\int_{T_i}\nabla\times[\boldsymbol{H}_i]\cdot l_j(\boldsymbol{x})|^2\\
&+\delta C\sum_{T_i}\sum_{j=1}^{N_p}|\sum_{k\in\nu_i}\int_{a_{ik}}\mathbf{n}_{ik}\times([\boldsymbol{H}_i]-\mathbf{n}_{ik}\times[\boldsymbol{E}_i])\cdot l_j(\boldsymbol{x})|^2\\
\leq&\frac{C_2}{h^2}(||\boldsymbol{H}_h||^2+||\boldsymbol{E}_h||^2) \qquad (2.45)
\end{aligned}
$$

and

$$
\begin{aligned}
&|\frac{1}{4}F(\boldsymbol{n}\times([\boldsymbol{H}_i]-\mathbf{n}\times[\boldsymbol{E}_i]))|_{\partial T_k}\cdot M^{-1}F(\boldsymbol{n}\times([\boldsymbol{H}_i]-\mathbf{n}\times[\boldsymbol{E}_i]))|_{\partial T_k}|\\
&\leq C_3\sum_{T_i}\sum_{j=1}^{N_p}\sum_{k\in\nu_i}|\int_{a_{ik}}\mathbf{n}_{ik}\times([\boldsymbol{H}_i]-\mathbf{n}_{ik}\times[\boldsymbol{E}_i])\cdot l_j(\boldsymbol{x})|^2\\
&\leq\frac{C_3}{h^2}(||\boldsymbol{H}_h||^2+||\boldsymbol{E}_h||^2). \qquad (2.46)
\end{aligned}
$$

Thus,

$$
\begin{aligned}
||L_N\boldsymbol{U}_N||^2&\leq\int_\Omega\nabla\times\boldsymbol{H}_h\cdot\nabla\times\boldsymbol{H}_h+\int_\Omega\nabla\times\boldsymbol{E}_h\cdot\nabla\times\boldsymbol{E}_h+\frac{C_4}{h^2}(||\boldsymbol{H}_h||^2+||\boldsymbol{E}_h||^2)\\
&\leq\frac{C_h}{h^2}(||\boldsymbol{E}_h||^2+||\boldsymbol{H}_h||^2)=\frac{C_h}{h^2}||\boldsymbol{U}_h||^2 \qquad (2.47)
\end{aligned}
$$

□

Now we can prove the Theorem 2.2.1:

Proof. From Lemma 2.2.1 and 2.2.2,

$$\frac{h^2}{C_1}||L_N\boldsymbol{U}_N||^2 \leq ||\boldsymbol{U}_N||^2 \leq \frac{h}{C}|R(L_N\boldsymbol{U}_N, \boldsymbol{U}_N)|.$$

Then we obtain

$$h \leq C_s \frac{|R(L_N\boldsymbol{U}_N, \boldsymbol{U}_N)|}{||L_N\boldsymbol{U}_N||^2}. \tag{2.48}$$

According to Theorem 3.1, Theorem 3.2 and 3.3 in [42], the s-order RK discretization of the DG scheme, (2.35) , is strongly stable, provided Δt satisfies for the appropriate C_s,

$$\Delta t \leq C_s\eta, \quad \eta := inf_{||u||=1}\frac{|R(Lu, u)|}{||Lu||^2}. \tag{2.49}$$

From (2.48), we can get the CFL condition

$$\Delta t \leq C_s h.$$

According to (2.31), the s-order RK discretization of the DG scheme, (2.18) to (2.19) , is also strongly stable, provided Δt satisfies the CFL condition

$$\frac{\Delta t}{\sqrt{\epsilon_0\mu_o}} \leq C_s h. \tag{2.50}$$

□

2.2.2 ERROR ESTIMATE

Here we give the error estimate of a fully discrete RK4 DG scheme. The error estimate of any other orders can be developed in the same way.

Consider

$$u_t = F(u), \tag{2.51}$$

subject to the given initial value

$$u(0) = u^0. \tag{2.52}$$

The RK4 approximation of (2.51) is :

$$
\begin{aligned}
u^{n,1} &= F(u^n) \\
u^{n,2} &= F(u^n + 1/2\Delta t u^{n,1}), \\
u^{n,3} &= F(u^n + 1/2\Delta t u^{n,2}), \\
u^{n,4} &= F(u^n + 1/2\Delta t u^{n,1}), \\
u^{n+1} &= u^n + 1/6\Delta t[u^{n,1} + 2u^{n,2} + 2u^{n,3} + u^{n,4}].
\end{aligned}
$$

We will apply the above RK4 scheme to Maxwell's equations for the case of linear, constant-coefficients. Recalling the semidiscrete problem, as in (2.24), these equations are

$$
\begin{aligned}
\frac{d\boldsymbol{E}_N}{dt} =& M^{-1}S \times \boldsymbol{H}_N + \frac{1}{2}M^{-1}F(\boldsymbol{n} \times ([\boldsymbol{H}_i] - \mathbf{n} \times [\boldsymbol{E}_i]))|_{\partial T_k} \\
\frac{d\boldsymbol{H}_N}{dt} =& - M^{-1}S \times \boldsymbol{H}_N - \frac{1}{2}M^{-1}F(\boldsymbol{n} \times (\mathbf{n} \times [\boldsymbol{H}_i] + [\boldsymbol{E}_i]))|_{\partial T_k}.
\end{aligned} \tag{2.53}
$$

This system is in the form

$$
\frac{\partial \boldsymbol{U}_N}{\partial t} = L_N \boldsymbol{U}_N. \tag{2.54}
$$

Applying RK4 to (2.54) gives

$$
\boldsymbol{U}_N^{n+1} = \boldsymbol{U}_N^n + \widetilde{L}_N \boldsymbol{U}_N^n + \frac{1}{2}\widetilde{L}_N^2 \boldsymbol{U}_N^n + \frac{1}{6}\widetilde{L}_N^3 \boldsymbol{U}_N^n + \frac{1}{24}\widetilde{L}_N^4 \boldsymbol{U}_N^n, \tag{2.55}
$$

where $\widetilde{L}_N = \Delta t L_N$.

In the previous section , we have proved (2.55) is stable under the CFL condition,

$$
\|\boldsymbol{E}_h^m\|_0^2 + \|\boldsymbol{H}_h^m\|_0^2 \leq \left\|\boldsymbol{E}_h^0\right\|_0^2 + \left\|\boldsymbol{H}_h^0\right\|_0^2.
$$

Before we can prove the optimal error estimate, we need another two lemmas.

Lemma 2.2.3. *Under the CFL condition* $\frac{\Delta t}{\sqrt{\epsilon_0 \mu_0}} \leq C_s h$,

$$
(\epsilon_0 ||\boldsymbol{E}_h^n - \boldsymbol{E}_h(t_n)||^2 + \mu_0 ||\boldsymbol{H}_h^n - \boldsymbol{H}_h(t_n)||^2)^{\frac{1}{2}} \leq C(\Delta t)^4 ||(\boldsymbol{H}, \boldsymbol{E})||_{C^5[0,T], L^2(\Omega)} \tag{2.56}
$$

Proof. Define $\boldsymbol{u}_N(t_n) = [\boldsymbol{u}_h(\boldsymbol{x}_1, t_n), \boldsymbol{u}_h(\boldsymbol{x}_2, t_n), \cdots, \boldsymbol{u}_h(\boldsymbol{x}_{N_p}, t_n)]^T$ for any $\boldsymbol{u}_h \in \mathrm{V}_h$.

Introduce $\widetilde{\boldsymbol{U}}_N^{n+1} = (\widetilde{\boldsymbol{E}}_N^{n+1}, \widetilde{\boldsymbol{H}}_N^{n+1})$ as

$$\widetilde{\boldsymbol{U}}_N^{n+1} = \boldsymbol{U}_N(t_n) + \widetilde{L}_N \boldsymbol{U}_N(t_n) + \frac{1}{2}\widetilde{L}_N^2 \boldsymbol{U}_N(t_n) + \frac{1}{6}\widetilde{L}_N^3 \boldsymbol{U}_N(t_n) + \frac{1}{24}\widetilde{L}_N^4 \boldsymbol{U}_N(t_n) \tag{2.57}$$

By a Taylor expansion, we get:

$$\begin{aligned}\boldsymbol{U}_N(t_{n+1}) =& \boldsymbol{U}_N(t_n) + \widetilde{L}_N \boldsymbol{U}_N(t_n) + \frac{1}{2}\widetilde{L}_N^2 \boldsymbol{U}_N(t_n) + \frac{1}{6}\widetilde{L}_N^3 \boldsymbol{U}_N(t_n) \\ &+ \frac{1}{24}\widetilde{L}_N^4 \boldsymbol{U}_N(t_n) + \frac{(\Delta t)^5}{5!}\frac{\partial^5 \boldsymbol{U}_h}{\partial t^5} + \cdots .\end{aligned} \tag{2.58}$$

Subtracting (2.58) from (2.57), we find

$$\widetilde{\boldsymbol{U}}_N^{n+1} - \boldsymbol{U}_N(t_{n+1}) = -\frac{(\Delta t)^5}{5!}\frac{\partial^5 \boldsymbol{U}_h}{\partial t^5}. \tag{2.59}$$

Squaring both sides and using (2.23) gives

$$\begin{aligned}&||\widetilde{\boldsymbol{U}}_h^{n+1} - \boldsymbol{U}_h(t_{n+1})|| \le C\Delta t^5 ||\frac{\partial^5}{\partial t^5}\boldsymbol{U}_h|| \\ &(||\widetilde{\boldsymbol{E}}_h^{n+1} - \boldsymbol{E}_h(t_{n+1})||^2 + ||\widetilde{\boldsymbol{H}}_h^{n+1} - \boldsymbol{H}_h^{(}t_{n+1})||^2)^{\frac{1}{2}} \le C\Delta t^5 ||(\boldsymbol{H}, \boldsymbol{E})||_{C^5([0,T],L^2(\Omega))}\end{aligned} \tag{2.60}$$

Subtracting (2.57) from (2.55), we have

$$\begin{aligned}&\boldsymbol{U}_N^{n+1} - \boldsymbol{U}_N(t_{n+1}) = \boldsymbol{U}_N^n - \boldsymbol{U}_N(t_n) + \widetilde{L}_N(\boldsymbol{U}_N^n - \boldsymbol{U}_N(t_n)) + \frac{1}{2}\widetilde{L}_N^2(\boldsymbol{U}_N^n - \boldsymbol{U}_N(t_n)) \\ &+ \frac{1}{6}\widetilde{L}_N^3(\boldsymbol{U}_N^n - \boldsymbol{U}_N(t_n)) + \frac{1}{24}\widetilde{L}_N^4(\boldsymbol{U}_N^n - \boldsymbol{U}_N(t_n)) + \widetilde{\boldsymbol{U}}_N^{n+1} - \boldsymbol{U}_N(t_{n+1}).\end{aligned} \tag{2.61}$$

Now Let $\xi_{\mathbf{h}}^{\mathbf{n}} = \boldsymbol{E}_{\mathbf{h}}^{\mathbf{n}} - \boldsymbol{E}_{\mathbf{h}}(\mathbf{t_n})$, $\eta_{\mathbf{h}}^{\mathbf{n}} = \boldsymbol{H}_{\mathbf{h}}^{\mathbf{n}} - \boldsymbol{H}_{\mathbf{h}}(\mathbf{t_n})$, and $\varsigma_h^n = (\xi_{\mathbf{h}}^{\mathbf{n}}, \eta_{\mathbf{h}}^{\mathbf{n}})$. Then $\xi_{\mathbf{N}}^{\mathbf{n}} = \boldsymbol{E}_{\mathbf{N}}^{\mathbf{n}} - \boldsymbol{E}_{\mathbf{N}}(\mathbf{t_n})$, $\eta_{\mathbf{N}}^{\mathbf{n}} = \boldsymbol{H}_{\mathbf{N}}^{\mathbf{n}} - \boldsymbol{H}_{\mathbf{N}}(\mathbf{t_n})$, and $\varsigma_N^n = (\xi_{\mathbf{N}}^{\mathbf{n}}, \eta_{\mathbf{N}}^{\mathbf{n}})$, so that (2.61) becomes

$$\varsigma_N^{n+1} = \varsigma_N^n + \widetilde{L}_N \varsigma_N^n + \frac{1}{2}\widetilde{L}_N^2 \varsigma_N^n + \frac{1}{6}\widetilde{L}_N^3 \varsigma_N^n + \frac{1}{24}\widetilde{L}_N^4 \varsigma_N^n + \widetilde{\boldsymbol{U}}_N^{n+1} - \boldsymbol{U}_N(t_{n+1}). \tag{2.62}$$

This is similar to (2.55). Along with the stability of (2.55), squaring both sides of the above

equations and using(2.23) gives

$$
\begin{aligned}
&||\xi_{\mathbf{h}}^{\mathbf{n+1}}||^{\mathbf{2}} + ||\eta_{\mathbf{h}}^{\mathbf{n+1}}||^{\mathbf{2}} \leq ||\xi_{\mathbf{h}}^{\mathbf{n}}||^{\mathbf{2}} + ||\eta_{\mathbf{h}}^{\mathbf{n}}||^{\mathbf{2}} \\
&+ ||\widetilde{\boldsymbol{E}}_h^{n+1} - \boldsymbol{E}_h(t_{n+1})||^2 + ||\widetilde{\boldsymbol{H}}_h^{n+1} - \boldsymbol{H}_h(t_{n+1})||^2 \\
&+ M(\widetilde{\boldsymbol{U}}_N^{n+1} - \boldsymbol{U}_N(t_{n+1})) \cdot (\varsigma_N^n + \widetilde{L}_N \varsigma_N^n + \frac{1}{2}\widetilde{L}_N^2 \varsigma_N^n + \frac{1}{6}\widetilde{L}_N^3 \varsigma_N^n + \frac{1}{24}\widetilde{L}_N^4 \varsigma_N^n). \qquad (2.63)
\end{aligned}
$$

Multiplying (2.59) by any $\phi_h \in \mathrm{V}_h$, and integrating over Ω_h, we arrive at

$$
\begin{aligned}
M(\widetilde{\boldsymbol{U}}_N^{n+1} - \boldsymbol{U}_N(t_{n+1})) \cdot \phi_N &= \int_\Omega (\widetilde{\boldsymbol{U}}_h^{n+1} - \boldsymbol{U}_h(t_{n+1})) \cdot \phi_h \\
= \int_\Omega -\frac{(\Delta t)^5}{5!} \frac{\partial^5 \boldsymbol{U}_h}{\partial t^5} \cdot \phi_h &\leq ||\frac{(\Delta t)^5}{5!} \frac{\partial^5 \boldsymbol{U}_h}{\partial t^5}||\, ||\phi_h||,
\end{aligned}
$$

so that if one defines:

$$
\psi_h^n(\phi_N) = M(\widetilde{\boldsymbol{U}}_N^{n+1} - \boldsymbol{U}_N(t_{n+1})) \cdot \phi_N = \int_\Omega \widetilde{\boldsymbol{U}}_h^{n+1} - \boldsymbol{U}_h(t_{n+1}) \cdot \phi_h,
$$

and

$$
|\psi_h^n(\phi_N)| \leq ||\frac{(\Delta t)^5}{5!} \frac{\partial^5 \boldsymbol{U}_h}{\partial t^5}||\, ||\phi_h||
$$

then

$$
|||\psi_h^n(\phi_N)||| \leq C(\Delta t)^5 ||(\boldsymbol{H}, \boldsymbol{E})||_{C^5([0,T],L^2(\Omega))}, \qquad (2.64)
$$

where $|||\cdot|||$ denotes a linear norm if one considers the linear form on $L^2(\Omega)$. Therefore, we can write (2.63) as

$$
\begin{aligned}
&||\xi_{\mathbf{h}}^{\mathbf{n+1}}||^{\mathbf{2}} + ||\eta_{\mathbf{h}}^{\mathbf{n+1}}||^{\mathbf{2}} \leq ||\xi_{\mathbf{h}}^{\mathbf{n}}||^{\mathbf{2}} + ||\eta_{\mathbf{h}}^{\mathbf{n}}||^{\mathbf{2}} \\
&+ ||\widetilde{\boldsymbol{E}}_h^{n+1} - \boldsymbol{E}_h(t_{n+1})||^2 + ||\widetilde{\boldsymbol{H}}_h^{n+1} - \boldsymbol{H}_h(t_{n+1})||^2 \\
&+ \psi_h^{n-1}(\varsigma_N^n + \widetilde{L}_N \varsigma_N^n + \frac{1}{2}\widetilde{L}_N^2 \varsigma_N^n + \frac{1}{6}\widetilde{L}_N^3 \varsigma_N^n + \frac{1}{24}\widetilde{L}_N^4 \varsigma_N^n).
\end{aligned}
$$

Using (2.64) and (2.60), we finally obtain

$$
||\xi_{\mathbf{h}}^{\mathbf{n+1}}||^{\mathbf{2}} + ||\eta_{\mathbf{h}}^{\mathbf{n+1}}||^{\mathbf{2}} \leq ||\xi_{\mathbf{h}}^{\mathbf{n}}||^{\mathbf{2}} + ||\eta_{\mathbf{h}}^{\mathbf{n}}||^{\mathbf{2}} + \mathbf{C}(\boldsymbol{\Delta t})^{\mathbf{5}} ||(\boldsymbol{H}, \boldsymbol{E})||_{\mathbf{C^5([0,T],L^2(\Omega))}} \qquad (2.65)
$$

Adding from $n = 0$ to $n - 1$, we obtain the result in Lemma 2.2.3. □

Lemma 2.2.4. *Let P_h denote the standard L^2-projection onto V_h or V_h^0, which is the subspace of V_h with the boundary condition $\boldsymbol{n} \times \boldsymbol{E} = 0$ imposed. It is known that the projection error estimate*

$$\|u - P_h u\|_{0,T} \leq C h_T^{min\{s,k\}+1} \|u\|_{s+1,T}\,, \tag{2.66}$$

holds true for any element T,and $u \in H^{s+1}(T)$. Let $(\boldsymbol{E}_h, \boldsymbol{H}_h)$ be the weak solution of (2.18)-(2.19), and $(\boldsymbol{E}, \boldsymbol{H})$ be the solution of (2.14)-(2.15). Then

$$(\epsilon_0 ||P_h \boldsymbol{E} - \boldsymbol{E}_h||^2 + \mu_0 ||P_h H - H_h||^2)^{\frac{1}{2}} \leq C h^{min\{s,k\}} ||(H, E)||_{C^0([0,T], H^{s+1}(\Omega))}. \tag{2.67}$$

Proof. Multiply (2.14) by $u_h \in \mathrm{V}_h$, (2.15) by $v_h \in \mathrm{V}_h$, and integrate them over $\mathcal{T}_i$. Adding all elements together gives

$$\int_{T_i} \epsilon_0 \frac{\partial \boldsymbol{E}}{\partial t} \cdot u_i \;=\; \int_{T_i} \nabla \times \boldsymbol{H} \cdot u_i + \sum_{k \in \nu_i} \int_{a_{ik}} u_i \cdot \frac{1}{2} \mathbf{n}_{ik} \times ([\boldsymbol{H}] - \mathbf{n}_{ik} \times [\boldsymbol{E}]) \tag{2.68}$$

$$\int_{T_i} \mu_0 \frac{\partial \boldsymbol{H}}{\partial t} \cdot v_i \;=\; -\int_{T_i} \nabla \times \boldsymbol{E} \cdot v_i - \sum_{k \in \nu_i} \int_{a_{ik}} v_i \cdot \frac{1}{2} \mathbf{n}_{ik} \times (\mathbf{n}_{ik} \times [\boldsymbol{H}] + [\boldsymbol{E}]) \tag{2.69}$$

Let $\xi_h = P_h \boldsymbol{E} - \boldsymbol{E}_h$ and $\eta_h = P_h \boldsymbol{H} - \boldsymbol{H}_h$. Then from(2.18)-(2.19) and (2.68)-(2.69),

$$\begin{aligned}
&\epsilon_0 (\frac{\partial}{\partial t} \xi_h, u_h) - (\nabla \times \eta_h, u_h) - \sum_{T_i} \sum_{k \in \nu_i} \int_{a_{ik}} u_i \cdot \frac{1}{2} \mathbf{n}_{ik} \times ([\eta_i] - \mathbf{n}_{ik} \times [\xi_i]) \\
=&\epsilon_0 (\frac{\partial}{\partial t} (P_h \boldsymbol{E} - \boldsymbol{E}), u_h) - (\nabla \times (P_h \boldsymbol{H} - \boldsymbol{H}), u_h) \\
&- \sum_{T_i} \sum_{k \in \nu_i} \int_{a_{ik}} u_i \cdot \frac{1}{2} \mathbf{n}_{ik} \times ([(P_h \boldsymbol{H} - \boldsymbol{H})] - \mathbf{n}_{ik} \times [(P_h \boldsymbol{E} - \boldsymbol{E})]) \\
&\mu_0 (\frac{\partial}{\partial t} \eta_h, v_h) + (\nabla \times \xi_h, v_h) + \sum_{T_i} \sum_{k \in \nu_i} \int_{a_{ik}} v_i \cdot \frac{1}{2} \mathbf{n}_{ik} \times (\mathbf{n}_{ik} \times [\eta_i] + [\xi_i]) \\
=&\mu_0 (\frac{\partial}{\partial t} (P_h \boldsymbol{H} - \boldsymbol{H}), v_h) + (\nabla \times (P_h \boldsymbol{E} - \boldsymbol{E}), v_h) \\
&+ \sum_{T_i} \sum_{k \in \nu_i} \int_{a_{ik}} v_i \cdot \frac{1}{2} \mathbf{n}_{ik} \times (\mathbf{n}_{ik} \times [(P_h \boldsymbol{H} - \boldsymbol{H})] + [(P_h \boldsymbol{E} - \boldsymbol{E})]).
\end{aligned} \tag{2.70}$$

Further Letting $u_h = \xi_h$ and $v_h = \eta_h$,

$$
\begin{aligned}
&\epsilon_0(\frac{\partial}{\partial t}\xi_h, \xi_h) + \mu_0(\frac{\partial}{\partial t}\eta_h, \eta_h) \\
=&-\sum_{f_i \in F_h} \int_{f_i} \frac{1}{2}\mathbf{n}_{ik} \times [\xi_i] \cdot \mathbf{n}_{ik} \times [\xi_i] - \sum_{f_i \in F_h} \int_{f_i} \frac{1}{2}\mathbf{n}_{ik} \times [\eta_i] \cdot \mathbf{n}_{ik} \times [\eta_i] \\
&+ \epsilon_0(\frac{\partial}{\partial t}(P_h\boldsymbol{E} - \boldsymbol{E}), \xi_h) - (\nabla \times (P_h\boldsymbol{H} - \boldsymbol{H}), \xi_h) \\
&- \sum_{T_i} \sum_{k \in \nu_i} \int_{a_{ik}} \xi_i \cdot \frac{1}{2}\mathbf{n}_{ik} \times ([(P_h\boldsymbol{H} - \boldsymbol{H})] - \mathbf{n}_{ik} \times [(P_h\boldsymbol{E} - \boldsymbol{E})]) \\
&+ \mu_0(\frac{\partial}{\partial t}(P_h\boldsymbol{H} - \boldsymbol{H}), \eta_h) + (\nabla \times (P_h\boldsymbol{E} - \boldsymbol{E}), \eta_h) \\
&+ \sum_{T_i} \sum_{k \in \nu_i} \int_{a_{ik}} \eta_i \cdot \frac{1}{2}\mathbf{n}_{ik} \times (\mathbf{n}_{ik} \times [(P_h\boldsymbol{H} - \boldsymbol{H})] + [(P_h\boldsymbol{E} - \boldsymbol{E})]) \\
\leq&\epsilon_0(\frac{\partial}{\partial t}(P_h\boldsymbol{E} - \boldsymbol{E}), \xi_h) - (\nabla \times (P_h\boldsymbol{H} - \boldsymbol{H}), \xi_h) \\
&- \sum_{T_i} \sum_{k \in \nu_i} \int_{a_{ik}} \xi_i \cdot \frac{1}{2}\mathbf{n}_{ik} \times ([(P_h\boldsymbol{H} - \boldsymbol{H})] - \mathbf{n}_{ik} \times [(P_h\boldsymbol{E} - \boldsymbol{E})]) \\
&+ \mu_0(\frac{\partial}{\partial t}(P_h\boldsymbol{H} - \boldsymbol{H}), \eta_h) + (\nabla \times (P_h\boldsymbol{E} - \boldsymbol{E}), \eta_h) \\
&+ \sum_{T_i} \sum_{k \in \nu_i} \int_{a_{ik}} \eta_i \cdot \frac{1}{2}\mathbf{n}_{ik} \times (\mathbf{n}_{ik} \times [(P_h\boldsymbol{H} - \boldsymbol{H})] + [(P_h\boldsymbol{E} - \boldsymbol{E})]) \\
=&\sum_{i=1}^{6} Err_i. \qquad (2.71)
\end{aligned}
$$

We see that $Err_1 = 0$, $Err_2 = 0$, $Err_4 = 0$ and $Err_5 = 0$ by the property of L^2 projections. Hence,

$$Err_3 \leq \frac{C_{inv}}{h}||\xi_h|| \cdot (||P_h\boldsymbol{H} - \boldsymbol{H}|| + ||P_h\boldsymbol{E} - \boldsymbol{E}||). \qquad (2.72)$$

Similarly,

$$Err_6 \leq \frac{C_{inv}}{h}||\eta_h|| \cdot (||P_h\boldsymbol{H} - \boldsymbol{H}|| + ||P_h\boldsymbol{E} - \boldsymbol{E}||) \qquad (2.73)$$

and so,

$$\epsilon_0(\frac{\partial}{\partial t}\xi_h, \xi_h) + \mu_0(\frac{\partial}{\partial t}\eta_h, \eta_h) \leq \frac{C_{inv}}{h}(||\xi_h|| + ||\eta_h||) \cdot (||P_h\boldsymbol{E} - \boldsymbol{E}|| + ||P_h\boldsymbol{H} - \boldsymbol{H}||). \qquad (2.74)$$

Since

$$\epsilon_0(\xi_h,\xi_h)+\mu_0(\eta_h,\eta_h)=\int_0^t(\epsilon_0(\frac{\partial}{\partial s}\xi_h,\xi_h)+\mu_0(\frac{\partial}{\partial s}\eta_h,\eta_h))ds+\epsilon_0(\xi_h^0,\xi_h^0)+\mu_0(\eta_h^0,\eta_h^0), \quad (2.75)$$

we must have that

$$\begin{aligned}&\epsilon_0(\xi_h,\xi_h)+\mu_0(\eta_h,\eta_h)-(\epsilon_0(\xi_h^0,\xi_h^0)+\mu_0(\eta_h^0,\eta_h^0))\\ \leq&\int_0^t\frac{1}{2\delta}(||\xi_h||^2+||\eta_h||^2)+2\delta\frac{C_{inv}^2}{h^2}(||P_h\boldsymbol{E}-\boldsymbol{E}||^2+||P_h\boldsymbol{H}-\boldsymbol{H}||^2). \qquad (2.76)\end{aligned}$$

Finally, let $\lambda=\max_{[0,T]}(||\xi_h(t)||^2+||\eta_h(t)||^2)$.

Since λ is well defined due to the regularity hypotheses on the solution $(\boldsymbol{H},\boldsymbol{E})$ and $(\boldsymbol{H}_h,\boldsymbol{E}_h)$, it follows that

$$\epsilon_0(\xi_h,\xi_h)+\mu_0(\eta_h,\eta_h)\leq TC_{inv}^2\delta h^{2min\{s,k\}}||(H,E)||^2_{C^0([0,T],H^{s+1}(\Omega))}+T\lambda\frac{1}{2\delta}.$$

which concludes the proof. □

Theorem 2.2.2. *Under the assumption that the time step Δt satisfies a CFL condition, we have the following error estimate*

$$\begin{aligned}&\max_{1\leq n}(||\boldsymbol{E}^n-\boldsymbol{E}_h^n||_0+||\boldsymbol{H}^n-\boldsymbol{H}_h^n||_0\\ \leq&C((\Delta t)^4+Th^{min\{s,k\}})(||(\boldsymbol{H},\boldsymbol{E})||_{C^5([0,T],L^2(\Omega))}+||(H,E)||_{C^0([0,T],H^{s+1}(\Omega))})\end{aligned}$$

where k is the degree of the basis function in the finite element space (2.17)

Proof. From Lemma(2.2.3), Lemma(2.2.4) and(2.66), using the triangle inequality, we can get the above error estimate. □

For the numerical results to support the error estimate, we can refer to [29, 44].

Chapter 3

DG METHODS FOR MAXWELL'S EQUATIONS IN METAMATERIALS

3.1 INTRODUCTION OF METAMATERIALS

A metamaterial refers to any material that gains its properties from its structure rather than from its composition. (They are often associated with electromagnetic materials whose refractive index is negative). The quantitative statement of refraction is embodied in Snell's law, which relates the exit angle of a light ray, θ_2, as measured with respect to a line drawn perpendicular to the interface of the material, to the ray's angle of incidence, θ_1, by the formula

$$\sin(\theta_1) = n \sin(\theta_2)$$

Here, n is the ratio of the exit medium's refractive index to the that of the entrance material. The refractive index therefore determines the amount by which the beam is deflected. If the index is positive, the exiting beam is deflected to the opposite side of the surface normal, whereas if the index is negative, the exiting beam is deflected to the same side of the normal. Fig.3.1

Maxwell's equations determine how electromagnetic waves propagate within a medium, and in special cases, can be reduced to a wave equation of the form,

$$\frac{\partial^2 \boldsymbol{E}(x,t)}{\partial x^2} = \epsilon\mu \frac{\partial^2 \boldsymbol{E}(x,t)}{\partial t^2},$$

where ϵ is the ratio of the electric permitivity in the material to its free space value and μ is the ratio of the magnetic permeability in the material to its free space value. Indeed, solutions of the wave equation have the form $\exp[i(kx - \omega t)]$ where $k = n\omega$ and $n = \sqrt{\epsilon\mu}$ is another way to express the refractive index. Propagating solutions exist in the material whether ϵ and μ are both positive or are both negative. We need to be careful

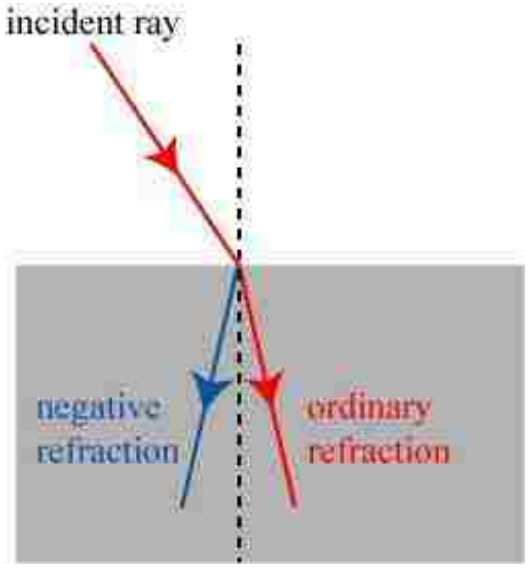

Figure 3.1: Negative refraction index. The direction of the light ray is mirror-imaged about the normal to the surface when the refraction index is negative (From:Metallurgy for skullsinthestars.com)

in taking the square root, as ϵ and μ are analytic functions that are generally complex valued. There is an ambiguity in the sign of the square root that can be resolved by a proper analysis. Since ϵ and μ are both negative, we need to obey the left-handed law. When we take the square root, we need to add a negative sign in the front of n. Hence, $n = -\sqrt{\epsilon\mu}$ for left handed metamaterials. The critical requirement is that mathematically the square root of product of ϵ and μ must take the negative sign in the left handed materials. In negative index metamaterials (NIM), both permittivity and permeability are negative resulting in a negative index of refraction. Because of these double negative parameters, some materials are classified as Double Negative Metamaterials or double negative materials (DNG). Other terminologies for NIMs are "left-handed media", "media with a negative refractive index", and "backward-wave media". In optical materials (i,e materials that are transparent to electro-magnetic waves), if both permittivity ϵ and permeability μ are positive, wave propagation in the forward direction results. If both ϵ and μ are negative, a backward wave is produced. If ϵ and μ have different polarities, then there is no wave propagation permitted.

Left-handed materials were first described theoretically by Victor Veselago in 1967.John Pendry was the first to theorize a practical way to make a left-handed metamaterial. Pendry's initial idea was that metallic wires aligned along the direction of propagation could provide a metamaterial with negative permittivity ($\epsilon < 0$). Note however that natural materials (such as ferroelectrics) were already known to exist with negative permittivity; the challenge was to construct a material which also showed negative permeability ($\mu < 0$). In 1999 Pendry demonstrated that a split ring resonator (SRR) with its axis placed along the direction of wave propagation could provide a negative permeability. The SRR consists of a planar set of concentric rings, each ring with a gap. Because the SRR is planar, it is easily fabricated by lithographic methods at scales appropriate for low frequencies to optical frequencies. Fig.3.2. In the same paper, he showed that a periodic array of wires and ring could give rise to a negative refractive index. A related negative-permeability particle, which was also proposed by Pendry, is the Swiss roll. The Swiss roll was claimed to be the most suited to MRI applications, Fig.3.3.

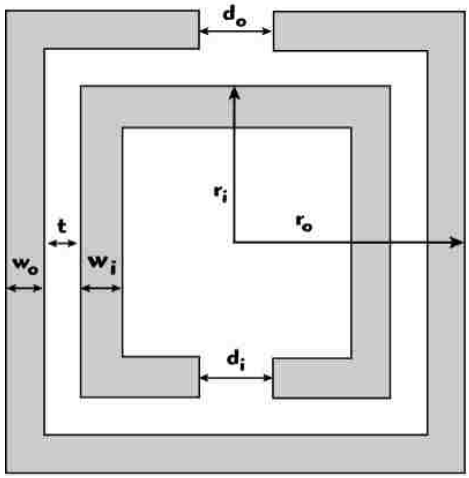

Figure 3.2: Structure of square split ring resonator from 'Metamaterial-based Compact Multilayer Filter with Skew-symmetric Feeds' on microwavejournal.com

The SRR, shown in Fig.3.2, is made of two concentric rings separated by a gap, both having splits at opposite sides. The geometrical parameters, such as the split gap width,

gap distance, metal width and radius are respectively represented by d, t, w and r. The subscripts i and o denote the inner and outer rings. Besides the electric and magnetic coupling, the incident field also induces the magnetoelectric coupling. The SRR not only has an electric resonance, but also a magnetic resonance. Moreover, the magnetic resonance frequency is lower than the electric resonance frequency. Using the magnetic resonance of the SRR in the filter design, a significant size reduction can be obtained.

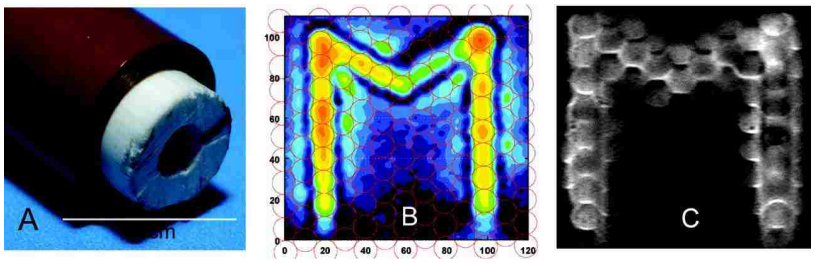

Figure 3.3: Structure of swissroll (from http://www.sciencemag.org)

In 2000, Smith et. al. successfully introduced a composite structure based on SRRs, which was shown to have a frequency band over which ϵ and μ were both negative. The negative μ occurred at frequencies above the resonant frequency of SRR structure. The negative ϵ was introduced by interleaving the SRR lattice with a lattice of conducting wires. Fig.3.4

Metamaterials applications in various fields such as design of invisibility cloak, sub-wavelength imaging, antenna and radar technology Figs.3.5-3.8.

Due to many potential interesting applications in various fields such as design of invisibility cloak, sub-wavelength imaging, antenna and radar technology, the study of metamaterials has attracted a great attention of scientists and engineers since 2000. Numerical simulation plays a very important role in the study of metamaterial and its applications due to its cost effectiveness compared to the physical experiments. However, simulations are mostly restricted to either the classic finite-difference time-domain (FDTD) method [27] or commercial packages such as COMSOL Multiphysics Finite Element Analysis Software. It is known that the FDTD method has a big disadvantage for solving problems with complex

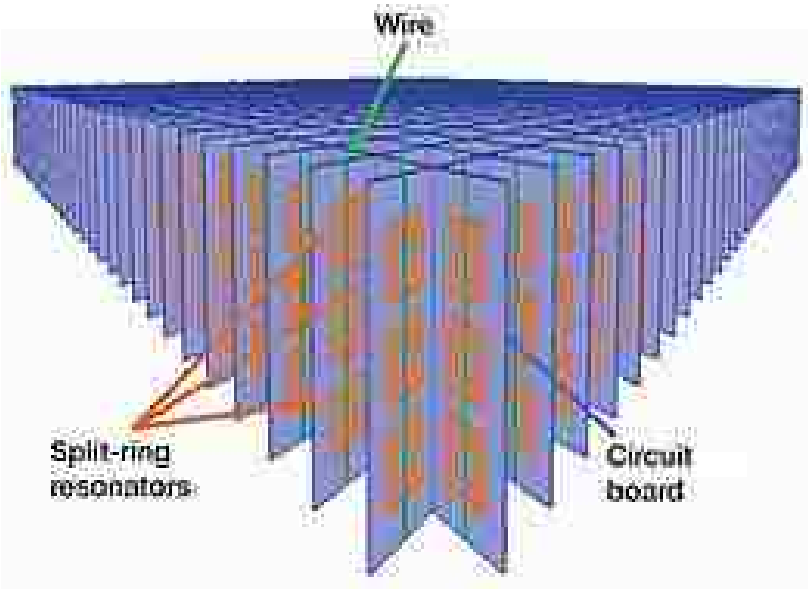

Figure 3.4: A split ring etched into a copper circuit board combined with copper wires leads to a material with negative μ and negative ϵ. From: http://en.wikipedia.org

geometries.Hence it would be quite interesting and useful to develop efficient and robust finite element methods for modeling metamaterials.

The discontinuous Galerkin (DG) method, originally introduced by Reed and Hill back in 1973, has become one of the most popular methods used for solving various differential equations (e.g., [2, 4, 19, 22, 32, 33, 36, 41, 50, 53, 63]). The DG method has a great flexibility in mesh construction by allowing conforming or non-conforming meshes and using different orders of basis functions in different elements.In the past decade, there has been a growing interest in developing DG methods for solving Maxwell's equations in free space [13, 20, 23, 24, 26, 28, 31, 51]. Very recently, there were some DG investigations [35, 45, 49, 58] carried out for Maxwell's equations in dispersive media, whose permittivity depends on the wave frequency. However, to our best knowledge, the study of DG methods for solving Maxwell's equations in metamaterials is quite limited.

Figure 3.5: invisibility cloak (From:Metallurgy for Dummies.com /futuristic-materials)

3.2 LEAP-FROG DISCONTINUOUS GALERKIN METHOD FOR THE TIME DOMAIN MAXWELL'S EQUATIONS IN METAMATERIALS

This section is mainly based on our published work [47].[1] It continues our recent initial effort [44] on developing DG methods for solving Maxwell's equations in metamaterials. In [44], we extended the DG method developed by Hesthaven and Warburton [28, 29] for Maxwell's equations in free space to metamaterials. Preliminary numerical results were performed and good convergence rates were observed, but detailed theoretical analysis was not carried out. Here we extend the framework of [28, 29] to develop a leap-frog type DG method for solving the time-domain Maxwell's equations in metamaterials and provide detailed stability results and error estimates for the scheme. Numerical results consistent with the theoretical analysis are also presented.

The governing equations for modeling wave propagation in metamaterials described by

[1]Reprinted from Computer Methods in Applied Mechanics and Engineering, 223-224(0), J. Li and J. Waters and E. A. Machorro, An implicit leap-frog discontinuous Galerkin method for the time-domain Maxwell's equations in metamaterials, 43-54, Copyright (2012), with permission from Elsevier.

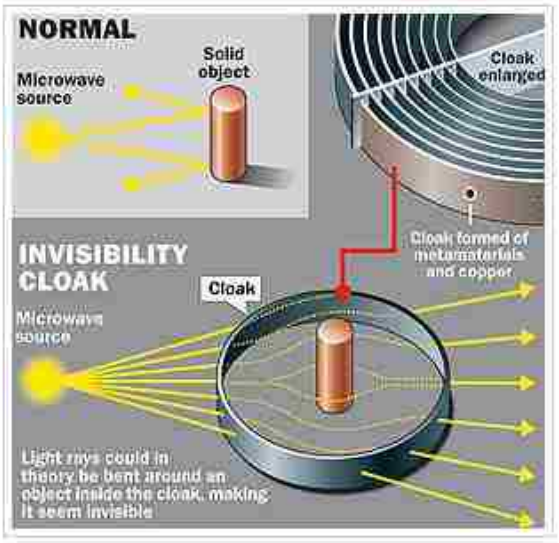

Figure 3.6: Light rays could in theory be bent around an object inside the cloak, making it seem invisible. From: livescience.com

the Drude model has been derived in our earlier work [48]:

$$\epsilon_0 \frac{\partial \boldsymbol{E}}{\partial t} = \nabla \times \boldsymbol{H} - \boldsymbol{J}, \quad \text{in} \ \ \Omega \times (0,T), \tag{3.1}$$

$$\mu_0 \frac{\partial \boldsymbol{H}}{\partial t} = -\nabla \times \boldsymbol{E} - \boldsymbol{K}, \quad \text{in} \ \ \Omega \times (0,T), \tag{3.2}$$

$$\frac{\partial \boldsymbol{J}}{\partial t} + \Gamma_e \boldsymbol{J} = \epsilon_0 \omega_{pe}^2 \boldsymbol{E}, \quad \text{in} \ \ \Omega \times (0,T), \tag{3.3}$$

$$\frac{\partial \boldsymbol{K}}{\partial t} + \Gamma_m \boldsymbol{K} = \mu_0 \omega_{pm}^2 \boldsymbol{H}, \quad \text{in} \ \ \Omega \times (0,T), \tag{3.4}$$

where $\boldsymbol{E}(\boldsymbol{x},t)$ and $\boldsymbol{H}(\boldsymbol{x},t)$ are the electric and magnetic fields, $\boldsymbol{J}(\boldsymbol{x},t)$ and $\boldsymbol{K}(\boldsymbol{x},t)$ are the induced electric and magnetic currents, ϵ_0 and μ_0 are the permittivity and permeability in free space, respectively, ω_{pe} and ω_{pm} are the electric and magnetic plasma frequencies, respectively, and Γ_e and Γ_m are the electric and magnetic damping frequencies, respectively. For simplicity, we assume that Ω is a bounded polyhedral domain of R^3 (note that our analysis below holds true for R^2 also), and the system (3.1)-(3.4) is supplemented with

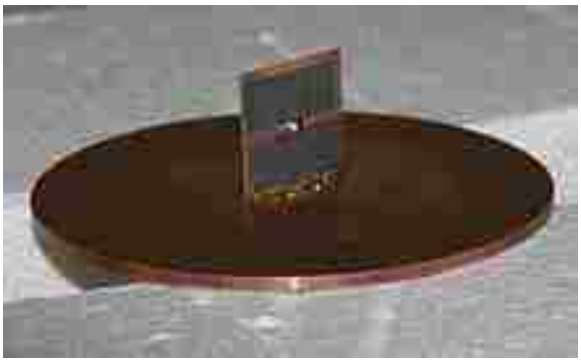

Figure 3.7: This Z antenna tested at the National Institute of Standards and Technology is smaller than a standard antenna with comparable properties. Its high efficiency is derived from the "Z element" inside the square that acts as a metamaterial, greatly boosting the signal sent over the air. The square is 30 millimeters on a side.(From:nextbigfuture.com)

metallic boundary conditions (i.e. a perfectly conducting surface), in which

$$\mathbf{n} \times \boldsymbol{E} = 0 \quad \text{on } \partial\Omega_m, \tag{3.5}$$

and initial conditions

$$\boldsymbol{E}(\boldsymbol{x}, 0) = \boldsymbol{E}_0(\boldsymbol{x}), \quad \boldsymbol{H}(\boldsymbol{x}, 0) = \boldsymbol{H}_0(\boldsymbol{x}), \boldsymbol{J}(\boldsymbol{x}, 0) = \boldsymbol{J}_0(\boldsymbol{x}), \quad \boldsymbol{K}(\boldsymbol{x}, 0) = \boldsymbol{K}_0(\boldsymbol{x}), \tag{3.6}$$

where $\boldsymbol{n}$ denotes the unit outward normal to $\partial\Omega$, and $\boldsymbol{E}_0, \boldsymbol{H}_0, \boldsymbol{J}_0, \boldsymbol{K}_0$ are some given functions.

3.2.1 NOTATION AND THE DG SCHEME

We assume that the bounded Lipschitz polyhedral domain Ω is partitioned into disjoint tetrahedral elements T_i such that $\overline{\Omega} = \cup_i T_i$. For each internal face $a_{ik} = T_i \bigcap T_k$, we denote $\mathbf{n}_{ik}$ the unit normal, oriented from T_i towards T_k. We denote h the maximum mesh size, ν_i the set of indices of the neighboring elements of the T_i, F_h^{int} the union of internal faces, and $\partial\Omega^m$ the set of metallic boundaries.

Figure 3.8: LG Chocolate BL40, the first cellphone to use a metamaterial antenna. (From:nextbigfuture.com)

Furthermore, we denote the jump terms by

$$[\boldsymbol{E}_i] = \boldsymbol{E}_i^+ - \boldsymbol{E}_i^-, \quad [\boldsymbol{H}_i] = \boldsymbol{H}_i^+ - \boldsymbol{H}_i^-,$$

where superscripts " $+$ " and " $-$ " refer to field values from the neighbor element and the local element itself, respectively.

We introduce the discontinuous finite element space:

$$\mathrm{V}_h = \{\boldsymbol{v}_h \in L^2(\Omega)^3 : \quad \boldsymbol{v}_h|_{T_i} \in (\mathrm{P}_k(T_i))^3 \ \text{ for any } T_i \in \overline{\Omega}\}, \tag{3.7}$$

i.e., the basis function is a discontinuous polynomial of degree k over each element.

To define a fully discrete scheme, we divide the time interval $(0, T)$ into M uniform subintervals by points $0 = t_0 < t_1 < \cdots < t_M = T$, where $t_k = k\tau$ and τ is the time step size. Moreover, we define $\boldsymbol{E}_i^n = \boldsymbol{E}(\cdot, t_n)$ as the approximate field on element T_i, and $\boldsymbol{E}_h$ as the global approximate field, i.e., $\boldsymbol{E}_h|_{T_i} = \boldsymbol{E}_i$. Similar notation holds for other fields $\boldsymbol{H}_h, \boldsymbol{J}_h$ and $\boldsymbol{K}_h$. Below we also use the average notation

$$\boldsymbol{E}_i^{[n+\frac{1}{2}]} = (\boldsymbol{E}_i^n + \boldsymbol{E}_i^{n+1})/2, \quad \boldsymbol{H}_i^{[n+1]} = (\boldsymbol{H}_i^{n+\frac{1}{2}} + \boldsymbol{H}_i^{n+\frac{3}{2}})/2.$$

With the above preparation, now we can construct our leap-frog DG method. Multiplying (3.1)-(3.4) by test functions $\boldsymbol{u}_i$,$\boldsymbol{v}_i$,$\boldsymbol{\phi}_i$,$\boldsymbol{\psi}_i$ respectively, integrating the resultants over each

element T_i, and choosing the upwind flux for the first two equations, we obtain the following leap-frog DG scheme: given initial approximations $\boldsymbol{E}_i^0, \boldsymbol{K}_i^0, \boldsymbol{H}_i^{\frac{1}{2}}, \boldsymbol{J}_i^{\frac{1}{2}}$, for $n = 0, 1, \cdots$, find $\boldsymbol{E}_i^{n+1}, \boldsymbol{K}_i^{n+1}, \boldsymbol{H}_i^{n+\frac{3}{2}}, \boldsymbol{J}_i^{n+\frac{3}{2}} \in \mathrm{V}_h$ such that

$$\begin{aligned}\int_{T_i} \epsilon_0 \frac{\boldsymbol{E}_i^{n+1} - \boldsymbol{E}_i^n}{\tau} \cdot \boldsymbol{u}_i &= \int_{T_i} \boldsymbol{u}_i \cdot \nabla \times \boldsymbol{H}_i^{n+\frac{1}{2}} - \int_{T_i} \boldsymbol{J}_i^{n+\frac{1}{2}} \cdot \boldsymbol{u}_i \\ &\quad + \sum_{k \in \nu_i} \int_{a_{ik}} \boldsymbol{u}_i \cdot \frac{1}{2} \mathbf{n}_{ik} \times ([\boldsymbol{H}_i^{n+\frac{1}{2}}] - \mathbf{n}_{ik} \times [\boldsymbol{E}_i^{[n+\frac{1}{2}]}]), \quad (3.8)\end{aligned}$$

$$\begin{aligned}\int_{T_i} \mu_0 \frac{\boldsymbol{H}_i^{n+\frac{3}{2}} - \boldsymbol{H}_i^{n+\frac{1}{2}}}{\tau} \cdot \boldsymbol{v}_i &= -\int_{T_i} \boldsymbol{v}_i \cdot \nabla \times \boldsymbol{E}_i^{n+1} - \int_{T_i} \boldsymbol{K}_i^{n+1} \cdot \boldsymbol{v}_i \\ &\quad - \sum_{k \in \nu_i} \int_{a_{ik}} \boldsymbol{v}_i \cdot \frac{1}{2} \mathbf{n}_{ik} \times (\mathbf{n}_{ik} \times [\boldsymbol{H}_i^{[n+1]}] + [\boldsymbol{E}_i^{n+1}]), \quad (3.9)\end{aligned}$$

$$\frac{1}{\epsilon_0 \omega_{pe}^2} \int_{T_i} \frac{\boldsymbol{J}_i^{n+\frac{3}{2}} - \boldsymbol{J}_i^{n+\frac{1}{2}}}{\tau} \cdot \boldsymbol{\phi}_i + \frac{\Gamma_e}{\epsilon_0 \omega_{pe}^2} \int_{T_i} \frac{\boldsymbol{J}_i^{n+\frac{3}{2}} + \boldsymbol{J}_i^{n+\frac{1}{2}}}{2} \cdot \boldsymbol{\phi}_i = \int_{T_i} \boldsymbol{E}_i^{n+1} \cdot \boldsymbol{\phi}_i, \quad (3.10)$$

$$\frac{1}{\mu_0 \omega_{pm}^2} \int_{T_i} \frac{\boldsymbol{K}_i^{n+1} - \boldsymbol{K}_i^n}{\tau} \cdot \boldsymbol{\psi}_i + \frac{\Gamma_m}{\mu_0 \omega_{pm}^2} \int_{T_i} \frac{\boldsymbol{K}_i^{n+1} + \boldsymbol{K}_i^n}{2} \cdot \boldsymbol{\psi}_i = \int_{T_i} \boldsymbol{H}_i^{n+\frac{1}{2}} \cdot \boldsymbol{\psi}_i. \quad (3.11)$$

For a metallic boundary face a_{ik}, the boundary condition $\mathbf{n}_{ik} \times \boldsymbol{E}|_{a_{ik}} = 0$ is implemented as

$$\boldsymbol{E}_k^n|_{a_{ik}} = -\boldsymbol{E}_i^n|_{a_{ik}}, \quad (3.12)$$

$$\boldsymbol{H}_k^{n+\frac{1}{2}}|_{a_{ik}} = \boldsymbol{H}_i^{n+\frac{1}{2}}|_{a_{ik}}. \quad (3.13)$$

For our scheme (3.8)-(3.11), we can prove the following conditional stability.

Theorem 3.2.1. *Denote $C_v = 1/\sqrt{\epsilon_0 \mu_0}$ for the wave propagation speed in free space. Under the CFL condition*

$$\tau \leq min\{\frac{1}{8}, \frac{h}{5C_{inv}^2 C_v}, \frac{h}{5C_{inv} C_v}, \frac{1}{2\omega_{pm}}, \frac{1}{2\omega_{pe}}\}, \quad (3.14)$$

where $C_{inv} > 0$ is the constant appearing in the standard inverse estimates [14]:

$$|u|_{0,\partial T_i} \leq C_{inv} h_{T_i}^{-\frac{1}{2}} \|u\|_{0,T_i}, \quad |u|_{1,T_i} \leq C_{inv} h_{T_i}^{-1} \|u\|_{0,T_i}, \quad \forall\ u \in V_h. \quad (3.15)$$

Here and below $|u|_{k,T_i}$ and $||u||_{k,T_i}$ denote the semi-norm and norm for a function u in the Sobolev space $H^k(T_i)$, respectively. The scheme (3.8)-(3.11) is stable and has the following stability:

$$\begin{aligned}
&\epsilon_0 \left\|\boldsymbol{E}_h^n\right\|_{0,\Omega}^2 + \mu_0 \left\|\boldsymbol{H}_h^{n+\frac{1}{2}}\right\|_{0,\Omega}^2 + \frac{1}{\epsilon_0\omega_{pe}^2}\left\|\boldsymbol{J}_h^{n+\frac{1}{2}}\right\|_{0,\Omega}^2 + \frac{1}{\mu_0\omega_{pm}^2}\left\|\boldsymbol{K}_h^n\right\|_{0,\Omega}^2 \\
&\leq C\left(\left\|\boldsymbol{E}_h^0\right\|_{0,\Omega}^2 + \left\|\boldsymbol{H}_h^{\frac{1}{2}}\right\|_{0,\Omega}^2 + \left\|\boldsymbol{J}_h^{\frac{1}{2}}\right\|_{0,\Omega}^2 + \left\|\boldsymbol{K}_h^0\right\|_{0,\Omega}^2\right),
\end{aligned}$$

where the constant $C > 0$ depends on the physical parameters $\epsilon_0, \mu_0, \omega_{pe}, \omega_{pm}, \Gamma_e$ and Γ_m, but is independent of the time step size τ and mesh size h.

Proof. Let us denote $EGY_i^n = EGY_{i1}^n + EGY_{i2}^n$, where

$$EGY_{i1}^n = \frac{1}{2}\int_{T_i} \epsilon_0 \boldsymbol{E}_i^n \cdot \boldsymbol{E}_i^n + \frac{1}{2}\int_{T_i} \mu_0 \boldsymbol{H}_i^{n+\frac{1}{2}} \cdot \boldsymbol{H}_i^{n+\frac{1}{2}}, \tag{3.16}$$

$$EGY_{i2}^n = \frac{1}{2}\int_{T_i} \frac{1}{\epsilon_0\omega_{pe}^2}\boldsymbol{J}_i^{n+\frac{1}{2}} \cdot \boldsymbol{J}_i^{n+\frac{1}{2}} + \frac{1}{2}\int_{T_i} \frac{1}{\mu_0\omega_{pm}^2}\boldsymbol{K}_i^n \cdot \boldsymbol{K}_i^n. \tag{3.17}$$

Choosing $\boldsymbol{u}_i = \tau \boldsymbol{E}_i^{[n+\frac{1}{2}]}$ in (3.8) and $\boldsymbol{v}_i = \tau \boldsymbol{H}_i^{[n+1]}$ in (3.9), and adding the resultants together, we have

$$\begin{aligned}
EGY_{i1}^{n+1} = \; & EGY_{i1}^n - \tau\int_{T_i} \frac{\boldsymbol{H}_i^{n+\frac{3}{2}} + \boldsymbol{H}_i^{n+\frac{1}{2}}}{2} \cdot \nabla \times \boldsymbol{E}_i^{n+1} - \tau\int_{T_i} \frac{\boldsymbol{H}_i^{n+\frac{3}{2}} + \boldsymbol{H}_i^{n+\frac{1}{2}}}{2} \cdot \boldsymbol{K}_i^{n+1} \\
& - \sum_{k\in\nu_i} \frac{\tau}{2}\int_{a_{ik}} \boldsymbol{H}_i^{[n+1]} \cdot \mathbf{n}_{ik} \times (\mathbf{n}_{ik} \times [\boldsymbol{H}_i^{[n+1]}] + [\boldsymbol{E}_i^{n+1}]) \\
& + \tau\int_{T_i} \frac{\boldsymbol{E}_i^n + \boldsymbol{E}_i^{n+1}}{2} \cdot \nabla \times \boldsymbol{H}_i^{n+\frac{1}{2}} - \tau\int_{T_i} \boldsymbol{J}_i^{n+\frac{1}{2}} \cdot \boldsymbol{E}_i^{[n+\frac{1}{2}]} \\
& + \sum_{k\in\nu_i} \frac{\tau}{2}\int_{a_{ik}} \boldsymbol{E}_i^{[n+\frac{1}{2}]} \cdot \mathbf{n}_{ik} \times ([\boldsymbol{H}_i^{n+\frac{1}{2}}] - \mathbf{n}_{ik} \times [\boldsymbol{E}_i^{[n+\frac{1}{2}]}]).
\end{aligned} \tag{3.18}$$

Using the identity

$$\int_{T_i} \boldsymbol{H}_i^{n+\frac{1}{2}} \cdot \nabla \times \boldsymbol{E}_i^{n+1} = \int_{T_i} \nabla \times \boldsymbol{H}_i^{n+\frac{1}{2}} \cdot \boldsymbol{E}_i^{n+1} + \int_{\partial T_i} \boldsymbol{E}_i^{n+1} \cdot (\boldsymbol{H}_i^{n+\frac{1}{2}} \times \mathbf{n}_i)$$

and the jump definition $[\boldsymbol{E}_i] = \boldsymbol{E}_i^+ - \boldsymbol{E}_i^- = \boldsymbol{E}_k - \boldsymbol{E}_i$, $[\boldsymbol{H}_i] = \boldsymbol{H}_i^+ - \boldsymbol{H}_i^- = \boldsymbol{H}_k - \boldsymbol{H}_i$ in

(3.18), we have

$$
\begin{aligned}
EGY_{i1}^{n+1} &= EGY_{i1}^{n} - \frac{\tau}{2}\int_{T_i} \boldsymbol{H}_i^{n+\frac{3}{2}} \cdot \nabla \times \boldsymbol{E}_i^{n+1} - \frac{\tau}{2}\int_{\partial T_i} \boldsymbol{E}_i^{n+1} \cdot (\boldsymbol{H}_i^{n+\frac{1}{2}} \times \mathbf{n}_i) \\
&\quad -\tau \int_{T_i} \boldsymbol{H}_i^{[n+1]} \cdot \boldsymbol{K}_i^{n+1} - \sum_{k\in\nu_i} \frac{\tau}{2}\int_{a_{ik}} \boldsymbol{H}_i^{[n+1]} \cdot \mathbf{n}_{ik} \times \boldsymbol{E}_k^{n+1} \\
&\quad + \sum_{k\in\nu_i} \frac{\tau}{2}\int_{a_{ik}} \boldsymbol{H}_i^{[n+1]} \cdot \mathbf{n}_{ik} \times \boldsymbol{E}_i^{n+1} - \sum_{k\in\nu_i} \frac{\tau}{2}\int_{a_{ik}} \boldsymbol{H}_i^{[n+1]} \cdot \mathbf{n}_{ik} \times (\mathbf{n}_{ik} \times [\boldsymbol{H}_i^{[n+1]}]) \\
&\quad + \frac{\tau}{2}\int_{T_i} \boldsymbol{E}_i^{n} \cdot \nabla \times \boldsymbol{H}_i^{n+\frac{1}{2}} - \tau \int_{T_i} \boldsymbol{J}_i^{n+\frac{1}{2}} \cdot \boldsymbol{E}_i^{[n+\frac{1}{2}]} + \sum_{k\in\nu_i} \frac{\tau}{2}\int_{a_{ik}} \boldsymbol{E}_i^{[n+\frac{1}{2}]} \cdot \mathbf{n}_{ik} \times \boldsymbol{H}_k^{n+\frac{1}{2}} \\
&\quad - \sum_{k\in\nu_i} \frac{\tau}{2}\int_{a_{ik}} \boldsymbol{E}_i^{[n+\frac{1}{2}]} \cdot \mathbf{n}_{ik} \times \boldsymbol{H}_i^{n+\frac{1}{2}} - \sum_{k\in\nu_i} \frac{\tau}{2}\int_{a_{ik}} \boldsymbol{E}_i^{[n+\frac{1}{2}]} \cdot \mathbf{n}_{ik} \times (\mathbf{n}_{ik} \times [\boldsymbol{E}_i^{[n+\frac{1}{2}]}])
\end{aligned}
$$

$$
\begin{aligned}
&= EGY_{i1}^{n} - \frac{\tau}{2}\int_{T_i} \boldsymbol{H}_i^{n+\frac{3}{2}} \cdot \nabla \times \boldsymbol{E}_i^{n+1} - \frac{\tau}{2}\int_{\partial T_i} \boldsymbol{E}_i^{n+1} \cdot (\boldsymbol{H}_i^{n+\frac{1}{2}} \times \mathbf{n}_i) \\
&\quad -\tau \int_{T_i} \boldsymbol{H}_i^{[n+1]} \cdot \boldsymbol{K}_i^{n+1} - \sum_{k\in\nu_i} \frac{\tau}{4}\int_{a_{ik}} \boldsymbol{H}_i^{n+\frac{3}{2}} \cdot \mathbf{n}_{ik} \times \boldsymbol{E}_k^{n+1} \\
&\quad - \sum_{k\in\nu_i} \frac{\tau}{4}\int_{a_{ik}} \boldsymbol{H}_i^{n+\frac{1}{2}} \cdot \mathbf{n}_{ik} \times \boldsymbol{E}_k^{n+1} + \sum_{k\in\nu_i} \frac{\tau}{4}\int_{a_{ik}} \boldsymbol{H}_i^{n+\frac{3}{2}} \cdot \mathbf{n}_{ik} \times \boldsymbol{E}_i^{n+1} \\
&\quad + \sum_{k\in\nu_i} \frac{\tau}{4}\int_{a_{ik}} \boldsymbol{H}_i^{n+\frac{1}{2}} \cdot \mathbf{n}_{ik} \times \boldsymbol{E}_i^{n+1-\sum_{k\in\nu_i}\frac{\tau}{2}\int_{a_{ik}} \boldsymbol{H}_i^{[n+1]}\cdot\mathbf{n}_{ik}\times(\mathbf{n}_{ik}\times[\boldsymbol{H}_i^{[n+1]}])} \\
&\quad + \frac{\tau}{2}\int_{T_i} \boldsymbol{E}_i^{n} \cdot \nabla \times \boldsymbol{H}_i^{n+\frac{1}{2}} - \tau \int_{T_i} \boldsymbol{J}_i^{n+\frac{1}{2}} \cdot \boldsymbol{E}_i^{[n+\frac{1}{2}]} + \sum_{k\in\nu_i} \frac{\tau}{4}\int_{a_{ik}} \boldsymbol{E}_i^{n+1} \cdot \mathbf{n}_{ik} \times \boldsymbol{H}_k^{n+\frac{1}{2}} \\
&\quad + \sum_{k\in\nu_i} \frac{\tau}{4}\int_{a_{ik}} \boldsymbol{E}_i^{n} \cdot \mathbf{n}_{ik} \times \boldsymbol{H}_k^{n+\frac{1}{2}} - \sum_{k\in\nu_i} \frac{\tau}{4}\int_{a_{ik}} \boldsymbol{E}_i^{n+1} \cdot \mathbf{n}_{ik} \times \boldsymbol{H}_i^{n+\frac{1}{2}} \\
&\quad - \sum_{k\in\nu_i} \frac{\tau}{4}\int_{a_{ik}} \boldsymbol{E}_i^{n} \cdot \mathbf{n}_{ik} \times \boldsymbol{H}_i^{n+\frac{1}{2}} - \sum_{k\in\nu_i} \frac{\tau}{2}\int_{a_{ik}} \boldsymbol{E}_i^{[n+\frac{1}{2}]} \cdot \mathbf{n}_{ik} \times (\mathbf{n}_{ik} \times [\boldsymbol{E}_i^{[n+\frac{1}{2}]}]). \quad (3.19)
\end{aligned}
$$

Using the identity

$$
\frac{\tau}{2}\int_{\partial T_i} \boldsymbol{E}_i^{n+1} \cdot (\boldsymbol{H}_i^{n+\frac{1}{2}} \times \mathbf{n}_i) = \sum_{k\in\nu_i} \frac{\tau}{4}\int_{a_{ik}} \boldsymbol{H}_i^{n+\frac{1}{2}} \cdot \mathbf{n}_{ik} \times \boldsymbol{E}_i^{n+1} - \sum_{k\in\nu_i} \frac{\tau}{4}\int_{a_{ik}} \boldsymbol{E}_i^{n+1} \cdot \mathbf{n}_{ik} \times \boldsymbol{H}_i^{n+\frac{1}{2}}
$$

in (3.19), and moving the 6th term to the last and the 12th term to the second last, we obtain

$$
\begin{aligned}
EGY_{i1}^{n+1} &= EGY_{i1}^{n} - \frac{\tau}{2}\int_{T_i} \boldsymbol{H}_i^{n+\frac{3}{2}} \cdot \nabla \times \boldsymbol{E}_i^{n+1} - \tau \int_{T_i} \boldsymbol{H}_i^{[n+1]} \cdot \boldsymbol{K}_i^{n+1} \\
&\quad - \sum_{k\in\nu_i} \frac{\tau}{4}\int_{a_{ik}} \boldsymbol{H}_i^{n+\frac{3}{2}} \cdot \mathbf{n}_{ik} \times \boldsymbol{E}_k^{n+1} + \sum_{k\in\nu_i} \frac{\tau}{4}\int_{a_{ik}} \boldsymbol{H}_i^{n+\frac{3}{2}} \cdot \mathbf{n}_{ik} \times \boldsymbol{E}_i^{n+1} \\
&\quad - \sum_{k\in\nu_i} \frac{\tau}{2}\int_{a_{ik}} \boldsymbol{H}_i^{[n+1]} \cdot \mathbf{n}_{ik} \times (\mathbf{n}_{ik} \times [\boldsymbol{H}_i^{[n+1]}]) + \frac{\tau}{2}\int_{T_i} \boldsymbol{E}_i^{n} \cdot \nabla \times \boldsymbol{H}_i^{n+\frac{1}{2}} \\
&\quad - \tau \int_{T_i} \boldsymbol{J}_i^{n+\frac{1}{2}} \cdot \boldsymbol{E}_i^{[n+\frac{1}{2}]} + \sum_{k\in\nu_i} \frac{\tau}{4}\int_{a_{ik}} \boldsymbol{E}_i^{n} \cdot \mathbf{n}_{ik} \times \boldsymbol{H}_k^{n+\frac{1}{2}} \\
&\quad - \sum_{k\in\nu_i} \frac{\tau}{4}\int_{a_{ik}} \boldsymbol{E}_i^{n} \cdot \mathbf{n}_{ik} \times \boldsymbol{H}_i^{n+\frac{1}{2}} - \sum_{k\in\nu_i} \frac{\tau}{2}\int_{a_{ik}} \boldsymbol{E}_i^{[n+\frac{1}{2}]} \cdot \mathbf{n}_{ik} \times (\mathbf{n}_{ik} \times [\boldsymbol{E}_i^{[n+\frac{1}{2}]}]) \\
&\quad + \sum_{k\in\nu_i} \frac{\tau}{4}\int_{a_{ik}} \boldsymbol{E}_i^{n+1} \cdot \mathbf{n}_{ik} \times \boldsymbol{H}_k^{n+\frac{1}{2}} - \sum_{k\in\nu_i} \frac{\tau}{4}\int_{a_{ik}} \boldsymbol{H}_i^{n+\frac{1}{2}} \cdot \mathbf{n}_{ik} \times \boldsymbol{E}_k^{n+1}. \qquad (3.20)
\end{aligned}
$$

Choosing $\boldsymbol{\phi}_i = \frac{\tau}{2}(\boldsymbol{J}_i^{n+\frac{3}{2}} + \boldsymbol{J}_i^{n+\frac{1}{2}})$ in (3.10) and $\boldsymbol{\psi}_i = \frac{\tau}{2}(\boldsymbol{K}_i^{n+1} + \boldsymbol{K}_i^{n})$ in (3.11), and adding the resultants, we obtain

$$
\begin{aligned}
EGY_{i2}^{n+1} &= EGY_{i2}^{n} - \frac{\Gamma_e \tau}{\epsilon_0 \omega_{pe}^2}\int_{T_i} \boldsymbol{J}_i^{[n+1]} \cdot \boldsymbol{J}_i^{[n+1]} + \frac{\tau}{2}\int_{T_i} \boldsymbol{E}_i^{n+1} \cdot \boldsymbol{J}_i^{n+\frac{3}{2}} + \frac{\tau}{2}\int_{T_i} \boldsymbol{E}_i^{n+1} \cdot \boldsymbol{J}_i^{n+\frac{1}{2}} \\
&\quad - \frac{\Gamma_m \tau}{\mu_0 \omega_{pm}^2}\int_{T_i} \boldsymbol{K}_i^{[n+\frac{1}{2}]} \cdot \boldsymbol{K}_i^{[n+\frac{1}{2}]} + \frac{\tau}{2}\int_{T_i} \boldsymbol{H}_i^{n+\frac{1}{2}} \cdot \boldsymbol{K}_i^{n+1} + \frac{\tau}{2}\int_{T_i} \boldsymbol{H}_i^{n+\frac{1}{2}} \cdot \boldsymbol{K}_i^{n} \qquad (3.21)
\end{aligned}
$$

Adding (3.20) to (3.21), expanding $\boldsymbol{H}_i^{[n+1]}, \boldsymbol{E}_i^{[n+\frac{1}{2}]}$ and simplifying the results, we have

$$
\begin{aligned}
&EGY_i^{n+1} = EGY_{i1}^{n+1} + EGY_{i2}^{n+1} \\
&= EGY_i^n - \frac{\tau}{2}\int_{T_i} \boldsymbol{H}_i^{n+\frac{3}{2}} \cdot \nabla \times \boldsymbol{E}_i^{n+1} - \frac{\tau}{2}\int_{T_i} \boldsymbol{H}_i^{n+\frac{3}{2}} \cdot \boldsymbol{K}_i^{n+1} - \sum_{k\in\nu_i} \frac{\tau}{4}\int_{a_{ik}} \boldsymbol{H}_i^{n+\frac{3}{2}} \cdot \mathbf{n}_{ik} \times \boldsymbol{E}_k^{n+1} \\
&\quad + \sum_{k\in\nu_i} \frac{\tau}{4}\int_{a_{ik}} \boldsymbol{H}_i^{n+\frac{3}{2}} \cdot \mathbf{n}_{ik} \times \boldsymbol{E}_i^{n+1} - \sum_{k\in\nu_i} \frac{\tau}{2}\int_{a_{ik}} \boldsymbol{H}_i^{[n+1]} \cdot \mathbf{n}_{ik} \times (\mathbf{n}_{ik} \times [\boldsymbol{H}_i^{[n+1]}]) \\
&\quad + \frac{\tau}{2}\int_{T_i} \boldsymbol{E}_i^n \cdot \nabla \times \boldsymbol{H}_i^{n+\frac{1}{2}} - \frac{\tau}{2}\int_{T_i} \boldsymbol{J}_i^{n+\frac{1}{2}} \cdot \boldsymbol{E}_i^n + \sum_{k\in\nu_i} \frac{\tau}{4}\int_{a_{ik}} \boldsymbol{E}_i^n \cdot \mathbf{n}_{ik} \times \boldsymbol{H}_k^{n+\frac{1}{2}} \\
&\quad - \sum_{k\in\nu_i} \frac{\tau}{4}\int_{a_{ik}} \boldsymbol{E}_i^n \cdot \mathbf{n}_{ik} \times \boldsymbol{H}_i^{n+\frac{1}{2}} - \sum_{k\in\nu_i} \frac{\tau}{2}\int_{a_{ik}} \boldsymbol{E}_i^{[n+\frac{1}{2}]} \cdot \mathbf{n}_{ik} \times (\mathbf{n}_{ik} \times [\boldsymbol{E}_i^{[n+\frac{1}{2}]}]) \\
&\quad + \sum_{k\in\nu_i} \frac{\tau}{4}\int_{a_{ik}} \boldsymbol{E}_i^{n+1} \cdot \mathbf{n}_{ik} \times \boldsymbol{H}_k^{n+\frac{1}{2}} + \sum_{k\in\nu_i} \frac{\tau}{4}\int_{a_{ik}} \boldsymbol{E}_k^{n+1} \cdot \mathbf{n}_{ik} \times \boldsymbol{H}_i^{n+\frac{1}{2}} \\
&\quad - \frac{\Gamma_e \tau}{\epsilon_0 \omega_{pe}^2}\int_{T_i} \boldsymbol{J}_i^{[n+1]} \cdot \boldsymbol{J}_i^{[n+1]} + \frac{\tau}{2}\int_{T_i} \boldsymbol{E}_i^{n+1} \cdot \boldsymbol{J}_i^{n+\frac{3}{2}} \\
&\quad - \frac{\Gamma_m \tau}{\mu_0 \omega_{pm}^2}\int_{T_i} \boldsymbol{K}_i^{[n+\frac{1}{2}]} \cdot \boldsymbol{K}_i^{[n+\frac{1}{2}]} + \frac{\tau}{2}\int_{T_i} \boldsymbol{H}_i^{n+\frac{1}{2}} \cdot \boldsymbol{K}_i^n. \qquad (3.22)
\end{aligned}
$$

Substituting the identity

$$
-\frac{\tau}{2}\int_{T_i} \boldsymbol{H}_i^{n+\frac{3}{2}} \cdot \nabla \times \boldsymbol{E}_i^{n+1} = -\frac{\tau}{2}\int_{T_i} \boldsymbol{E}_i^{n+1} \cdot \nabla \times \boldsymbol{H}_i^{n+\frac{3}{2}} - \sum_{k\in\nu_i} \frac{\tau}{2}\int_{a_{ik}} \boldsymbol{H}_i^{n+\frac{3}{2}} \cdot \mathbf{n}_{ik} \times \boldsymbol{E}_i^{n+1}
$$

into (3.22), we can rewrite (3.22) as

$$
\begin{aligned}
& EGY_i^{n+1} + \frac{\tau}{2}\int_{T_i} \boldsymbol{E}_i^{n+1} \cdot \nabla \times \boldsymbol{H}_i^{n+\frac{3}{2}} - \sum_{k\in\nu_i} \frac{\tau}{4}\int_{a_{ik}} \boldsymbol{E}_i^{n+1} \cdot \mathbf{n}_{ik} \times \boldsymbol{H}_i^{n+\frac{3}{2}} \\
& + \frac{\tau}{2}\int_{T_i} \boldsymbol{H}_i^{n+\frac{3}{2}} \cdot \boldsymbol{K}_i^{n+1} - \frac{\tau}{2}\int_{T_i} \boldsymbol{E}_i^{n+1} \cdot \boldsymbol{J}_i^{n+\frac{3}{2}} \\
= \quad & EGY_i^n + \frac{\tau}{2}\int_{T_i} \boldsymbol{E}_i^n \cdot \nabla \times \boldsymbol{H}_i^{n+\frac{1}{2}} - \sum_{k\in\nu_i} \frac{\tau}{4}\int_{a_{ik}} \boldsymbol{E}_i^n \cdot \mathbf{n}_{ik} \times \boldsymbol{H}_i^{n+\frac{1}{2}}
\end{aligned}
$$

$$
\begin{aligned}
&+\frac{\tau}{2}\int_{T_i}\boldsymbol{H}_i^{n+\frac{1}{2}}\cdot\boldsymbol{K}_i^n-\frac{\tau}{2}\int_{T_i}\boldsymbol{J}_i^{n+\frac{1}{2}}\cdot\boldsymbol{E}_i^n\\
&-\sum_{k\in\nu_i}\frac{\tau}{4}\int_{a_{ik}}\boldsymbol{H}_i^{n+\frac{3}{2}}\cdot\mathbf{n}_{ik}\times\boldsymbol{E}_k^{n+1}-\sum_{k\in\nu_i}\frac{\tau}{2}\int_{a_{ik}}\boldsymbol{H}_i^{[n+1]}\cdot\mathbf{n}_{ik}\times(\mathbf{n}_{ik}\times[\boldsymbol{H}_i^{[n+1]}])\\
&+\sum_{k\in\nu_i}\frac{\tau}{4}\int_{a_{ik}}\boldsymbol{E}_i^{n}\cdot\mathbf{n}_{ik}\times\boldsymbol{H}_k^{n+\frac{1}{2}}-\sum_{k\in\nu_i}\frac{\tau}{2}\int_{a_{ik}}\boldsymbol{E}_i^{[n+\frac{1}{2}]}\cdot\mathbf{n}_{ik}\times(\mathbf{n}_{ik}\times[\boldsymbol{E}_i^{[n+\frac{1}{2}]}])\\
&+\sum_{k\in\nu_i}\frac{\tau}{4}\int_{a_{ik}}\boldsymbol{E}_i^{n+1}\cdot\mathbf{n}_{ik}\times\boldsymbol{H}_k^{n+\frac{1}{2}}+\sum_{k\in\nu_i}\frac{\tau}{4}\int_{a_{ik}}\boldsymbol{E}_k^{n+1}\cdot\mathbf{n}_{ik}\times\boldsymbol{H}_i^{n+\frac{1}{2}}\\
&-\frac{\Gamma_e\tau}{\epsilon_0\omega_{pe}^2}\int_{T_i}\boldsymbol{J}_i^{[n+1]}\cdot\boldsymbol{J}_i^{[n+1]}-\frac{\Gamma_m\tau}{\mu_0\omega_{pm}^2}\int_{T_i}\boldsymbol{K}_i^{[n+\frac{1}{2}]}\cdot\boldsymbol{K}_i^{[n+\frac{1}{2}]}.
\end{aligned}
\tag{3.23}
$$

Let us denote

$$
\begin{aligned}
F1_i^n=&EGY_i^n+\frac{\tau}{2}\int_{T_i}\boldsymbol{E}_i^n\cdot\nabla\times\boldsymbol{H}_i^{n+\frac{1}{2}}-\sum_{k\in\nu_i}\frac{\tau}{4}\int_{a_{ik}}\boldsymbol{E}_i^n\cdot\mathbf{n}_{ik}\times\boldsymbol{H}_i^{n+\frac{1}{2}}\\
&+\frac{\tau}{2}\int_{T_i}\boldsymbol{H}_i^{n+\frac{1}{2}}\cdot\boldsymbol{K}_i^n-\frac{\tau}{2}\int_{T_i}\boldsymbol{J}_i^{n+\frac{1}{2}}\cdot\boldsymbol{E}_i^n.
\end{aligned}
$$

Then we can rewrite (3.23) as

$$
\begin{aligned}
F1_i^{n+1} \;=\;& F1_i^n-\sum_{k\in\nu_i}\frac{\tau}{4}\int_{a_{ik}}\boldsymbol{H}_i^{n+\frac{3}{2}}\cdot\mathbf{n}_{ik}\times\boldsymbol{E}_k^{n+1}+\sum_{k\in\nu_i}\frac{\tau}{4}\int_{a_{ik}}\boldsymbol{E}_i^{n}\cdot\mathbf{n}_{ik}\times\boldsymbol{H}_k^{n+\frac{1}{2}}\\
&-\sum_{k\in\nu_i}\frac{\tau}{2}\int_{a_{ik}}\boldsymbol{H}_i^{[n+1]}\cdot\mathbf{n}_{ik}\times(\mathbf{n}_{ik}\times[\boldsymbol{H}_i^{[n+1]}])\\
&-\sum_{k\in\nu_i}\frac{\tau}{2}\int_{a_{ik}}\boldsymbol{E}_i^{[n+\frac{1}{2}]}\cdot\mathbf{n}_{ik}\times(\mathbf{n}_{ik}\times[\boldsymbol{E}_i^{[n+\frac{1}{2}]}])\\
&+\sum_{k\in\nu_i}\frac{\tau}{4}\int_{a_{ik}}\boldsymbol{E}_i^{n+1}\cdot\mathbf{n}_{ik}\times\boldsymbol{H}_k^{n+\frac{1}{2}}+\sum_{k\in\nu_i}\frac{\tau}{4}\int_{a_{ik}}\boldsymbol{E}_k^{n+1}\cdot\mathbf{n}_{ik}\times\boldsymbol{H}_i^{n+\frac{1}{2}}\\
&-\frac{\tau_e\tau}{\epsilon_0\omega_{pe}^2}\int_{T_i}\boldsymbol{J}_i^{[n+1]}\cdot\boldsymbol{J}_i^{[n+1]}-\frac{\Gamma_m\tau}{\mu_0\omega_{pm}^2}\int_{T_i}\boldsymbol{K}_i^{[n+\frac{1}{2}]}\cdot\boldsymbol{K}_i^{[n+\frac{1}{2}]}.
\end{aligned}
\tag{3.24}
$$

Now summing up (3.24) over all elements T_i of Ω, and noting that all terms of

$$
\sum_{k\in\nu_i}\frac{\tau}{4}\int_{a_{ik}}\boldsymbol{E}_i^{n+1}\cdot\mathbf{n}_{ik}\times\boldsymbol{H}_k^{n+\frac{1}{2}}+\sum_{k\in\nu_i}\frac{\tau}{4}\int_{a_{ik}}\boldsymbol{E}_k^{n+1}\cdot\mathbf{n}_{ik}\times\boldsymbol{H}_i^{n+\frac{1}{2}}
$$

vanish on the internal faces F_h^{int} and metallic boundaries $\partial\Omega^m$, we obtain

$$
\begin{aligned}
F1_{\Omega_h}^{n+1} = F1_{\Omega_h}^{n} &+ \sum_{a_{ik}\in\partial\Omega_h^m} \frac{\tau}{4}\int_{a_{ik}} \boldsymbol{H}_i^{n+\frac{3}{2}}\cdot\mathbf{n}_{ik}\times\boldsymbol{E}_i^{n+1} + \sum_{a_{ik}\in\partial\Omega_h^m} \frac{\tau}{4}\int_{a_{ik}} \boldsymbol{E}_i^{n}\cdot\mathbf{n}_{ik}\times\boldsymbol{H}_i^{n+\frac{1}{2}} \\
&- \sum_{T_i}\sum_{k\in\nu_i} \frac{\tau}{4}\int_{a_{ik}\in F_h^{int}} \boldsymbol{H}_i^{n+\frac{3}{2}}\cdot\mathbf{n}_{ik}\times\boldsymbol{E}_k^{n+1} + \sum_{T_i}\sum_{k\in\nu_i} \frac{\tau}{4}\int_{a_{ik}\in F_h^{int}} \boldsymbol{E}_i^{n}\cdot\mathbf{n}_{ik}\times\boldsymbol{H}_k^{n+\frac{1}{2}} \\
&- \sum_{f_i\in F_h^{int}} \frac{\tau}{2}\int_{f_i} (\mathbf{n}_{ik}\times[\boldsymbol{H}_i^{[n+1]}])\cdot(\mathbf{n}_{ik}\times[\boldsymbol{H}_i^{[n+1]}]) \\
&- \sum_{f_i\in F_h^{int}} \frac{\tau}{2}\int_{f_i} (\mathbf{n}_{ik}\times[\boldsymbol{E}_i^{[n+\frac{1}{2}]}])\cdot(\mathbf{n}_{ik}\times[\boldsymbol{E}_i^{[n+\frac{1}{2}]}]) \\
&- \sum_{a_{ik}\in\partial\Omega_h^m} \tau\int_{a_{ik}} (\mathbf{n}_{ik}\times[\boldsymbol{E}_i^{[n+\frac{1}{2}]}])\cdot(\mathbf{n}_{ik}\times[\boldsymbol{E}_i^{[n+\frac{1}{2}]}]) \\
&- \frac{\Gamma_e\tau}{\epsilon_0\omega_{pe}^2}\left\|\boldsymbol{J}_i^{[n+1]}\right\|_{0,\Omega}^2 - \frac{\Gamma_m\tau}{\mu_0\omega_{pm}^2}\left\|\boldsymbol{K}_i^{[n+\frac{1}{2}]}\right\|_{0,\Omega}^2 .
\end{aligned}
\tag{3.25}
$$

Denote

$$
F_{\Omega_h}^{n} = F1_{\Omega_h}^{n} + \sum_{a_{ik}\in\partial\Omega_h^m} \frac{\tau}{4}\int_{a_{ik}} \boldsymbol{E}_i^{n}\cdot\mathbf{n}_{ik}\times\boldsymbol{H}_i^{n+\frac{1}{2}}.
$$

Then we can rewrite (3.25) as

$$
\begin{aligned}
F_{\Omega_h}^{n+1} = F_{\Omega_h}^{n} &- \sum_{T_i}\sum_{k\in\nu_i} \frac{\tau}{4}\int_{a_{ik}\in F_h^{int}} \boldsymbol{H}_i^{n+\frac{3}{2}}\cdot\mathbf{n}_{ik}\times\boldsymbol{E}_k^{n+1} \\
&+ \sum_{T_i}\sum_{k\in\nu_i} \frac{\tau}{4}\int_{a_{ik}\in F_h^{int}} \boldsymbol{E}_i^{n}\cdot\mathbf{n}_{ik}\times\boldsymbol{H}_k^{n+\frac{1}{2}} \\
&- \sum_{f_i\in F_h^{int}} \frac{\tau}{2}\int_{f_i} (\mathbf{n}_{ik}\times[\boldsymbol{H}_i^{[n+1]}])\cdot(\mathbf{n}_{ik}\times[\boldsymbol{H}_i^{[n+1]}]) \\
&- \sum_{f_i\in F_h^{int}} \frac{\tau}{2}\int_{f_i} (\mathbf{n}_{ik}\times[\boldsymbol{E}_i^{[n+\frac{1}{2}]}])\cdot(\mathbf{n}_{ik}\times[\boldsymbol{E}_i^{[n+\frac{1}{2}]}]) \\
&- \sum_{a_{ik}\in\partial\Omega_h^m} \tau\int_{a_{ik}} (\mathbf{n}_{ik}\times[\boldsymbol{E}_i^{[n+\frac{1}{2}]}])\cdot(\mathbf{n}_{ik}\times[\boldsymbol{E}_i^{[n+\frac{1}{2}]}]) \\
&- \frac{\Gamma_e\tau}{\epsilon_0\omega_{pe}^2}\left\|\boldsymbol{J}_h^{[n+1]}\right\|_{0,\Omega} - \frac{\Gamma_m\tau}{\mu_0\omega_{pm}^2}\left\|\boldsymbol{K}_h^{[n+\frac{1}{2}]}\right\|_{0,\Omega}^2 .
\end{aligned}
\tag{3.26}
$$

Summing (3.26) from $n = 0$ to $m - 1$ (for any $m \geq 1$), we obtain

$$
\begin{aligned}
F^m_{\Omega_h} = F^0_{\Omega_h} &- \sum_{T_i} \sum_{k \in \nu_i} \frac{\tau}{4} \int_{a_{ik} \in F^{int}_h} \boldsymbol{H}_i^{m+\frac{1}{2}} \cdot \mathbf{n}_{ik} \times \boldsymbol{E}_k^m \\
&+ \sum_{T_i} \sum_{k \in \nu_i} \frac{\tau}{4} \int_{a_{ik} \in F^{int}_h} \boldsymbol{E}_i^0 \cdot \mathbf{n}_{ik} \times \boldsymbol{H}_k^{\frac{1}{2}} \\
&- \sum_{j=0}^{m} \sum_{f_i \in F^{int}_h} \frac{\tau}{2} \int_{\mathrm{f}_i} (\mathbf{n}_{ik} \times [\boldsymbol{H}_i^{[j]}]) \cdot (\mathbf{n}_{ik} \times [\boldsymbol{H}_i^{[j]}]) \\
&- \sum_{j=0}^{m} \sum_{f_i \in F^{int}_h} \frac{\tau}{2} \int_{\mathrm{f}_i} (\mathbf{n}_{ik} \times [\boldsymbol{E}_i^{j-\frac{1}{2}}]) \cdot (\mathbf{n}_{ik} \times [\boldsymbol{E}_i^{j-\frac{1}{2}}]) \\
&- \sum_{j=0}^{m} \sum_{a_{ik} \in \partial\Omega^m_h} \tau \int_{a_{ik}} (\mathbf{n}_{ik} \times [\boldsymbol{E}_i^{j-\frac{1}{2}}]) \cdot (\mathbf{n}_{ik} \times [\boldsymbol{E}_i^{j-\frac{1}{2}}]) \\
&- \sum_{j=0}^{m} \frac{\Gamma_e \tau}{\epsilon_0 \omega_{pe}^2} \left\| \boldsymbol{J}_i^{[j]} \right\|^2_{0,\Omega} - \sum_{j=0}^{m} \frac{\Gamma_m \tau}{\mu_0 \omega_{pm}^2} \left\| \boldsymbol{K}_i^{[j-\frac{1}{2}]} \right\|^2_{0,\Omega},
\end{aligned} \tag{3.27}
$$

which leads to

$$
F^m_{\Omega_h} \leq F^0_{\Omega_h} - \sum_{T_i} \sum_{k \in \nu_i} \frac{\tau}{4} \int_{a_{ik} \in F^{int}_h} \boldsymbol{H}_i^{m+\frac{1}{2}} \cdot \mathbf{n}_{ik} \times \boldsymbol{E}_k^m + \sum_{T_i} \sum_{k \in \nu_i} \frac{\tau}{4} \int_{a_{ik} \in F^{int}_h} \boldsymbol{E}_i^0 \cdot \mathbf{n}_{ik} \times \boldsymbol{H}_k^{\frac{1}{2}}.
$$

Recalling the definition of $F^m_{\Omega_h}$, we obtain

$$
\begin{aligned}
F^m_{\Omega_h} \equiv & \frac{1}{2}\epsilon_0 \left\|\boldsymbol{E}^m\right\|^2_{0,\Omega} + \frac{1}{2}\mu_0 \left\|\boldsymbol{H}^{m+\frac{1}{2}}\right\|^2_{0,\Omega} + \frac{1}{2\epsilon_0\omega_{pe}^2}\left\|\boldsymbol{J}^{m+\frac{1}{2}}\right\|^2_{0,\Omega} \\
& + \frac{1}{2\mu_0\omega_{pm}^2}\left\|\boldsymbol{K}^m\right\|^2_{0,\Omega} + \frac{\tau}{2}\int_{\Omega_h} \boldsymbol{E}^m \cdot \nabla \times \boldsymbol{H}^{m+\frac{1}{2}} - \frac{\tau}{4}\sum_{T_i}\int_{\partial T_i} \boldsymbol{E}_i^m \cdot \mathbf{n}_i \times \boldsymbol{H}_i^{m+\frac{1}{2}} \\
& + \frac{\tau}{2}\int_{\Omega_h} \boldsymbol{H}^{m+\frac{1}{2}} \cdot \boldsymbol{K}^m - \frac{\tau}{2}\int_{\Omega_h} \boldsymbol{J}^{m+\frac{1}{2}} \cdot \boldsymbol{E}^m + \sum_{a_{ik}\in\partial\Omega_h^m}\frac{\tau}{4}\int_{a_{ik}} \boldsymbol{E}_i^m \cdot \mathbf{n}_{ik} \times \boldsymbol{H}_i^{m+\frac{1}{2}} \\
\leq & F^0_{\Omega_h} - \sum_{T_i}\sum_{k\in\nu_i}\frac{\tau}{4}\int_{a_{ik}\in F_h^{int}} \boldsymbol{H}_i^{m+\frac{1}{2}} \cdot \mathbf{n}_{ik} \times \boldsymbol{E}_k^m + \sum_{T_i}\sum_{k\in\nu_i}\frac{\tau}{4}\int_{a_{ik}\in F_h^{int}} \boldsymbol{E}_i^0 \cdot \mathbf{n}_{ik} \times \boldsymbol{H}_k^{\frac{1}{2}} \\
\equiv & \frac{1}{2}\epsilon_0 \left\|\boldsymbol{E}^0\right\|^2_{0,\Omega} + \frac{1}{2}\mu_0 \left\|\boldsymbol{H}^{\frac{1}{2}}\right\|^2_{0,\Omega} + \frac{1}{2\epsilon_0\omega_{pe}^2}\left\|\boldsymbol{J}^{\frac{1}{2}}\right\|^2_{0,\Omega} \\
& + \frac{1}{2\mu_0\omega_{pm}^2}\left\|\boldsymbol{K}^0\right\|^2_{0,\Omega} + \frac{\tau}{2}\int_{\Omega_h} \boldsymbol{E}^0 \cdot \nabla \times \boldsymbol{H}^{\frac{1}{2}} - \frac{\tau}{4}\sum_{T_i}\int_{\partial T_i} \boldsymbol{E}_i^0 \cdot \mathbf{n}_i \times \boldsymbol{H}_i^{\frac{1}{2}} \\
& + \frac{\tau}{2}\int_{\Omega_h} \boldsymbol{H}^{\frac{1}{2}} \cdot \boldsymbol{K}^0 - \frac{\tau}{2}\int_{\Omega_h} \boldsymbol{J}^{\frac{1}{2}} \cdot \boldsymbol{E}^0 + \sum_{a_{ik}\in\partial\Omega_h^m}\frac{\tau}{4}\int_{a_{ik}} \boldsymbol{E}_i^0 \cdot \mathbf{n}_{ik} \times \boldsymbol{H}_i^{\frac{1}{2}} \\
& - \sum_{T_i}\sum_{k\in\nu_i}\frac{\tau}{4}\int_{a_{ik}\in F_h^{int}} \boldsymbol{H}_i^{m+\frac{1}{2}} \cdot \mathbf{n}_{ik} \times \boldsymbol{E}_k^m + \sum_{T_i}\sum_{k\in\nu_i}\frac{\tau}{4}\int_{a_{ik}\in F_h^{int}} \boldsymbol{E}_i^0 \cdot \mathbf{n}_{ik} \times \boldsymbol{H}_k^{\frac{1}{2}}. \quad (3.28)
\end{aligned}
$$

Simplifying the above equation, we obtain

$$
\begin{aligned}
& \frac{1}{2}\epsilon_0 \left\|\boldsymbol{E}^m\right\|^2_{0,\Omega} + \frac{1}{2}\mu_0 \left\|\boldsymbol{H}^{m+\frac{1}{2}}\right\|^2_{0,\Omega} + \frac{1}{2\epsilon_0\omega_{pe}^2}\left\|\boldsymbol{J}^{m+\frac{1}{2}}\right\|^2_{0,\Omega} + \frac{1}{2\mu_0\omega_{pm}^2}\left\|\boldsymbol{K}^m\right\|^2_{0,\Omega} \\
& \leq \frac{1}{2}\epsilon_0 \left\|\boldsymbol{E}^0\right\|^2_{0,\Omega} + \frac{1}{2}\mu_0 \left\|\boldsymbol{H}^{\frac{1}{2}}\right\|^2_{0,\Omega} + \frac{1}{2\epsilon_0\omega_{pe}^2}\left\|\boldsymbol{J}^{\frac{1}{2}}\right\|^2_{0,\Omega} + \frac{1}{2\mu_0\omega_{pm}^2}\left\|\boldsymbol{K}^0\right\|^2_{0,\Omega} \\
& - \frac{\tau}{2}\int_{\Omega_h} \boldsymbol{E}^m \cdot \nabla \times \boldsymbol{H}^{m+\frac{1}{2}} + \frac{\tau}{4}\sum_{T_i}\int_{\partial T_i} \boldsymbol{E}_i^m \cdot \mathbf{n}_i \times \boldsymbol{H}_i^{m+\frac{1}{2}} \\
& - \frac{\tau}{2}\int_{\Omega_h} \boldsymbol{H}^{m+\frac{1}{2}} \cdot \boldsymbol{K}^m + \frac{\tau}{2}\int_{\Omega_h} \boldsymbol{J}^{m+\frac{1}{2}} \cdot \boldsymbol{E}^m - \sum_{a_{ik}\in\partial\Omega_h^m}\frac{\tau}{4}\int_{a_{ik}} \boldsymbol{E}_i^m \cdot \mathbf{n}_{ik} \times \boldsymbol{H}_i^{m+\frac{1}{2}} \\
& + \frac{\tau}{2}\int_{\Omega_h} \boldsymbol{E}^0 \cdot \nabla \times \boldsymbol{H}^{\frac{1}{2}} - \frac{\tau}{4}\sum_{T_i}\int_{\partial T_i} \boldsymbol{E}_i^0 \cdot \mathbf{n}_i \times \boldsymbol{H}_i^{\frac{1}{2}} \\
& + \frac{\tau}{2}\int_{\Omega_h} \boldsymbol{H}^{\frac{1}{2}} \cdot \boldsymbol{K}^0 - \frac{\tau}{2}\int_{\Omega_h} \boldsymbol{J}^{\frac{1}{2}} \cdot \boldsymbol{E}^0 + \sum_{a_{ik}\in\partial\Omega_h^m}\frac{\tau}{4}\int_{a_{ik}} \boldsymbol{E}_i^0 \cdot \mathbf{n}_{ik} \times \boldsymbol{H}_i^{\frac{1}{2}} \\
& - \sum_{T_i}\sum_{k\in\nu_i}\frac{\tau}{4}\int_{a_{ik}\in F_h^{int}} \boldsymbol{H}_i^{m+\frac{1}{2}} \cdot \mathbf{n}_{ik} \times \boldsymbol{E}_k^m + \sum_{T_i}\sum_{k\in\nu_i}\frac{\tau}{4}\int_{a_{ik}\in F_h^{int}} \boldsymbol{E}_i^0 \cdot \mathbf{n}_{ik} \times \boldsymbol{H}_k^{\frac{1}{2}}. \quad (3.29)
\end{aligned}
$$

By the standard inverse estimates (3.15), we have

$$\left|\frac{\tau}{2}\int_{\Omega_h}\boldsymbol{E}^m\cdot\nabla\times\boldsymbol{H}^{m+\frac{1}{2}}\right| \le \frac{C_{inv}\tau h^{-1}}{4\sqrt{\epsilon_0\mu_0}}(\epsilon_0\left\|\boldsymbol{E}^m\right\|_{0,\Omega}^2+\mu_0\left\|\boldsymbol{H}^{m+\frac{1}{2}}\right\|_{0,\Omega}^2),$$

$$\left|\frac{\tau}{4}\sum_{T_i}\int_{\partial T_i}\boldsymbol{E}_i^m\cdot\mathbf{n}_i\times\boldsymbol{H}_i^{m+\frac{1}{2}}\right| \le \frac{C_{inv}^2\tau h^{-1}}{8\sqrt{\epsilon_0\mu_0}}(\epsilon_0\left\|\boldsymbol{E}^m\right|_{0,\Omega}^2+\mu_0\left\|\boldsymbol{H}^{m+\frac{1}{2}}\right\|_{0,\Omega}^2),$$

$$\left|\frac{\tau}{2}\int_{\Omega_h}\boldsymbol{H}^{m+\frac{1}{2}}\cdot\boldsymbol{K}^m\right| \le \frac{\omega_{pm}\tau}{4}(\mu_0\left\|\boldsymbol{H}^{m+\frac{1}{2}}\right\|_{0,\Omega}^2+\frac{1}{\mu_0\omega_{pm}^2}\left\|\boldsymbol{K}^m\right|_{0,\Omega}^2),$$

$$\left|\frac{\tau}{2}\int_{\Omega_h}\boldsymbol{J}^{m+\frac{1}{2}}\cdot\boldsymbol{E}^m\right| \le \frac{\omega_{pe}\tau}{4}(\epsilon_0\left\|\boldsymbol{E}^m\right\|_{0,\Omega}^2+\frac{1}{\epsilon_0\omega_{pe}^2}\left\|\boldsymbol{J}^{m+\frac{1}{2}}\right|_{0,\Omega}^2),$$

$$\left|\sum_{a_{ik}\in\partial\Omega_h^m}\frac{\tau}{4}\int_{a_{ik}}\boldsymbol{E}_i^m\cdot\mathbf{n}_{ik}\times\boldsymbol{H}_i^{m+\frac{1}{2}}\right| \le \frac{C_{inv}^2\tau h^{-1}}{8\sqrt{\epsilon_0\mu_0}}(\epsilon_0\left\|\boldsymbol{E}^m\right\|_{0,\Omega}^2+\mu_0\left\|\boldsymbol{H}^{m+\frac{1}{2}}\right\|_{0,\Omega}^2),$$

$$\left|\sum_{T_i}\sum_{k\in\nu_i}\frac{\tau}{4}\int_{a_{ik}\in F_h^{int}}\boldsymbol{H}_i^{m+\frac{1}{2}}\cdot\mathbf{n}_{ik}\times\boldsymbol{E}_k^m\right| \le \frac{C_{inv}^2\tau h^{-1}}{8\sqrt{\epsilon_0\mu_0}}(\epsilon_0\left\|\boldsymbol{E}^m\right\|_{0,\Omega}^2+\mu_0\left\|\boldsymbol{H}^{m+\frac{1}{2}}\right\|_{0,\Omega}^2).$$

By choosing the time step τ small enough so that the right hand side terms can be controlled by the corresponding terms on the left hand side of (3.29), we can obtain a stability result. An exemplary choice is

$$\tau \le \min\{\frac{1}{8},\frac{h}{5C_{inv}^2C_v},\frac{h}{5C_{inv}C_v},\frac{1}{2\omega_{pm}},\frac{1}{2\omega_{pe}}\},$$

and substituting all above estimates into (3.29), we have

$$\begin{aligned}&\epsilon_0\left\|\boldsymbol{E}^n\right\|_{0,\Omega}^2+\mu_0\left\|\boldsymbol{H}^{n+\frac{1}{2}}\right\|_{0,\Omega}^2+\frac{1}{\epsilon_0\omega_{pe}^2}\left\|\boldsymbol{J}^{n+\frac{1}{2}}\right\|_{0,\Omega}^2+\frac{1}{\mu_0\omega_{pm}^2}\left\|\boldsymbol{K}^n\right\|_{0,\Omega}^2\\ &\le C[\left\|\boldsymbol{E}^0\right\|_{0,\Omega}^2+\left\|\boldsymbol{H}^{\frac{1}{2}}\right\|_{0,\Omega}^2+\left\|\boldsymbol{J}^{\frac{1}{2}}\right\|_{0,\Omega}^2+\left\|\boldsymbol{K}^0\right\|_{0,\Omega}^2],\end{aligned}$$

where the physical parameters $\epsilon_0,\mu_0,\omega_{pe},\omega_{pm},\Gamma_e$ and Γ_m have been absorbed into the generic constant C. □

3.2.2 THE ERROR ESTIMATE

Before we prove the error estimate, we need the following two lemmas.

Lemma 3.2.1. *[43, Lemma 5.1] Denote $u^j = u(.,j\tau)$. For any $u \in H^2(0,T;L^2(\Omega))$, we have*

$$(i) \quad \left\| u^j - \frac{1}{\tau}\int_{t_{j-\frac{1}{2}}}^{t_{j-\frac{1}{2}}} u(s)ds \right\|_0^2 \leq \frac{\tau^3}{4}\int_{t_{j-\frac{1}{2}}}^{t_{j-\frac{1}{2}}} \|u_{tt}(s)\|_0^2\, ds,$$

$$(ii) \quad \left\| u^{j-\frac{1}{2}} - \frac{1}{\tau}\int_{t_{j-1}}^{t_j} u(s)ds \right\|_0^2 \leq \frac{\tau^3}{4}\int_{t_{j-1}}^{t_j} \|u_{tt}(s)\|_0^2\, ds,$$

$$(iii) \quad \left\| \frac{1}{2}(u^j + u^{j+1}) - \frac{1}{\tau}\int_{t_j}^{t_{j+1}} u(s)ds \right\|_0^2 \leq \frac{\tau^3}{4}\int_{t_j}^{t_{j+1}} \|u_{tt}(s)\|_0^2\, ds,$$

$$(iv) \quad \left\| \frac{1}{2}(u^{j-\frac{1}{2}} + u^{j+\frac{1}{2}}) - \frac{1}{\tau}\int_{t_{j-\frac{1}{2}}}^{t_{j+\frac{1}{2}}} u(s)ds \right\|_0^2 \leq \frac{\tau^3}{4}\int_{t_{j-\frac{1}{2}}}^{t_{j+\frac{1}{2}}} \|u_{tt}(s)\|_0^2\, ds.$$

Let P_h denote the standard L^2-projection onto V_h or V_h^0, which is the subspace of V_h with the boundary condition $\boldsymbol{n} \times \boldsymbol{E} = 0$ imposed. It is known that the projection error estimate

$$\|u - P_h u\|_{0,T} \leq C h_T^{min\{s,k\}+1} \|u\|_{s+1,T}\,, \tag{3.30}$$

holds true for any element T, and $u \in H^{s+1}(T)$.

Lemma 3.2.2. *For any functions $\eta_i^{j-\frac{1}{2}}, \eta_i^{j+\frac{1}{2}}, \xi_i^j, \xi_i^{j-1} \in \mathrm{V}_h$, we have*

$$
\begin{aligned}
&-\sum_i \int_{\partial T_i} \mathbf{n}_i \times \eta_i^{j-\frac{1}{2}} \cdot (\xi_i^j + \xi_i^{j-1}) \\
&-\sum_{T_i} \sum_{k\in\nu_i} \int_{a_{ik}} (\xi_i^j + \xi_i^{j-1}) \cdot \frac{1}{2}\mathbf{n}_{ik} \times ([\eta_i^{j-\frac{1}{2}}] - \mathbf{n}_{ik} \times [\frac{\xi_i^j + \xi_i^{j-1}}{2}]) \\
&+\sum_{T_i} \sum_{k\in\nu_i} \int_{a_{ik}} (\eta_i^{j+\frac{1}{2}} + \eta_i^{j-\frac{1}{2}}) \cdot \frac{1}{2}\mathbf{n}_{ik} \times (\mathbf{n}_{ik} \times [\frac{\eta_i^{j+\frac{1}{2}} + \eta_i^{j-\frac{1}{2}}}{2}] + [\xi_i^j]) \\
=&\sum_i \int_{\partial T_i} \frac{1}{2}\mathbf{n}_i \times \xi_i^{j-1} \cdot \eta_i^{j-\frac{1}{2}} - \sum_{T_i} \sum_{k\in\nu_i} \int_{a_{ik}} \xi_i^{j-1} \cdot \frac{1}{2}\mathbf{n}_{ik} \times \eta_k^{j-\frac{1}{2}} \\
&+\sum_{T_i} \sum_{k\in\nu_i} \int_{a_{ik}} \eta_i^{j+\frac{1}{2}} \cdot \frac{1}{2}\mathbf{n}_{ik} \times \xi_k^j - \sum_{T_i} \sum_{k\in\nu_i} \int_{a_{ik}} \eta_i^{j+\frac{1}{2}} \cdot \frac{1}{2}\mathbf{n}_{ik} \times \xi_i^j \\
&+\sum_{T_i} \sum_{k\in\nu_i} \int_{a_{ik}} \frac{\xi_i^j + \xi_i^{j-1}}{2} \cdot \mathbf{n}_{ik} \times (\mathbf{n}_{ik} \times [\frac{\xi_i^j + \xi_i^{j-1}}{2}]) \\
&+\sum_{T_i} \sum_{k\in\nu_i} \int_{a_{ik}} \frac{\eta_i^{j+\frac{1}{2}} + \eta_i^{j-\frac{1}{2}}}{2} \cdot \mathbf{n}_{ik} \times (\mathbf{n}_{ik} \times [\frac{\eta_i^{j+\frac{1}{2}} + \eta_i^{j-\frac{1}{2}}}{2}]).
\end{aligned} \tag{3.31}
$$

Proof. Using the jump definition

$$
[\eta_i^{j-\frac{1}{2}}] = \eta_k^{j-\frac{1}{2}} - \eta_i^{j-\frac{1}{2}}, \quad [\xi_i^j] = \xi_k^j - \xi_i^j
$$

in the left hand-side (LHS) of (3.31), we have

$$
\begin{aligned}
LHS = &-\sum_i \int_{\partial T_i} \mathbf{n}_i \times \eta_i^{j-\frac{1}{2}} \cdot (\xi_i^j + \xi_i^{j-1}) - \sum_{T_i} \sum_{k\in\nu_i} \int_{a_{ik}} (\xi_i^j + \xi_i^{j-1}) \cdot \frac{1}{2}\mathbf{n}_{ik} \times \eta_k^{j-\frac{1}{2}} \\
&+\sum_{T_i} \sum_{k\in\nu_i} \int_{a_{ik}} (\xi_i^j + \xi_i^{j-1}) \cdot \frac{1}{2}\mathbf{n}_{ik} \times \eta_i^{j-\frac{1}{2}} \\
&+\sum_{T_i} \sum_{k\in\nu_i} \int_{a_{ik}} \frac{\xi_i^j + \xi_i^{j-1}}{2} \cdot \mathbf{n}_{ik} \times (\mathbf{n}_{ik} \times [\frac{\xi_i^j + \xi_i^{j-1}}{2}]) \\
&+\sum_{T_i} \sum_{k\in\nu_i} \int_{a_{ik}} (\eta_i^{j+\frac{1}{2}} + \eta_i^{j-\frac{1}{2}}) \cdot \frac{1}{2}\mathbf{n}_{ik} \times \xi_k^j - \sum_{T_i} \sum_{k\in\nu_i} \int_{a_{ik}} (\eta_i^{j+\frac{1}{2}} + \eta_i^{j-\frac{1}{2}}) \cdot \frac{1}{2}\mathbf{n}_{ik} \times \xi_i^j \\
&+\sum_{T_i} \sum_{k\in\nu_i} \int_{a_{ik}} \frac{\eta_i^{j+\frac{1}{2}} + \eta_i^{j-\frac{1}{2}}}{2} \cdot \mathbf{n}_{ik} \times (\mathbf{n}_{ik} \times [\frac{\eta_i^{j+\frac{1}{2}} + \eta_i^{j-\frac{1}{2}}}{2}])
\end{aligned}
$$

$$
\begin{aligned}
&= \sum_i \int_{\partial T_i} \frac{1}{2}\mathbf{n}_i \times \xi_i^{j-1} \cdot \eta_i^{j-\frac{1}{2}} - \sum_{T_i}\sum_{k\in\nu_i}\int_{a_{ik}} \xi_i^j \cdot \frac{1}{2}\mathbf{n}_{ik} \times \eta_k^{j-\frac{1}{2}} \\
&\quad - \sum_{T_i}\sum_{k\in\nu_i}\int_{a_{ik}} \xi_i^{j-1} \cdot \frac{1}{2}\mathbf{n}_{ik} \times \eta_k^{j-\frac{1}{2}} + \sum_{T_i}\sum_{k\in\nu_i}\int_{a_{ik}} \eta_i^{j+\frac{1}{2}} \cdot \frac{1}{2}\mathbf{n}_{ik} \times \xi_k^{j} \\
&\quad + \sum_{T_i}\sum_{k\in\nu_i}\int_{a_{ik}} \eta_i^{j-\frac{1}{2}} \cdot \frac{1}{2}\mathbf{n}_{ik} \times \xi_k^{j} - \sum_{T_i}\sum_{k\in\nu_i}\int_{a_{ik}} \eta_i^{j+\frac{1}{2}} \cdot \frac{1}{2}\mathbf{n}_{ik} \times \xi_i^{j} \\
&\quad + \sum_{T_i}\sum_{k\in\nu_i}\int_{a_{ik}} \frac{\xi_i^j + \xi_i^{j-1}}{2} \cdot \mathbf{n}_{ik} \times (\mathbf{n}_{ik} \times [\frac{\xi_i^j + \xi_i^{j-1}}{2}]) \\
&\quad + \sum_{T_i}\sum_{k\in\nu_i}\int_{a_{ik}} \frac{\eta_i^{j+\frac{1}{2}} + \eta_i^{j-\frac{1}{2}}}{2} \cdot \mathbf{n}_{ik} \times (\mathbf{n}_{ik} \times [\frac{\eta_i^{j+\frac{1}{2}} + \eta_i^{j-\frac{1}{2}}}{2}]) \\
&= \sum_i \int_{\partial T_i} \frac{1}{2}\mathbf{n}_i \times \xi_i^{j-1} \cdot \eta_i^{j-\frac{1}{2}} - \sum_{T_i}\sum_{k\in\nu_i}\int_{a_{ik}} \xi_i^{j-1} \cdot \frac{1}{2}\mathbf{n}_{ik} \times \eta_k^{j-\frac{1}{2}} \\
&\quad + \sum_{T_i}\sum_{k\in\nu_i}\int_{a_{ik}} \eta_i^{j+\frac{1}{2}} \cdot \frac{1}{2}\mathbf{n}_{ik} \times \xi_k^{j} - \sum_{T_i}\sum_{k\in\nu_i}\int_{a_{ik}} \eta_i^{j+\frac{1}{2}} \cdot \frac{1}{2}\mathbf{n}_{ik} \times \xi_i^{j} \\
&\quad + \sum_{T_i}\sum_{k\in\nu_i}\int_{a_{ik}} \frac{\xi_i^j + \xi_i^{j-1}}{2} \cdot \mathbf{n}_{ik} \times (\mathbf{n}_{ik} \times [\frac{\xi_i^j + \xi_i^{j-1}}{2}]) \\
&\quad + \sum_{T_i}\sum_{k\in\nu_i}\int_{a_{ik}} \frac{\eta_i^{j+\frac{1}{2}} + \eta_i^{j-\frac{1}{2}}}{2} \cdot \mathbf{n}_{ik} \times (\mathbf{n}_{ik} \times [\frac{\eta_i^{j+\frac{1}{2}} + \eta_i^{j-\frac{1}{2}}}{2}]),
\end{aligned}
$$

which concludes the proof. □

Theorem 3.2.2. *Under the assumptions that the time step τ satisfies a CFL condition such as:*

$$
\tau = \min\left\{\frac{1}{8}, \frac{1}{2\omega_{pe}}, \frac{1}{2\omega_{pm}}, \frac{1}{10\Gamma_e}, \frac{1}{10\Gamma_m}, \frac{h}{5C_{inv}C_v}, \frac{h}{5C_{inv}^2 C_v}\right\}, \tag{3.32}
$$

and that the solution of (3.1)-(3.4) has the following regularity:

$$
\begin{aligned}
&\boldsymbol{E}_{tt}, \boldsymbol{H}_{tt}, \boldsymbol{J}_{tt}, \boldsymbol{K}_{tt}, \nabla\times\boldsymbol{E}_{tt}, \nabla\times\boldsymbol{H}_{tt} \in L^2(0,T;L^2(\Omega)^3), \\
&\boldsymbol{E}, \boldsymbol{H} \in L^\infty(0,T;H^{s+1}(\Omega)^3), \quad \forall\ s \geq 0,
\end{aligned}
$$

we have the following error estimate

$$
\begin{aligned}
&\max_{1\leq n}(||\boldsymbol{E}^n - \boldsymbol{E}_h^n||_0 + ||\boldsymbol{H}^{n+\frac{1}{2}} - \boldsymbol{H}_h^{n+\frac{1}{2}}||_0 + ||\boldsymbol{J}^{n+\frac{1}{2}} - \boldsymbol{J}_h^{n+\frac{1}{2}}||_0 + ||\boldsymbol{K}^n - \boldsymbol{K}_h^n||_0) \\
\leq\ & C(\tau^2 + Th^{min\{s,k\}}) + C\Big(||\boldsymbol{E}^0 - \boldsymbol{E}_h^0||_0 + ||\boldsymbol{H}^{\frac{1}{2}} - \boldsymbol{H}_h^{\frac{1}{2}}||_0 + ||\boldsymbol{J}^{\frac{1}{2}} - \boldsymbol{J}_h^{\frac{1}{2}}||_0 + ||\boldsymbol{K}^0 - \boldsymbol{K}_h^0||_0\Big),
\end{aligned}
$$

where k is the degree of the basis function in the finite element space (3.7), and the constant

$$C = C(\epsilon_0, \mu_0, \omega_{pe}, \omega_{pm}, \Gamma_e, \Gamma_m, \boldsymbol{E}, \boldsymbol{H}, \boldsymbol{J}, \boldsymbol{K})$$

is independent of both the time step τ and the mesh size h.

Remark 3.2.1. *When the initial approximations are accurate enough, such as*

$$||\boldsymbol{E}^0 - \boldsymbol{E}_h^0||_0 + ||\boldsymbol{H}^{\frac{1}{2}} - \boldsymbol{H}_h^{\frac{1}{2}}||_0 + ||\boldsymbol{J}^{\frac{1}{2}} - \boldsymbol{J}_h^{\frac{1}{2}}||_0 + ||\boldsymbol{K}^0 - \boldsymbol{K}_h^0||_0 \leq C(\tau^2 + h^{min\{s,k\}}),$$

then the error estimate of Theorem 3.2.2 becomes

$$\begin{aligned} & \max_{1\leq n}(||\boldsymbol{E}^n - \boldsymbol{E}_h^n||_0 + ||\boldsymbol{H}^{n+\frac{1}{2}} - \boldsymbol{H}_h^{n+\frac{1}{2}}||_0 + ||\boldsymbol{J}^{n+\frac{1}{2}} - \boldsymbol{J}_h^{n+\frac{1}{2}}||_0 + ||\boldsymbol{K}^n - \boldsymbol{K}_h^n||_0) \\ \leq \;& C(\tau^2 + Th^{min\{s,k\}}), \end{aligned}$$

which shows that the error grows linearly with time.

3.2.3 PROOF OF THEOREM 3.2.2

Integrating the governing equations (3.1) and (3.4) from t_{j-1} to t_j, and (3.2) and (3.3) from $t_{j-\frac{1}{2}}$ to $t_{j+\frac{1}{2}}$, then multiplying the respective resultants by $\frac{\boldsymbol{u}_h}{\tau}, \frac{\boldsymbol{v}_h}{\tau}, \frac{\boldsymbol{\phi}_h}{\tau}, \frac{\boldsymbol{\psi}_h}{\tau}$ and integrating over Ω, we obtain

$$\epsilon_0(\frac{\boldsymbol{E}^j - \boldsymbol{E}^{j-1}}{\tau}, \boldsymbol{u}_h) - (\frac{1}{\tau}\int_{t_{j-1}}^{t_j} \nabla \times \boldsymbol{H}(s)ds, \boldsymbol{u}_h) + (\frac{1}{\tau}\int_{t_{j-1}}^{t_j} \boldsymbol{J}(s)ds, \boldsymbol{u}_h) = 0, \tag{3.33}$$

$$\mu_0(\frac{\boldsymbol{H}^{j+\frac{1}{2}} - \boldsymbol{H}^{j-\frac{1}{2}}}{\tau}, \boldsymbol{v}_h) + (\frac{1}{\tau}\int_{t_{j-\frac{1}{2}}}^{t_{j+\frac{1}{2}}} \nabla \times \boldsymbol{E}(s)ds, \boldsymbol{v}_h) + (\frac{1}{\tau}\int_{t_{j-\frac{1}{2}}}^{t_{j+\frac{1}{2}}} \boldsymbol{K}(s)ds, \boldsymbol{v}_h) = 0, \tag{3.34}$$

$$\frac{1}{\epsilon_0\omega_{pe}^2}(\frac{\boldsymbol{J}^{j+\frac{1}{2}} - \boldsymbol{J}^{j-\frac{1}{2}}}{\tau}, \boldsymbol{\phi}_h) + \frac{\Gamma_e}{\epsilon_0\omega_{pe}^2}(\frac{1}{\tau}\int_{t_{j-\frac{1}{2}}}^{t_{j+\frac{1}{2}}} \boldsymbol{J}(s)ds, \boldsymbol{\phi}_h) = (\frac{1}{\tau}\int_{t_{j-\frac{1}{2}}}^{t_{j+\frac{1}{2}}} \boldsymbol{E}(s)ds, \boldsymbol{\phi}_h), \tag{3.35}$$

$$\frac{1}{\mu_0\omega_{pm}^2}(\frac{\boldsymbol{K}^j - \boldsymbol{K}^{j-1}}{\tau}, \boldsymbol{\psi}_h) + \frac{\Gamma_m}{\mu_0\omega_{pm}^2}(\frac{1}{\tau}\int_{t_{j-1}}^{t_j} \boldsymbol{K}(s)ds, \boldsymbol{\psi}_h) = (\frac{1}{\tau}\int_{t_{j-1}}^{t_j} \boldsymbol{H}(s)ds, \boldsymbol{\psi}_h). \tag{3.36}$$

Summing all elements together for (3.8)-(3.11) with $n = j-1$, we have

$$(\epsilon_0 \frac{\boldsymbol{E}_h^j - \boldsymbol{E}_h^{j-1}}{\tau}, \boldsymbol{u}_h) - (\nabla \times \boldsymbol{H}_h^{j-\frac{1}{2}}, \boldsymbol{u}_h) + (\boldsymbol{J}_h^{j-\frac{1}{2}}, \boldsymbol{u}_h) - \sum_{T_i} \sum_{k \in \nu_i} \int_{a_{ik}} \boldsymbol{u}_i \cdot \frac{1}{2} \mathbf{n}_{ik} \times ([\boldsymbol{H}_i^{j-\frac{1}{2}}] - \mathbf{n}_{ik} \times [\boldsymbol{E}_i^{[j-\frac{1}{2}]}]) = 0, \tag{3.37}$$

$$(\mu_0 \frac{\boldsymbol{H}_h^{j+\frac{1}{2}} - \boldsymbol{H}_h^{j-\frac{1}{2}}}{\tau}, \boldsymbol{v}_h) + (\nabla \times \boldsymbol{E}_h^j, \boldsymbol{v}_h) + (\boldsymbol{K}_h^j, \boldsymbol{v}_h) + \sum_{T_i} \sum_{k \in \nu_i} \int_{a_{ik}} \boldsymbol{v}_i \cdot \frac{1}{2} \mathbf{n}_{ik} \times (\mathbf{n}_{ik} \times [\boldsymbol{H}_i^{[j]}] + [\boldsymbol{E}_i^j]) = 0, \tag{3.38}$$

$$\frac{1}{\epsilon_0 \omega_{pe}^2} (\frac{\boldsymbol{J}_h^{j+\frac{1}{2}} - \boldsymbol{J}_h^{j-\frac{1}{2}}}{\tau}, \boldsymbol{\phi}_h) + \frac{\Gamma_e}{\epsilon_0 \omega_{pe}^2} (\frac{\boldsymbol{J}_h^{j+\frac{1}{2}} + \boldsymbol{J}_h^{j-\frac{1}{2}}}{2}, \boldsymbol{\phi}_h) = (\boldsymbol{E}_h^j, \boldsymbol{\phi}_h), \tag{3.39}$$

$$\frac{1}{\mu_0 \omega_{pm}^2} (\frac{\boldsymbol{K}_h^j - \boldsymbol{K}_h^{j-1}}{\tau}, \boldsymbol{\psi}_h) + \frac{\Gamma_m}{\mu_0 \omega_{pm}^2} (\frac{\boldsymbol{K}_h^j + \boldsymbol{K}_h^{j-1}}{2}, \boldsymbol{\psi}_h) = (\boldsymbol{H}_h^{j-\frac{1}{2}}, \boldsymbol{\psi}_h). \tag{3.40}$$

Denote $\xi_h^j = P_h \boldsymbol{E}^j - \boldsymbol{E}_h^j, \eta_h^j = P_h \boldsymbol{H}^j - \boldsymbol{H}_h^j, \tilde{\xi}_h^j = P_h \boldsymbol{J}^j - \boldsymbol{J}_h^j, \tilde{\eta}_h^j = P_h \boldsymbol{K}^j - \boldsymbol{K}_h^j$, and the backward operator $\delta_\tau u^j = (u^j - u^{j-1})/\tau$.

Subtracting (3.37)-(3.40) from (3.33)-(3.36) with the corresponding flux terms added, and using the identity

$$(\nabla \times \eta_h^{j-\frac{1}{2}}, \boldsymbol{u}_h) = (\eta_h^{j-\frac{1}{2}}, \nabla \times \boldsymbol{u}_h) + \sum_i \int_{\partial T_i} \mathbf{n}_i \times \eta_i^{j-\frac{1}{2}} \cdot \boldsymbol{u}_i,$$

we can obtain the following error equations:

$$
\begin{aligned}
(i)\quad & \epsilon_0(\frac{\xi_h^j-\xi_h^{j-1}}{\tau},\boldsymbol{u}_h)-(\eta_h^{j-\frac{1}{2}},\nabla\times\boldsymbol{u}_h)-\sum_i\int_{\partial T_i}\mathbf{n}_i\times\eta_i^{j-\frac{1}{2}}\cdot\boldsymbol{u}_i\\
&-\sum_{T_i}\sum_{k\in\nu_i}\int_{a_{ik}}u_i\cdot\frac{1}{2}\mathbf{n}_{ik}\times([\eta_i^{j-\frac{1}{2}}]-\mathbf{n}_{ik}\times[\frac{\xi_h^j+\xi_h^{j-1}}{2}])\\
&=\epsilon_0(\delta_t(P_h\boldsymbol{E}^j-\boldsymbol{E}^j),\boldsymbol{u}_h)-(\nabla\times(P_h\boldsymbol{H}^{j-\frac{1}{2}}-\frac{1}{\tau}\int_{t_{j-1}}^{t_j}\boldsymbol{H}(s)ds),\boldsymbol{u}_h)\\
&+(-\tilde{\xi}_h^{j-\frac{1}{2}}+P_h\boldsymbol{J}^{j-\frac{1}{2}}-\frac{1}{\tau}\int_{t_{j-1}}^{t_j}\boldsymbol{J}(s)ds,\boldsymbol{u}_h)\\
&-\sum_{T_i}\sum_{k\in\nu_i}\int_{a_{ik}}u_i\cdot\frac{1}{2}\mathbf{n}_{ik}\times([P_h\boldsymbol{H}^{j-\frac{1}{2}}-\boldsymbol{H}^{j-\frac{1}{2}}]-\mathbf{n}_{ik}\times[\frac{P_h\boldsymbol{E}^j-\boldsymbol{E}^j+P_h\boldsymbol{E}^{j-1}-\boldsymbol{E}^{j-1}}{2}]),
\end{aligned}
\tag{3.41}
$$

$$
\begin{aligned}
(ii)\quad & \mu_0(\frac{\eta_h^{j+\frac{1}{2}}-\eta_h^{j-\frac{1}{2}}}{\tau},\boldsymbol{v}_h)+(\nabla\times\xi_h^j,\boldsymbol{v}_h)\\
&+\sum_{T_i}\sum_{k\in\nu_i}\int_{a_{ik}}v_i\cdot\frac{1}{2}\mathbf{n}_{ik}\times(\mathbf{n}_{ik}\times[\frac{\eta_i^{j+\frac{1}{2}}+\eta_i^{j-\frac{1}{2}}}{2}]+[\xi_i^j])\\
&=\mu_0(\delta_t(P_h\boldsymbol{H}^{j+\frac{1}{2}}-\boldsymbol{H}^{j+\frac{1}{2}}),\boldsymbol{v}_h)+(\nabla\times(P_h\boldsymbol{E}^j-\frac{1}{\tau}\int_{t_{j-\frac{1}{2}}}^{t_{j+\frac{1}{2}}}\boldsymbol{E}(s)ds,\boldsymbol{v}_h)\\
&+(-\tilde{\eta}_h^j+P_h\boldsymbol{K}^j-\frac{1}{\tau}\int_{t_{j-\frac{1}{2}}}^{t_{j+\frac{1}{2}}}\boldsymbol{K}(s)ds,\boldsymbol{v}_h)\\
&+\sum_{T_i}\sum_{k\in\nu_i}\int_{a_{ik}}v_i\cdot\frac{1}{2}\mathbf{n}_{ik}\times(\mathbf{n}_{ik}\times[\frac{P_h\boldsymbol{H}^{j+\frac{1}{2}}-\boldsymbol{H}^{j+\frac{1}{2}}+P_h\boldsymbol{H}^{j-\frac{1}{2}}-\boldsymbol{H}^{j-\frac{1}{2}}}{2}]+[P_h\boldsymbol{E}^j-\boldsymbol{E}^j]),
\end{aligned}
\tag{3.42}
$$

$$
\begin{aligned}
(iii)\quad & \frac{1}{\epsilon_0\omega_{pe}^2}(\frac{\tilde{\xi}_h^{j+\frac{1}{2}}-\tilde{\xi}_h^{j-\frac{1}{2}}}{\tau},\boldsymbol{\phi}_h)+\frac{\Gamma_e}{\epsilon_0\omega_{pe}^2}(\frac{\tilde{\xi}_h^{j+\frac{1}{2}}+\tilde{\xi}_h^{j-\frac{1}{2}}}{2},\boldsymbol{\phi}_h)=\frac{1}{\epsilon_0\omega_{pe}^2}(\delta_\tau(P_h\boldsymbol{J}^{j+\frac{1}{2}}-\boldsymbol{J}^{j-\frac{1}{2}}),\boldsymbol{\phi}_h)\\
&+\frac{\Gamma_e}{\epsilon_0\omega_{pe}^2}(\frac{P_h\boldsymbol{J}^{j+\frac{1}{2}}+P_h\boldsymbol{J}^{j-\frac{1}{2}}}{2}-\frac{1}{\tau}\int_{t_{j-\frac{1}{2}}}^{t_{j+\frac{1}{2}}}\boldsymbol{J}(s)ds,\boldsymbol{\phi}_h)\\
&+(\frac{1}{\tau}\int_{t_{j-\frac{1}{2}}}^{t_{j+\frac{1}{2}}}\boldsymbol{E}(s)ds-P_h\boldsymbol{E}^j+\xi_h^j,\boldsymbol{\phi}_h),
\end{aligned}
\tag{3.43}
$$

$$(iv)\quad \frac{1}{\mu_0\omega_{pm}^2}(\frac{\tilde{\eta}_h^j-\tilde{\eta}_h^{j-1}}{\tau},\boldsymbol{\psi}_h)+\frac{\Gamma_m}{\mu_0\omega_{pm}^2}(\frac{\tilde{\eta}_h^j+\tilde{\eta}_h^{j-1}}{2},\boldsymbol{\psi}_h)=\frac{1}{\mu_0\omega_{pm}^2}(\delta_\tau(P_h\boldsymbol{K}^j-\boldsymbol{K}^j),\boldsymbol{\psi}_h)$$
$$+\frac{\Gamma_m}{\mu_0\omega_{pm}^2}(\frac{P_h\boldsymbol{K}^j+P_h\boldsymbol{K}^{j+1}}{2}-\frac{1}{\tau}\int_{t_{j-1}}^{t_j}\boldsymbol{K}(s)ds,\boldsymbol{\psi}_h)$$
$$+(\frac{1}{\tau}\int_{t_{j-1}}^{t_j}\boldsymbol{H}(s)ds-P_h\boldsymbol{H}^{j-\frac{1}{2}}+\eta_h^{j-\frac{1}{2}},\boldsymbol{\psi}_h). \tag{3.44}$$

Choosing $\boldsymbol{u}_h=\tau(\xi_h^j+\xi_h^{j-1}),\boldsymbol{v}_h=\tau(\eta_h^{j+\frac{1}{2}}+\eta_h^{j-\frac{1}{2}})$, $\boldsymbol{\phi}_h=\tau(\tilde{\xi}_h^{j+\frac{1}{2}}+\tilde{\xi}_h^{j-\frac{1}{2}})$, $\boldsymbol{\psi}_h=\tau(\tilde{\eta}_h^j+\tilde{\eta}_h^{j-1})$ in (3.41)-(3.44), respectively, then summing up the resultants from $j=1$ to $j=n$, dropping those zero terms by the projection property of P_h, and using (3.31) and the following identities:

$$\begin{aligned}&(\nabla\times\xi_h^j,\eta_h^{j+\frac{1}{2}}+\eta_h^{j-\frac{1}{2}})-(\eta_h^{j-\frac{1}{2}},\nabla\times(\xi_h^j+\xi_h^{j-1}))\\ =\;&(\nabla\times\xi_h^j,\eta_h^{j+\frac{1}{2}})-(\nabla\times\xi_h^{j-1},\eta_h^{j-\frac{1}{2}}),\end{aligned}$$

and

$$\begin{aligned}&-(\tilde{\xi}_h^{j-\frac{1}{2}},\xi_h^j+\xi_h^{j-1})-(\tilde{\eta}_h^j,\eta_h^{j+\frac{1}{2}}+\eta_h^{j-\frac{1}{2}})+(\xi_h^j,\tilde{\xi}_h^{j+\frac{1}{2}}+\tilde{\xi}_h^{j-\frac{1}{2}})+(\eta_h^{j-\frac{1}{2}},\tilde{\eta}_h^j+\tilde{\eta}_h^{j-1})\\ =\;&[(\tilde{\xi}_h^{j+\frac{1}{2}},\xi_h^j)-(\tilde{\xi}_h^{j-\frac{1}{2}},\xi_h^{j-1})]-[(\tilde{\eta}_h^j,\eta_h^{j+\frac{1}{2}})-(\tilde{\eta}_h^{j-1},\eta_h^{j-\frac{1}{2}})],\end{aligned}$$

we obtain

$$\begin{aligned}&\epsilon_0(||\xi_h^n||_0^2-||\xi_h^0||_0^2)+\mu_0(||\eta_h^{n+\frac{1}{2}}||_0^2-||\eta_h^{\frac{1}{2}}||_0^2)\\ &\quad+\frac{1}{\epsilon_0\omega_{pe}^2}(||\tilde{\xi}_h^{n+\frac{1}{2}}||_0^2-||\tilde{\xi}_h^{\frac{1}{2}}||_0^2)+\frac{1}{\mu_0\omega_{pm}^2}(||\tilde{\eta}_h^n||_0^2-||\tilde{\eta}_h^0||_0^2)\\ &\le-\tau\sum_{j=1}^n(\nabla\times(P_h\boldsymbol{H}^{j-\frac{1}{2}}-\frac{1}{\tau}\int_{t_{j-1}}^{t_j}\boldsymbol{H}(s)ds),\xi_h^j+\xi_h^{j-1})\\ &+\tau\sum_{j=1}^n(P_h\boldsymbol{J}^{j-\frac{1}{2}}-\frac{1}{\tau}\int_{t_{j-1}}^{t_j}\boldsymbol{J}(s)ds,\xi_h^j+\xi_h^{j-1})\\ &+\tau\sum_{j=1}^n(\nabla\times(P_h\boldsymbol{E}^j-\frac{1}{\tau}\int_{t_{j-\frac{1}{2}}}^{t_{j+\frac{1}{2}}}\boldsymbol{E}(s)ds),\eta_h^{j+\frac{1}{2}}+\eta_h^{j-\frac{1}{2}})\end{aligned}$$

$$
\begin{aligned}
&+\tau\sum_{j=1}^{n}(P_h\boldsymbol{K}^j-\frac{1}{\tau}\int_{t_{j-\frac{1}{2}}}^{t_{j+\frac{1}{2}}}\boldsymbol{K}(s)ds,\eta_h^{j+\frac{1}{2}}+\eta_h^{j-\frac{1}{2}})\\
&+\frac{\tau\Gamma_e}{\epsilon_0\omega_{pe}^2}\sum_{j=1}^{n}(\frac{1}{2}(P_h\boldsymbol{J}^{j+\frac{1}{2}}+P_h\boldsymbol{J}^{j-\frac{1}{2}})-\frac{1}{\tau}\int_{t_{j-\frac{1}{2}}}^{t_{j+\frac{1}{2}}}\boldsymbol{J}(s)ds,\tilde{\xi}_h^{j+\frac{1}{2}}+\tilde{\xi}_h^{j-\frac{1}{2}})\\
&+\tau\sum_{j=1}^{n}(\frac{1}{\tau}\int_{t_{j-\frac{1}{2}}}^{t_{j+\frac{1}{2}}}\boldsymbol{E}(s)ds-P_h\boldsymbol{E}^j,\tilde{\xi}_h^{j+\frac{1}{2}}+\tilde{\xi}_h^{j-\frac{1}{2}})\\
&+\frac{\tau\Gamma_m}{\mu_0\omega_{pm}^2}\sum_{j=1}^{n}(\frac{1}{2}(P_h\boldsymbol{K}^j+P_h\boldsymbol{K}^{j-1})-\frac{1}{\tau}\int_{t_{j-1}}^{t_j}\boldsymbol{K}(s)ds,\tilde{\eta}_h^j+\tilde{\eta}_h^{j-1})\\
&+\tau\sum_{j=1}^{n}(\frac{1}{\tau}\int_{t_{j-1}}^{t_j}\boldsymbol{H}(s)ds-P_h\boldsymbol{H}^{j-\frac{1}{2}},\tilde{\eta}_h^j+\tilde{\eta}_h^{j-1})\\
&+\tau(\tilde{\xi}_h^{n+\frac{1}{2}},\xi_h^n)-\tau(\tilde{\xi}_h^{\frac{1}{2}},\xi_h^0)-\tau(\tilde{\eta}_h^n,\eta_h^{n+\frac{1}{2}})+\tau(\tilde{\eta}_h^0,\eta_h^{\frac{1}{2}})\\
&+\tau(\nabla\times\xi_h^0,\eta_h^{\frac{1}{2}})-\tau(\nabla\times\xi_h^n,\eta_h^{n+\frac{1}{2}})\\
&+\sum_i\frac{\tau}{2}\int_{\partial T_i}\eta_i^{n+\frac{1}{2}}\cdot\mathbf{n}_{ik}\times\xi_i^n-\sum_i\frac{\tau}{2}\int_{\partial T_i}\mathbf{n}_i\times\xi_i^0\cdot\eta_i^{\frac{1}{2}}\\
&-\sum_{T_i}\sum_{k\in\nu_i}\frac{\tau}{2}\int_{a_{ik}}\eta_i^{n+\frac{1}{2}}\cdot\mathbf{n}_{ik}\times\xi_k^n+\sum_{T_i}\sum_{k\in\nu_i}\frac{\tau}{2}\int_{a_{ik}}\xi_i^0\cdot\mathbf{n}_{ik}\times\eta_k^{\frac{1}{2}}\\
&-\sum_{j=1}^{n}\sum_{T_i}\sum_{k\in\nu_i}\frac{\tau}{2}\int_{a_{ik}}(\xi_i^j+\xi_i^{j-1})\cdot\mathbf{n}_{ik}\times([P_h\boldsymbol{H}^{j-\frac{1}{2}}-\boldsymbol{H}^{j-\frac{1}{2}}]\\
&\qquad\qquad-\mathbf{n}_{ik}\times[\frac{P_h\boldsymbol{E}^j-\boldsymbol{E}^j+P_h\boldsymbol{E}^{j-1}-\boldsymbol{E}^{j-1}}{2}])\\
&+\sum_{j=1}^{n}\sum_{T_i}\sum_{k\in\nu_i}\frac{\tau}{2}\int_{a_{ik}}(\eta_i^{j+\frac{1}{2}}+\eta_i^{j-\frac{1}{2}})\cdot\mathbf{n}_{ik}\times(\mathbf{n}_{ik}\times[\frac{P_h\boldsymbol{H}^{j+\frac{1}{2}}-\boldsymbol{H}^{j+\frac{1}{2}}+P_h\boldsymbol{H}^{j-\frac{1}{2}}-\boldsymbol{H}^{j-\frac{1}{2}}}{2}]\\
&\qquad\qquad+[P_h\boldsymbol{E}^j-\boldsymbol{E}^j])\\
&=\sum_{i=1}^{20}Err_i.
\end{aligned}
\tag{3.45}
$$

Below we will estimate each term Err_i. During the proof, we frequently use the arithmetic-geometric mean inequality

$$
(a,b)\le\frac{\delta}{2}||a||_0^2+\frac{1}{2\delta}||b||_0^2, \tag{3.46}
$$

where δ is an arbitrary positive constant.

Using integration by parts, the projection property, and Lemma 3.2.1 (ii), we obtain

$$\begin{aligned} Err_1 &\le \tau\delta_1 \sum_{j=1}^{n}(||\xi_h^j||_0^2 + ||\xi_h^{j-1}||_0^2) + \frac{\tau}{2\delta_1}\sum_{j=1}^{n}||\nabla\times \boldsymbol{H}^{j-\frac{1}{2}} - \frac{1}{\tau}\int_{t_{j-1}}^{t_j}\nabla\times\boldsymbol{H}(s)ds||_0^2 \\ &\le \tau\delta_1\cdot 2\sum_{j=1}^{n}||\xi_h||_{l^\infty(L^2)}^2 + \tau\delta_1||\xi_h^0||_0^2 + \frac{\tau}{2\delta_1}\sum_{j=1}^{n}\frac{\tau^3}{4}\int_{t_{j-1}}^{t_j}||\nabla\times\boldsymbol{H}_{tt}(s)||_0^2 ds \\ &\le 2T\delta_1||\xi_h||_{l^\infty(L^2)}^2 + \tau\delta_1||\xi_h^0||_0^2 + \frac{\tau^4}{8\delta_1}||\nabla\times\boldsymbol{H}_{tt}||_{L^2(0,T;L^2(\Omega)^3)}, \end{aligned}$$

where we introduced the notation $||\xi_h||_{l^\infty(L^2)} = \max_{j\ge 1}||\xi_h^j||_0$.

Similarly, we can obtain

$$\begin{aligned} Err_2 &= \tau\sum_{j=1}^{n}(\boldsymbol{J}^{j-\frac{1}{2}} - \frac{1}{\tau}\int_{t_{j-1}}^{t_j}\boldsymbol{J}(s)ds, \xi_h^j + \xi_h^{j-1}) \\ &\le 2T\delta_2||\xi_h||_{l^\infty(L^2)}^2 + \tau\delta_2||\xi_h^0||_0^2 + \frac{\tau^4}{8\delta_2}||\boldsymbol{J}_{tt}||_{L^2(0,T;L^2(\Omega)^3)}. \end{aligned}$$

Using integration by parts, the projection property, and Lemma 3.2.1 (i), we have

$$\begin{aligned} Err_3 &= \tau\sum_{j=1}^{n}(\nabla\times\boldsymbol{E}^j - \frac{1}{\tau}\int_{t_{j-\frac{1}{2}}}^{t_{j+\frac{1}{2}}}\nabla\times\boldsymbol{E}(s)ds, \eta_h^{j+\frac{1}{2}} + \eta_h^{j-\frac{1}{2}}) \\ &\le \tau\sum_{j=1}^{n}\delta_3(||\eta_h^{j+\frac{1}{2}}||_0^2 + ||\eta_h^{j-\frac{1}{2}}||_0^2) + \frac{\tau}{2\delta_3}\sum_{j=1}^{n}\frac{\tau^3}{4}\int_{t_{j-\frac{1}{2}}}^{t_{j+\frac{1}{2}}}||\nabla\times\boldsymbol{E}_{tt}(s)||_0^2 ds \\ &\le 2T\delta_3||\eta_h||_{l^\infty(L^2)}^2 + \tau\delta_3||\eta_h^{\frac{1}{2}}||_0^2 + \frac{\tau^4}{8\delta_3}\int_{t_{\frac{1}{2}}}^{t_{n+\frac{1}{2}}}||\nabla\times\boldsymbol{E}_{tt}(s)||_0^2 ds. \end{aligned}$$

By similar arguments, we have

$$Err_4 \le 2T\delta_4||\eta_h||_{l^\infty(L^2)}^2 + \tau\delta_4||\eta_h^{\frac{1}{2}}||_0^2 + \frac{\tau^4}{8\delta_4}\int_{t_{\frac{1}{2}}}^{t_{n+\frac{1}{2}}}||\boldsymbol{K}_{tt}(s)||_0^2 ds;$$

$$\begin{aligned} Err_5 &\le \frac{\tau\Gamma_e}{\epsilon_0\omega_{pe}^2}[\sum_{j=1}^{n}\delta_5(||\tilde{\xi}_h^{j+\frac{1}{2}}||_0^2 + ||\tilde{\xi}_h^{j-\frac{1}{2}}||_0^2) + \sum_{j=1}^{n}\frac{1}{2\delta_5}||\frac{1}{2}(\boldsymbol{J}^{j+\frac{1}{2}} + \boldsymbol{J}^{j-\frac{1}{2}}) - \frac{1}{\tau}\int_{t_{j-\frac{1}{2}}}^{t_{j+\frac{1}{2}}}\boldsymbol{J}(s)ds||_0^2] \\ &\le \frac{\Gamma_e}{\epsilon_0\omega_{pe}^2}\left[2T\delta_5||\tilde{\xi}_h||_{l^\infty(L^2)}^2 + \tau\delta_5||\tilde{\xi}_h^{\frac{1}{2}}||_0^2 + \frac{\tau^4}{8\delta_5}\int_{t_{\frac{1}{2}}}^{t_{n+\frac{1}{2}}}||\boldsymbol{J}_{tt}(s)||_0^2 ds\right]; \end{aligned}$$

$$Err_6 \leq 2T\delta_6||\tilde{\xi}_h||^2_{l^\infty(L^2)} + \tau\delta_6||\tilde{\xi}_h^{\frac{1}{2}}||_0^2 + \frac{\tau^4}{8\delta_6}\int_{t_{\frac{1}{2}}}^{t_{n+\frac{1}{2}}} ||\boldsymbol{E}_{tt}(s)||_0^2 ds;$$

$$Err_7 \leq \frac{\Gamma_m}{\mu_0\omega_{pm}^2}\left[2T\delta_7||\tilde{\eta}_h||^2_{l^\infty(L^2)} + \tau\delta_7||\tilde{\eta}_h^0||_0^2 + \frac{\tau^4}{8\delta_7}\int_{t_0}^{t_n} ||\boldsymbol{K}_{tt}(s)||_0^2 ds\right];$$

and

$$Err_8 \leq 2T\delta_8||\tilde{\eta}_h||^2_{l^\infty(L^2)} + \tau\delta_8||\tilde{\eta}_h^0||_0^2 + \frac{\tau^4}{8\delta_8}\int_{t_0}^{t_n} ||\boldsymbol{H}_{tt}(s)||_0^2 ds.$$

Using the Cauchy-Schwartz inequality, we obtain

$$Err_9 = \tau(\tilde{\xi}_h^{n+\frac{1}{2}}, \xi_h^n) \leq \frac{\epsilon_0\omega_{pe}^2\tau^2}{2}||\xi_h^n||_0^2 + \frac{1}{2\epsilon_0\omega_{pe}^2}||\tilde{\xi}_h^{n+\frac{1}{2}}||_0^2, \tag{3.47}$$

$$Err_{10} = \tau(\tilde{\xi}_h^{\frac{1}{2}}, \xi_h^0) \leq \frac{\epsilon_0\omega_{pe}^2\tau^2}{2}||\xi_h^0||_0^2 + \frac{1}{2\epsilon_0\omega_{pe}^2}||\tilde{\xi}_h^{\frac{1}{2}}||_0^2, \tag{3.48}$$

$$Err_{11} = \tau(\tilde{\eta}_h^n, \eta_h^{n+\frac{1}{2}}) \leq \frac{\mu_0\omega_{pm}^2\tau^2}{2}||\eta_h^{n+\frac{1}{2}}||_0^2 + \frac{1}{2\mu_0\omega_{pm}^2}||\tilde{\eta}_h^n||_0^2, \tag{3.49}$$

$$Err_{12} = \tau(\tilde{\eta}_h^0, \eta_h^{\frac{1}{2}}) \leq \frac{\mu_0\omega_{pm}^2\tau^2}{2}||\eta_h^{\frac{1}{2}}||_0^2 + \frac{1}{2\mu_0\omega_{pm}^2}||\tilde{\eta}_h^0||_0^2. \tag{3.50}$$

By the Cauchy-Schwartz inequality and the inverse estimate (3.15), and recalling the notation $C_v = 1/\sqrt{\mu_0\epsilon_0}$, we have

$$\begin{aligned}
Err_{13} &\leq \tau \cdot C_{inv}h^{-1}||\xi_h^0||_0||\eta_h^{\frac{1}{2}}||_0 = \tau C_{inv}h^{-1}C_v\sqrt{\epsilon_0}||\xi_h^0||_0 \cdot \sqrt{\mu_0}||\eta_h^{\frac{1}{2}}||_0 \\
&\leq \frac{C_{inv}C_v\tau}{2h}\left[\epsilon_0||\xi_h^0||_0^2 + \mu_0||\eta_h^{\frac{1}{2}}||_0^2\right], \\
Err_{14} &\leq \tau \cdot C_{inv}h^{-1}||\xi_h^n||_0||\eta_h^{n+\frac{1}{2}}||_0 = \tau C_{inv}h^{-1}C_v\sqrt{\epsilon_0}||\xi_h^n||_0 \cdot \sqrt{\mu_0}||\eta_h^{n+\frac{1}{2}}||_0 \\
&\leq \frac{C_{inv}C_v\tau}{2h}\left[\epsilon_0||\xi_h^n||_0^2 + \mu_0||\eta_h^{n+\frac{1}{2}}||_0^2\right], \\
Err_{15} &= \sum_i \frac{\tau}{2}\int_{\partial T_i} \eta_i^{n+\frac{1}{2}} \cdot \mathbf{n}_{ik} \times \xi_i^n \leq \frac{\tau}{2}C_{inv}^2h^{-1}c_v\sum_i \sqrt{\epsilon_0}\,\|\xi_i^n\|_{0,T_i}\sqrt{\mu_0}\left\|\eta_i^{n+\frac{1}{2}}\right\|_{0,T_i} \\
&\leq \frac{\tau C_{inv}^2C_v}{4h}\left[\epsilon_0\,\|\xi_h^n\|_0^2 + \mu_0\left\|\eta_h^{n+\frac{1}{2}}\right\|_0^2\right].
\end{aligned}$$

Similar to Err_{15}, we have

$$Err_{16} \leq \frac{\tau C_{inv}^2 C_v}{4h}(\epsilon_0 \left\|\xi_h^0\right\|_0^2 + \mu_0 \left\|\eta_h^{\frac{1}{2}}\right\|_0^2),$$
$$Err_{17} \leq \frac{\tau C_{inv}^2 C_v}{4h}(\epsilon_0 \left\|\xi_h^n\right\|_0^2 + \mu_0 \left\|\eta_h^{n+\frac{1}{2}}\right\|_0^2),$$
$$Err_{18} \leq \frac{\tau C_{inv}^2 C_v}{4h}(\left\|\xi_h^0\right\|_0^2 + \left\|\eta_h^{\frac{1}{2}}\right\|_0^2).$$

By the Cauchy-Schwartz inequality, the inverse estimate (3.15) and the projection error estimate (3.30), we have

$$\begin{aligned} Err_{19} &\leq \sum_{j=1}^{n} \frac{\tau}{2} C_{inv}^2 h^{-1} \sum_{T_i} \left\|\xi_i^j + \xi_i^{j-1}\right\|_{0,T_i} \cdot Ch^{min(s,k)+1}(||\boldsymbol{H}||_{L^\infty(0,T;H^{s+1}(\Omega))} + ||\boldsymbol{E}||_{L^\infty(0,T;H^{s+1}(\Omega))}) \\ &\leq \tau \sum_{j=1}^{n} [\delta_{19} \sum_{T_i} (\left\|\xi_h^j\right\|_0^2 + \left\|\xi_h^{j-1}\right\|_0^2) + \frac{C_{inv}^4}{2\delta_{19}} \cdot Ch^{2min(s,k)}] \\ &\leq 2T\delta_{19} \left\|\xi_h\right\|_{l^\infty(L^2)}^2 + \tau\delta_{19} \left\|\xi_h^0\right\|_0^2 + \frac{TC_{inv}^4}{2\delta_{19}} \cdot Ch^{2min(s,k)}. \end{aligned}$$

By the same arguments, we have

$$Err_{20} \quad \leq \quad 2T\delta_{20} \left\|\eta_h\right\|_{l^\infty(L^2)}^2 + \tau\delta_{20} \left\|\eta_h^0\right\|_0^2 + \frac{TC_{inv}^2}{2\delta_{20}} \cdot Ch^{2min(s,k)}.$$

Substituting the above estimates Err_i into (3.45) by first choosing τ small enough (such as (3.32)) so that those terms $||\xi_h^n||_0^2, ||\eta_h^{n+\frac{1}{2}}||_0^2, ||\tilde{\xi}_h^{n+\frac{1}{2}}||_0^2$ and $||\tilde{\eta}_h^n||_0^2$ on the right-hand sides of $Err_i, i = 9, \cdots, 18$, can be controlled by the corresponding terms on the left-hand side of (3.45), and then taking the maximum of the resultant for n and choosing parameters δ_i small enough such as

$$\delta_1 = \delta_2 = \delta_{19} = \frac{\epsilon_0}{8T}, \quad \delta_3 = \delta_4 = \delta_{20} = \frac{\mu_0}{8T}, \tag{3.51}$$
$$\delta_5 = \delta_7 = \frac{1}{10T\Gamma_e}, \quad \delta_6 = \frac{1}{10T\epsilon_0\omega_{pe}^2}, \quad \delta_8 = \frac{1}{10T\mu_0\omega_{pm}^2}, \tag{3.52}$$

we obtain

$$\begin{aligned} & \epsilon_0||\xi_h^n||_0^2+\mu_0||\eta_h^{n+\frac{1}{2}}||_0^2+\frac{1}{\epsilon_0\omega_{pe}^2}||\tilde{\xi}_h^{n+\frac{1}{2}}||_0^2+\frac{1}{\mu_0\omega_{pm}^2}||\tilde{\eta}_h^n||_0^2 \\ \leq\ & C(\tau^4+T^2h^{min\{s,k\}})+C\Big(\epsilon_0||\xi_h^0||_0^2+\mu_0||\eta_h^{\frac{1}{2}}||_0^2+\frac{1}{\epsilon_0\omega_{pe}^2}||\tilde{\xi}_h^{\frac{1}{2}}||_0^2+\frac{1}{\mu_0\omega_{pm}^2}||\tilde{\eta}_h^0||_0^2\Big) \end{aligned} \tag{3.53}$$

Using the triangle inequality, (3.53), and the estimates (3.30), we get

$$\begin{aligned} & \max_{1\leq n}(||\boldsymbol{E}^n-\boldsymbol{E}_h^n||_0+||\boldsymbol{H}^{n+\frac{1}{2}}-\boldsymbol{H}_h^{n+\frac{1}{2}}||_0+||\boldsymbol{J}^{n+\frac{1}{2}}-\boldsymbol{J}_h^{n+\frac{1}{2}}||_0+||\boldsymbol{K}^n-\boldsymbol{K}_h^n||_0) \\ \leq\ & C(\tau^2+Th^{min\{s,k\}})+C\Big(||\boldsymbol{E}^0-\boldsymbol{E}_h^0||_0+||\boldsymbol{H}^{\frac{1}{2}}-\boldsymbol{H}_h^{\frac{1}{2}}||_0+||\boldsymbol{J}^{\frac{1}{2}}-\boldsymbol{J}_h^{\frac{1}{2}}||_0+||\boldsymbol{K}^0-\boldsymbol{K}_h^0||_0\Big), \end{aligned}$$

which completes the proof.

3.2.4 NUMERICAL RESULTS

In this section, we present 2D numerical results supporting our prior theoretical analysis. Recall that our prior 3D analysis holds true for 2D problems, in which case the scalar and vector curl operators are

$$\nabla\times\boldsymbol{H}=\frac{\partial H_y}{\partial x}-\frac{\partial H_x}{\partial y},\quad \nabla\times\boldsymbol{E}=(\frac{\partial E}{\partial y},-\frac{\partial E}{\partial x})',$$

where we consider the TM_z mode, which involves a vector magnetic field $\boldsymbol{H}=(H_x,H_y)$ and a scalar electric field E.

Example 3.2.1. In the first example, we create an exact solution to check the optimal order convergence rate. For simplicity, we assume that $\Omega=[0,1]^2$, $\epsilon_0=\mu_0=1$, $\omega_{pe}=\omega_{pm}=\Gamma_m=\Gamma_e=\pi$, and the exact solution to (3.1)-(3.4) with added right-hand side

source terms f and $\boldsymbol{g}$ is given by

$$
\begin{aligned}
H_x(x,y,t) &= \sin(\pi x)\cdot\cos(\pi y)e^{-\pi t},\\
H_y(x,y,t) &= -\cos(\pi x)\cdot\sin(\pi y)e^{-\pi t},\\
E(x,y,t) &= \sin(\pi x)\cdot\sin(\pi y)e^{-\pi t},\\
K_x(x,y,t) &= \pi^2 t\cdot\sin(\pi x)\cdot\cos(\pi y)e^{-\pi t},\\
K_y(x,y,t) &= -\pi^2 t\cdot\cos(\pi x)\cdot\sin(\pi y)e^{-\pi t},\\
J(x,y,t) &= \pi^2 t\sin(\pi x)\cdot\sin(\pi y)e^{-\pi t},
\end{aligned}
$$

where the source terms

$$
\begin{aligned}
f(x,y,t) &= (-3\pi+\pi^2 t)e^{-\pi t}\sin(\pi x)\cdot\sin(\pi y),\\
g_x(x,y,t) &= \pi^2 t e^{-\pi t}\sin(\pi x)\cdot\cos(\pi y),\\
g_y(x,y,t) &= -\pi^2 t e^{-\pi t}\cos(\pi x)\cdot\sin(\pi y),
\end{aligned}
$$

are added to the right-hand sides of (3.1) and (3.2), respectively. In our implementation, we have to add a term $\int_{T_i} f^{n+\frac{1}{2}}\cdot u_i$ and a term $\int_{T_i}\boldsymbol{g}^{n+1}\cdot\boldsymbol{v}_i$ to the right-hand sides of (3.8) and (3.9), respectively.

We solved the problem using various time step sizes τ and mesh sizes with different orders of basis functions. For a fixed small time step τ and smooth solutions, our numerical results showed that the error estimate is as follows:

$$
\max_{1\le n}(||\boldsymbol{E}^n-\boldsymbol{E}_h^n||_0+||\boldsymbol{H}^{n+\frac{1}{2}}-\boldsymbol{H}_h^{n+\frac{1}{2}}||_0+||\boldsymbol{J}^{n+\frac{1}{2}}-\boldsymbol{J}_h^{n+\frac{1}{2}}||_0+||\boldsymbol{K}^n-\boldsymbol{K}_h^n||_0)\le CTh^{k+1},
$$

which has one order higher convergence rate than that proved in Theorem 3.2.2. Recall that k denotes the order of the basis function. This occurrence, which happened for the upwind flux, was already mentioned in [29, p.205]. In fact, the rigorous proof of $O(h^{k+1})$ for the upwind flux case is still open.

In Tables 3.1-3.3, we present the numerical results obtained using a fixed $\tau=10^{-6}$ on uniformly refined triangular meshes. The results show the convergence rate $O(h^{k+1})$ clearly.

Table 3.1: The L^2 errors obtained after 100 steps on uniform triangular meshes with $\tau = 10^{-6}$ and $k = 1$.

Meshes	$h = \frac{1}{4}$	$h = \frac{1}{8}$	rate	$h = \frac{1}{16}$	rate	$h = \frac{1}{32}$	rate	$h = \frac{1}{64}$	rate
H_x	0.0455	0.0118	1.9471	0.0030	1.9758	7.5453e-4	1.9913	1.8875e-4	1.9991
H_y	0.0517	0.0128	2.0140	0.0032	2.0000	7.9346e-4	2.0118	1.9849e-4	1.9991
E	0.0486	0.0123	1.9823	0.0031	1.9883	7.7451e-4	2.0009	1.9370e-4	1.9995
K_x	4.4914e-5	1.1673e-5	1.9440	2.9630e-6	1.9780	7.4472e-7	1.9923	1.8634e-7	1.9988
K_y	5.1037e-5	1.2628e-5	2.0149	3.1376e-6	2.0089	7.8287e-7	2.0028	1.9582e-7	1.9992
J	4.8251e-5	1.2236e-5	1.9794	3.0708e-6	1.9944	7.6850e-7	1.9985	1.9217e-7	1.9997

Table 3.2: The L^2 errors obtained after 100 steps on uniform triangular meshes with $\tau = 10^{-6}$ and $k = 2$.

Meshes	$h = \frac{1}{4}$	$h = \frac{1}{8}$	rate	$h = \frac{1}{16}$	rate	$h = \frac{1}{32}$	rate	$h = \frac{1}{64}$	rate
H_x	0.0047	6.4854e-4	2.8574	8.6694e-5	2.9032	1.1357e-5	2.9324	1.4646e-6	2.9550
H_y	0.0047	6.4894e-4	2.8565	8.7021e-5	2.8986	1.1404e-5	2.9318	1.4699e-6	2.9558
E	0.0047	6.5112e-4	2.8517	8.6896e-5	2.9056	1.1322e-5	2.9402	1.4544e-6	2.9606
K_x	4.6862e-6	6.4001e-7	2.8723	8.5541e-8	2.9034	1.1202e-8	2.9329	1.4434e-9	2.9562
K_y	4.6398e-6	6.4030e-7	2.8572	8.5847e-8	2.8989	1.1245e-8	2.9325	1.4481e-9	2.9571
J	4.6696e-6	6.4594e-7	2.8538	8.6171e-8	2.9061	1.1216e-8	2.9416	1.4370e-9	2.9644

Table 3.3: The L^2 errors obtained after 100 steps on uniform triangular meshes with $\tau = 10^{-6}$ and $k = 3$.

Meshes	$h = \frac{1}{4}$	$h = \frac{1}{8}$	rate	$h = \frac{1}{16}$	rate	$h = \frac{1}{32}$	rate	$h = \frac{1}{64}$	rate
H_x	7.3281e-4	5.3071e-5	3.7874	3.6439e-6	3.8644	2.4100e-7	3.9184	1.5618e-8	3.9478
H_y	7.5179e-4	5.5864e-5	3.7503	3.8611e-6	3.8548	2.5572e-7	3.9164	1.6659e-8	3.9402
E	6.4847e-4	4.9042e-5	3.7250	3.4892e-6	3.8130	2.3667e-7	3.8819	1.5848e-8	3.9005
K_x	7.2325e-7	5.2389e-8	3.7872	3.5986e-9	3.8638	2.3817e-10	3.9174	1.5410e-11	3.9501
K_y	7.4200e-7	5.5150e-8	3.7500	3.8135e-9	3.8542	2.5272e-10	3.9155	1.6391e-11	3.9466
J	6.4357e-7	4.8697e-8	3.7242	3.4676e-9	3.8118	2.3542e-10	3.8806	1.5601e-11	3.9155

A linear growth of errors is also observed in our numerical tests. In Tables 3.4-3.5, we present the numerical results obtained with the same conditions as used for Tables 3.1-3.2 except the errors are recorded after 10 time steps. Comparing Tables 3.4-3.5 with Tables 3.1-3.2, we can see that the errors of K_x, K_y, J in Tables 3.1-3.2 are almost 10 times larger than those in Tables 3.4-3.5. The errors for the first three solutions do not change that much with the number of time steps. This is due to the fact that the exact solutions (H_x, H_y, E) change very little with respect to time since $e^{-\pi t} \approx 1$. We should mention that $O(\tau^2)$ could not be observed due to the CFL condition $\tau = O(h)$, since $O(\tau^2 + h^{k+1})$ is always dominated

by $O(\tau^2)$.

Table 3.4: The L^2 errors obtained after 10 steps on uniform triangular meshes with $\tau = 10^{-6}$ and $k = 1$.

Meshes	$h = \frac{1}{4}$	$h = \frac{1}{8}$	rate	$h = \frac{1}{16}$	rate	$h = \frac{1}{32}$	rate	$h = \frac{1}{64}$	rate
H_x	0.0455	0.0118	1.9471	0.0030	1.9758	7.5479e-4	1.9908	1.8890e-4	1.9985
H_y	0.0517	0.0128	2.0140	0.0032	2.0000	7.9325e-4	2.0122	1.9840e-4	1.9994
E_z	0.0487	0.0123	1.9853	0.0031	1.9883	7.7529e-4	1.9995	1.9388e-4	1.9996
K_x	4.4922e-6	1.1675e-6	1.9440	2.9636e-7	1.9780	7.4496e-8	1.9921	1.8644e-8	1.9985
K_y	5.1046e-6	1.2630e-6	2.0149	3.1378e-7	2.0090	7.8288e-8	2.0029	1.9580e-8	1.9994
J_z	5.0436e-6	1.2790e-6	1.9794	3.2102e-7	1.9943	8.0347e-8	1.9983	2.0093e-8	1.9996

Example 3.2.2. We use this example to demonstrate the effectiveness of our DG method in solving discontinuous media problems. For simplicity, we consider a case when the permittivity is discontinuous: $\epsilon_0 = 1$ in a subdomain $[0.25\ \ 0.75] \times [0.25\ \ 0.75]$ and $\epsilon_0 = 100$ in other area, $\mu_0 = 1$, $\omega_{pe} = \pi$, $\omega_{pm} = \pi$, $\Gamma_m = \pi$, $\Gamma_e = \pi$. The order of the basis function is 2.

The source functions:

$$f = (-3\pi + \pi^2 t)e^{-\pi t} sin(\pi x) \cdot sin(\pi y);$$

$$gx = \pi^2 t e^{-\pi t} sin(\pi x) \cdot cos(\pi y);$$

$$gy = -\pi^2 t e^{-\pi t} cos(\pi x) \cdot sin(\pi y).$$

Table 3.5: The L^2 errors obtained after 10 steps on uniform triangular meshes with $\tau = 10^{-6}$ and $k = 2$.

Meshes	$h = \frac{1}{4}$	$h = \frac{1}{8}$	rate	$h = \frac{1}{16}$	rate	$h = \frac{1}{32}$	rate	$h = \frac{1}{64}$	rate
H_x	0.0047	6.4858e-4	2.8573	8.6680e-5	2.9035	1.1349e-5	2.9331	1.4616e-6	2.9569
H_y	0.0047	6.4881e-4	2.8568	8.6976e-5	2.8991	1.1390e-5	2.9328	1.4659e-6	2.9579
E_z	0.0047	6.5149e-4	2.8508	8.6889e-5	2.9065	1.1302e-5	2.9426	1.4459e-6	2.9665
K_x	4.6873e-7	6.4012e-8	2.8723	8.5547e-9	2.9036	1.1200e-9	2.9332	1.4424e-10	2.9570
K_y	4.6404e-7	6.4033e-8	2.8574	8.5838e-9	2.8991	1.1241e-9	2.9328	1.4466e-10	2.9580
J_z	4.8815e-7	6.7516e-8	2.8540	9.0042e-9	2.9066	1.1712e-9	2.9426	1.4981e-10	2.9668

And the initial condition is

$$Hx = sin(\pi\frac{x}{4}) \cdot cos(\pi\frac{y}{4})e^{-\pi dt/2}; Hy = -cos(\pi\frac{x}{4}) \cdot sin(\pi\frac{y}{4})e^{-\pi dt/2};$$

$$E = sin(\pi x) \cdot sin(\pi y);$$

$$Kx = 0; Ky = 0;$$

$$J = \omega_{pe}^2 \frac{dt}{2} sin(\pi x) \cdot sin(\pi y)e^{-\Gamma_e dt/2}.$$

Since the exact solution to this problem is unknown, we just plot the numerical solutions obtained on different meshes. To verify the long term stability, we solved this example to 10000 time steps with $dt = 10^{-5}$. The resulting numerical magnetic field H = (Hx , Hy) and electric field E on various uniform triangular meshes are presented in Figures (3.9)-(3.12), Convergence was verified for the following different sizes $n = 4, 8, 16, 32$.

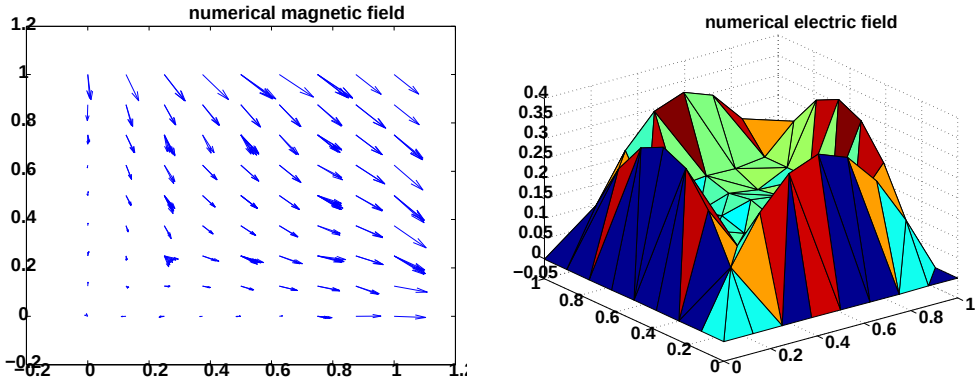

(a) magnetic field Hx,Hy (b) electric field E

Figure 3.9: Numerical solutions after 10000 time steps with h = 1/4: (Left) The magnetic field H = (Hx, Hy); (Right) The electric field E.

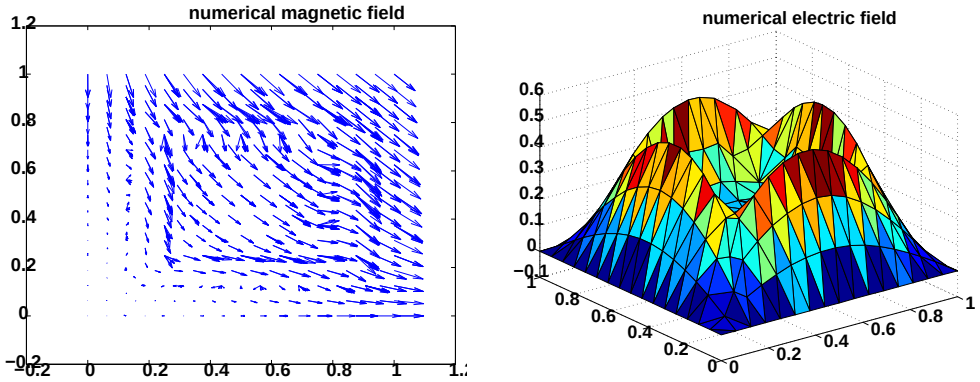

(a) magnetic field Hx,Hy (b) electric field E

Figure 3.10: Numerical solutions after 10000 time steps with h = 1/8: (Left) The magnetic field H = (Hx, Hy); (Right) The electric field E.

3.3 ANOTHER DGTD METHOD FOR MAXWELL'S EQUATIONS IN METAMATERIALS

For the same governing equations for modeling wave propagation in metamaterials (3.1-3.4), we also developed the following DGTD method:

$$\int_{T_i} \epsilon_0 \frac{\boldsymbol{E}_i^{n+1} - \boldsymbol{E}_i^n}{\tau} \cdot \boldsymbol{u}_i = \int_{T_i} \nabla \times \boldsymbol{u}_i \cdot \boldsymbol{H}_i^{n+\frac{1}{2}} - \int_{T_i} \boldsymbol{J}_i^{n+\frac{1}{2}} \cdot \boldsymbol{u}_i - \sum_{k \in \nu_i} \int_{a_{ik}} \boldsymbol{u}_i \cdot (\{\boldsymbol{H}_h^{n+\frac{1}{2}}\}_{ik} \times \boldsymbol{n}_{ik}) \tag{3.54}$$

$$\int_{T_i} \mu_0 \frac{\boldsymbol{H}_i^{n+\frac{3}{2}} - \boldsymbol{H}_i^{n+\frac{1}{2}}}{\tau} \cdot \boldsymbol{v}_i = -\int_{T_i} \nabla \times \boldsymbol{v}_i \cdot \boldsymbol{E}_i^{n+1} - \int_{T_i} \boldsymbol{K}_i^{n+1} \cdot \boldsymbol{v}_i + \sum_{k \in \nu_i} \int_{a_{ik}} \boldsymbol{v}_i \cdot (\{\boldsymbol{E}_h^{n+1}\}_{ik} \times \boldsymbol{n}_{ik}) \tag{3.55}$$

$$\frac{1}{\epsilon_0 \omega_{pe}^2} \int_{T_i} \frac{\boldsymbol{J}_i^{n+\frac{3}{2}} - \boldsymbol{J}_i^{n+\frac{1}{2}}}{\tau} \cdot \boldsymbol{\phi}_i + \frac{\Gamma_e}{\epsilon_0 \omega_{pe}^2} \int_{T_i} \frac{\boldsymbol{J}_i^{n+\frac{3}{2}} + \boldsymbol{J}_i^{n+\frac{1}{2}}}{2} \cdot \boldsymbol{\phi}_i = \int_{T_i} \boldsymbol{E}_i^{n+1} \cdot \boldsymbol{\phi}_i \tag{3.56}$$

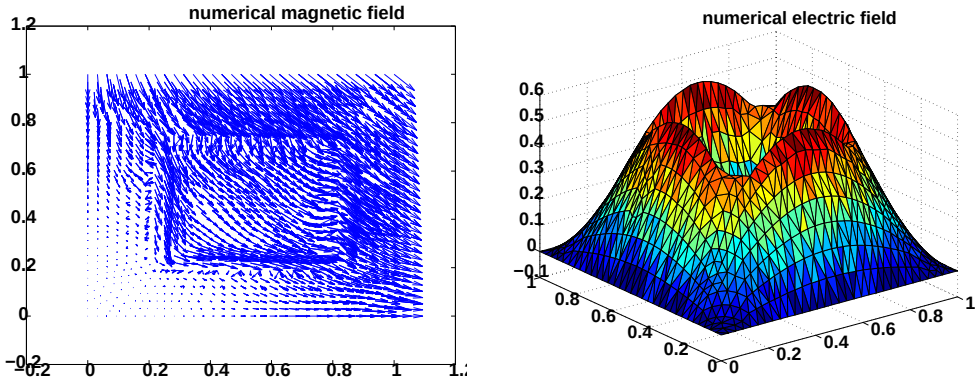

(a) magnetic field Hx,Hy (b) electric field E

Figure 3.11: Numerical solutions after 10000 time steps with h = 1/16: (Left) The magnetic field H = (Hx, Hy); (Right) The electric field E.

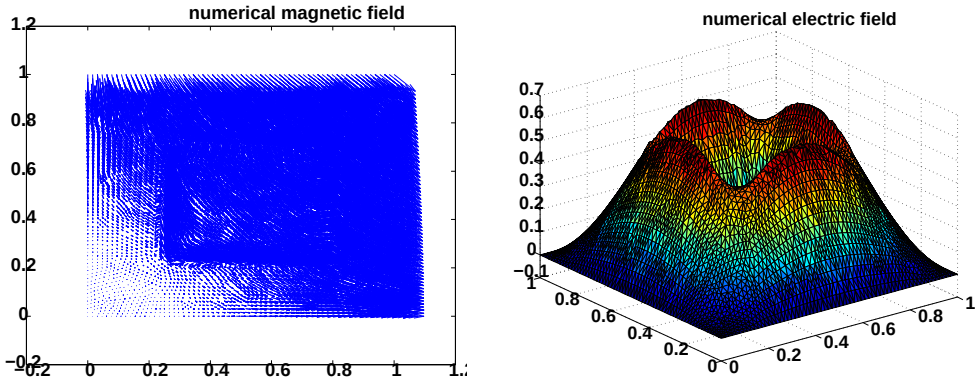

(a) magnetic field Hx,Hy (b) electric field E

Figure 3.12: magnetic field [Hx,Hy](left),electric field E(right),mesh size 1/32, time step 10000

$$\frac{1}{\mu_0\omega_{pm}^2}\int_{T_i}\frac{\boldsymbol{K}_i^{n+1}-\boldsymbol{K}_i^n}{\tau}\cdot\boldsymbol{\psi}_i+\frac{\Gamma_m}{\mu_0\omega_{pm}^2}\int_{T_i}\frac{\boldsymbol{K}_i^{n+1}+\boldsymbol{K}_i^n}{2}\cdot\boldsymbol{\psi}_i=\int_{T_i}\boldsymbol{H}_i^{n+\frac{1}{2}}\cdot\boldsymbol{\psi}_i. \tag{3.57}$$

Here we prove that the order of the convergence of the scheme is $O(\Delta t^2+h^{min(s,k)})$.

3.3.1 DISCRETE ENERGY

One defines the discrete energy at some time step n as:

$$\varepsilon^n=\sum_{T_i\in\Omega}\varepsilon_i^n,$$

where

$$\varepsilon_i^n = \frac{1}{2}\epsilon_0\langle \boldsymbol{E}_i^n, \boldsymbol{E}_i^n\rangle + \frac{1}{2}\mu_0\langle \boldsymbol{H}_i^{n-\frac{1}{2}}, \boldsymbol{H}_i^{n+\frac{1}{2}}\rangle + \frac{1}{2\mu_0\omega_{pm}^2}\langle \boldsymbol{K}_i^n, \boldsymbol{K}_i^n\rangle + \frac{1}{2\epsilon_0\omega_{pe}^2}\langle \boldsymbol{J}_i^{n-\frac{1}{2}}, \boldsymbol{J}_i^{n+\frac{1}{2}}\rangle. \quad (3.58)$$

Lemma 3.3.1. *(CFL condition) The discrete energy (3.58) defines a quadratic form of the unknowns* $\boldsymbol{E}^n$, $\boldsymbol{H}^{n-\frac{1}{2}}$, $\boldsymbol{K}^n$ *and* $\boldsymbol{J}^{n-\frac{1}{2}}$ *if:*

$$\frac{1}{\sqrt{\epsilon_0\mu_0}}\tau < Ch. \quad (3.59)$$

where $C > 0$ *is the constant.*

Lemma 3.3.2. *Under the CFL condition Lemma(3.3.1) the DGTD (3.54)-(3.57) is stable in the sense of the discrete energy (3.58):*

$$\varepsilon^n \leq \varepsilon^0$$

Proof. Denote $\boldsymbol{E}^{[n+\frac{1}{2}]} = \frac{\boldsymbol{E}^n + \boldsymbol{E}^{n+1}}{2}$ and $\boldsymbol{K}^{[n+\frac{1}{2}]} = \frac{\boldsymbol{K}^n + \boldsymbol{K}^{n+1}}{2}$. Let $\boldsymbol{u}_i$ be $\boldsymbol{E}_i^{[n+\frac{1}{2}]}$ in equation(3.54) and $\boldsymbol{\psi}_i$ be $\boldsymbol{K}_i^{[n+\frac{1}{2}]}$ in equation (3.57). Equations (3.55) and (3.56) are used at time steps $n+\frac{3}{2}$ and at time step $n+\frac{1}{2}$ with $\boldsymbol{v}_i$ as $\boldsymbol{H}_i^{n+\frac{1}{2}}/2$ in equation(3.55) and $\boldsymbol{\phi}_i$ as $\boldsymbol{J}_i^{n+\frac{1}{2}}/2$ in equation(3.56). This yields the following relations:

$$\int_{T_i} \epsilon_0 \frac{\boldsymbol{E}_i^{n+1} - \boldsymbol{E}_i^n}{\tau} \cdot \boldsymbol{E}^{[n+\frac{1}{2}]} = \int_{T_i} \nabla \times \boldsymbol{E}^{[n+\frac{1}{2}]} \cdot \boldsymbol{H}_i^{n+\frac{1}{2}} - \int_{T_i} \boldsymbol{J}_i^{n+\frac{1}{2}} \cdot \boldsymbol{E}^{[n+\frac{1}{2}]} - \sum_{k \in \nu_i} \int_{a_{ik}} \boldsymbol{E}^{[n+\frac{1}{2}]} \cdot (\{\boldsymbol{H}_h^{n+\frac{1}{2}}\}_{ik} \times \boldsymbol{n}_{ik}) \tag{3.60}$$

$$\int_{T_i} \mu_0 \frac{\boldsymbol{H}_i^{n+\frac{3}{2}} - \boldsymbol{H}_i^{n+\frac{1}{2}}}{\tau} \cdot \boldsymbol{H}^{n+\frac{1}{2}}/2 = -\int_{T_i} \nabla \times \boldsymbol{H}^{n+\frac{1}{2}}/2 \cdot \boldsymbol{E}_i^{n+1} - \int_{T_i} \boldsymbol{K}_i^{n+1} \cdot \boldsymbol{H}^{n+\frac{1}{2}}/2 + \sum_{k \in \nu_i} \int_{a_{ik}} \boldsymbol{H}^{n+\frac{1}{2}}/2 \cdot (\{\boldsymbol{E}_h^{n+1}\}_{ik} \times \boldsymbol{n}_{ik}) \tag{3.61}$$

$$\int_{T_i} \mu_0 \frac{\boldsymbol{H}_i^{n+\frac{1}{2}} - \boldsymbol{H}_i^{n-\frac{1}{2}}}{\tau} \cdot \boldsymbol{H}^{n+\frac{1}{2}}/2 = -\int_{T_i} \nabla \times \boldsymbol{H}^{n+\frac{1}{2}}/2 \cdot \boldsymbol{E}_i^{n} - \int_{T_i} \boldsymbol{K}_i^{n} \cdot \boldsymbol{H}^{n+\frac{1}{2}}/2 + \sum_{k \in \nu_i} \int_{a_{ik}} \boldsymbol{H}^{n+\frac{1}{2}}/2 \cdot (\{\boldsymbol{E}_h^{n}\}_{ik} \times \boldsymbol{n}_{ik}) \tag{3.62}$$

$$\frac{1}{\epsilon_0 \omega_{pe}^2} \int_{T_i} \frac{\boldsymbol{J}_i^{n+\frac{3}{2}} - \boldsymbol{J}_i^{n+\frac{1}{2}}}{\tau} \cdot \boldsymbol{J}^{n+\frac{1}{2}}/2 + \frac{\Gamma_e}{\epsilon_0 \omega_{pe}^2} \int_{T_i} \frac{\boldsymbol{J}_i^{n+\frac{3}{2}} + \boldsymbol{J}_i^{n+\frac{1}{2}}}{2} \cdot \boldsymbol{J}^{n+\frac{1}{2}}/2 = \int_{T_i} \boldsymbol{E}_i^{n+1} \cdot \boldsymbol{J}^{n+\frac{1}{2}}/2 \tag{3.63}$$

$$\frac{1}{\epsilon_0 \omega_{pe}^2} \int_{T_i} \frac{\boldsymbol{J}_i^{n+\frac{1}{2}} - \boldsymbol{J}_i^{n-\frac{1}{2}}}{\tau} \cdot \boldsymbol{J}^{n+\frac{1}{2}}/2 + \frac{\Gamma_e}{\epsilon_0 \omega_{pe}^2} \int_{T_i} \frac{\boldsymbol{J}_i^{n+\frac{1}{2}} + \boldsymbol{J}_i^{n-\frac{1}{2}}}{2} \cdot \boldsymbol{J}^{n+\frac{1}{2}}/2 = \int_{T_i} \boldsymbol{E}_i^{n} \cdot \boldsymbol{J}^{n+\frac{1}{2}}/2 \tag{3.64}$$

$$\frac{1}{\mu_0 \omega_{pm}^2} \int_{T_i} \frac{\boldsymbol{K}_i^{n+1} - \boldsymbol{K}_i^{n}}{\tau} \cdot \boldsymbol{K}^{[n+\frac{1}{2}]} + \frac{\Gamma_m}{\mu_0 \omega_{pm}^2} \int_{T_i} \frac{\boldsymbol{K}_i^{n+1} + \boldsymbol{K}_i^{n}}{2} \cdot \boldsymbol{K}^{[n+\frac{1}{2}]} = \int_{T_i} \boldsymbol{H}_i^{n+\frac{1}{2}} \cdot \boldsymbol{K}^{[n+\frac{1}{2}]}. \tag{3.65}$$

Adding equations(3.60)-(3.65), and rearranging, we find:

$$\begin{aligned}
&\frac{1}{2}\int_{T_i}\epsilon_0\boldsymbol{E}_i^{n+1}\cdot\boldsymbol{E}_i^{n+1}+\frac{1}{2}\int_{T_i}\mu_0\boldsymbol{H}_i^{n+\frac{3}{2}}\cdot\boldsymbol{H}_i^{n+\frac{1}{2}}\\
+&\frac{1}{\mu_0\omega_{pm}^2}\int_{T_i}\boldsymbol{K}_i^{n+1}\cdot\boldsymbol{K}_i^{n+1}+\frac{2+\tau\Gamma_e}{4\epsilon_0\omega_{pe}^2}\int_{T_i}\boldsymbol{J}_i^{n+\frac{3}{2}}\cdot\boldsymbol{J}_i^{n+\frac{1}{2}}\\
=&\frac{1}{2}\int_{T_i}\epsilon_0\boldsymbol{E}_i^{n}\cdot\boldsymbol{E}_i^{n}+\frac{1}{2}\int_{T_i}\mu_0\boldsymbol{H}_i^{n+\frac{1}{2}}\cdot\boldsymbol{H}_i^{n-\frac{1}{2}}\\
+&\frac{1}{\mu_0\omega_{pm}^2}\int_{T_i}\boldsymbol{K}_i^{n}\cdot\boldsymbol{K}_i^{n}-\frac{2+\tau\Gamma_e}{4\epsilon_0\omega_{pe}^2}\int_{T_i}\boldsymbol{J}_i^{n+\frac{1}{2}}\cdot\boldsymbol{J}_i^{n-\frac{1}{2}}\\
+&\tau\int_{T_i}\nabla\times\boldsymbol{E}^{[n+\frac{1}{2}]}\cdot\boldsymbol{H}_i^{n+\frac{1}{2}}-\tau\int_{T_i}\nabla\times\boldsymbol{H}^{n+\frac{1}{2}}\cdot\boldsymbol{E}_i^{[n+\frac{1}{2}]}\\
-&\sum_{k\in\nu_i}\int_{a_{ik}}\tau\boldsymbol{E}^{[n+\frac{1}{2}]}\cdot(\{\boldsymbol{H}_h^{n+\frac{1}{2}}\}_{ik}\times\boldsymbol{n}_{ik})+\sum_{k\in\nu_i}\int_{a_{ik}}\tau\boldsymbol{H}^{n+\frac{1}{2}}\cdot(\{\boldsymbol{E}_h^{[n+\frac{1}{2}]}\}_{ik}\times\boldsymbol{n}_{ik})\\
-&\frac{\Gamma_e\tau}{2\epsilon_0\omega_{pe}^2}\int_{T_i}\boldsymbol{J}_i^{n+\frac{1}{2}}\cdot\boldsymbol{J}_i^{n+\frac{1}{2}}-\frac{\Gamma_m\tau}{\mu_0\omega_{pm}^2}\int_{T_i}\frac{\boldsymbol{K}_i^{n+1}+\boldsymbol{K}_i^{n}}{2}\cdot\boldsymbol{K}^{[n+\frac{1}{2}]}
\end{aligned}$$

Integrating by parts yields:

$$\begin{aligned}
\varepsilon_i^{n+1}=&\varepsilon_i^{n}-\frac{\tau\Gamma_e}{4\epsilon_0\omega_{pe}^2}\int_{T_i}\boldsymbol{J}_i^{n+\frac{3}{2}}\cdot\boldsymbol{J}_i^{n+\frac{1}{2}}-\frac{\tau\Gamma_e}{4\epsilon_0\omega_{pe}^2}\int_{T_i}\boldsymbol{J}_i^{n+\frac{1}{2}}\cdot\boldsymbol{J}_i^{n-\frac{1}{2}}\\
&-\frac{\tau}{2}\sum_{k\in\nu_i}\int_{a_{ik}}(\boldsymbol{E}_i^{[n+\frac{1}{2}]}\times\boldsymbol{H}_k^{n+\frac{1}{2}}+\boldsymbol{E}_k^{[n+\frac{1}{2}]}\times\boldsymbol{H}_i^{n+\frac{1}{2}})\cdot\boldsymbol{n}_{ik}\\
&-\frac{\Gamma_e\tau}{2\epsilon_0\omega_{pe}^2}\int_{T_i}\boldsymbol{J}_i^{n+\frac{1}{2}}\cdot\boldsymbol{J}_i^{n+\frac{1}{2}}-\frac{\tau\Gamma_m}{\mu_0\omega_{pm}^2}\int_{T_i}\frac{\boldsymbol{K}_i^{n+1}+\boldsymbol{K}_i^{n}}{2}\cdot\boldsymbol{K}^{[n+\frac{1}{2}]}
\end{aligned}$$

We see that the term involving the sum over k vanished because interface contributions cancel out when adding all of the elements together, leaving only the boundary, which is 0 by the metallic boundary condition. Next, adding from $n=0$ to $n=m-1$, we obtain:

$$\varepsilon^m\leq\varepsilon^0 \tag{3.66}$$

□

3.3.2 ERROR ESTIMATE OF THE FULLY DISCRETE SCHEME

Before we give the proof for the error estimate, let us prepare two lemmas.

Lemma 3.3.3. *Let* $(\boldsymbol{E},\boldsymbol{H},\boldsymbol{J},\boldsymbol{K})\in C^3([0,T],L(\Omega))\cap C^0([0,T],(\boldsymbol{H}^{s+1}(\Omega))^3)$. *Under the*

CFL condition Lemma(3.3.1), the following error estimate holds:

$$max_{n=0,\ldots,N}(||\boldsymbol{E}_h(t_n)-\boldsymbol{E}_h^n||^2+||\boldsymbol{H}_h(t_{n+\frac{1}{2}})-\boldsymbol{H}_h^{n+\frac{1}{2}}||^2+||\boldsymbol{J}_h(t_{n+\frac{1}{2}})-\boldsymbol{J}_h^{n+\frac{1}{2}}||^2+||\boldsymbol{K}_h(t_n)-\boldsymbol{K}_h^n||^2)^{\frac{1}{2}}$$
$$\leq C\tau^2||(\boldsymbol{E},\boldsymbol{H},\boldsymbol{J},\boldsymbol{K})||_{C^3([0,T],L^2(\Omega))}.$$

Proof. The proof is developed in a manner similar to that given in [40].
Define $\tilde{\boldsymbol{E}}_h^{n+1}$, $\tilde{\boldsymbol{H}}_h^{n+\frac{3}{2}}$, $\tilde{\boldsymbol{J}}_h^{n+\frac{3}{2}}$ and $\tilde{\boldsymbol{K}}_h^{n+1}$ such that

$$\int_{T_i}\epsilon_0\frac{\tilde{\boldsymbol{E}}_i^{n+1}-\boldsymbol{E}_i(t_n)}{\tau}\cdot\boldsymbol{u}_i=\int_{T_i}\nabla\times\boldsymbol{u}_i\cdot\boldsymbol{H}_i(t_{n+\frac{1}{2}})-\int_{T_i}\boldsymbol{J}_i(t_{n+\frac{1}{2}})\cdot\boldsymbol{u}_i$$
$$-\sum_{k\in\nu_i}\int_{a_{ik}}\boldsymbol{u}_i\cdot(\{\boldsymbol{H}_h(t_{n+\frac{1}{2}})\}_{ik}\times\boldsymbol{n}_{ik}) \tag{3.67}$$

$$\int_{T_i}\mu_0\frac{\tilde{\boldsymbol{H}}_i^{n+\frac{3}{2}}-\boldsymbol{H}_i(t_{n+\frac{1}{2}})}{\tau}\cdot\boldsymbol{v}_i=-\int_{T_i}\nabla\times\boldsymbol{v}_i\cdot\boldsymbol{E}_i(t_{n+1})-\int_{T_i}\boldsymbol{K}_i(t_{n+1})\cdot\boldsymbol{v}_i$$
$$+\sum_{k\in\nu_i}\int_{a_{ik}}\boldsymbol{v}_i\cdot(\{\boldsymbol{E}_h(t_{n+1})\}_{ik}\times\boldsymbol{n}_{ik}) \tag{3.68}$$

$$\frac{1}{\epsilon_0\omega_{pe}^2}\int_{T_i}\frac{\tilde{\boldsymbol{J}}_i^{n+\frac{3}{2}}-\boldsymbol{J}_i(t_{n+\frac{1}{2}})}{\tau}\cdot\boldsymbol{\phi}_i+\frac{\Gamma_e}{\epsilon_0\omega_{pe}^2}\int_{T_i}\frac{\boldsymbol{J}_i(t_{n+\frac{3}{2}})+\boldsymbol{J}_i(t_{n+\frac{1}{2}})}{2}\cdot\boldsymbol{\phi}_i=\int_{T_i}\boldsymbol{E}_i(t_{n+1})\cdot\boldsymbol{\phi}_i \tag{3.69}$$

$$\frac{1}{\mu_0\omega_{pm}^2}\int_{T_i}\frac{\tilde{\boldsymbol{K}}_i^{n+1}-\boldsymbol{K}_i(t_n)}{\tau}\cdot\boldsymbol{\psi}_i+\frac{\Gamma_m}{\mu_0\omega_{pm}^2}\int_{T_i}\frac{\boldsymbol{K}_i(t_{n+1})+\boldsymbol{K}_i(t_n)}{2}\cdot\boldsymbol{\psi}_i=\int_{T_i}\boldsymbol{H}_i(t_{n+\frac{1}{2}})\cdot\boldsymbol{\psi}_i. \tag{3.70}$$

Using Taylor's formula gives:

$$\boldsymbol{E}_h(t_{n+1})-\boldsymbol{E}_h(t_n)=\tau\frac{\partial}{\partial t}\boldsymbol{E}_h(t_{n+\frac{1}{2}})+\frac{\tau^3}{28}(\frac{\partial^3}{\partial t^3}\boldsymbol{E}_h(c_{n+1})+\frac{\partial^3}{\partial t^3}\boldsymbol{E}_h(c_n))$$

where $(c_{n+1},c_n)\in[t_{n+\frac{1}{2}},t_{n+1}]\times[t_n,t_{n+\frac{1}{2}}]$. This leads to the estimate:

$$\begin{aligned}&(||\boldsymbol{E}_h(t_{n+1})-\tilde{\boldsymbol{E}}_h^{n+1}||^2+||\boldsymbol{H}_h(t_{n+\frac{3}{2}})-\tilde{\boldsymbol{H}}_h^{n+\frac{3}{2}}||^2+||\boldsymbol{K}_h(t_{n+1})-\tilde{\boldsymbol{K}}_h^{n+1}||^2+||\boldsymbol{J}_h(t_{n+\frac{3}{2}})-\tilde{\boldsymbol{J}}_h^{n+\frac{3}{2}}||^2)^{\frac{1}{2}}\\&\leq C\tau^3(||\frac{\partial^3}{\partial t^3}\boldsymbol{E}_h||+||\frac{\partial^3}{\partial t^3}\boldsymbol{H}_h||+||\frac{\partial^2}{\partial t^2}\boldsymbol{J}_h||+||\frac{\partial^2}{\partial t^2}\boldsymbol{K}_h||)\\&\leq C\tau^3||(\boldsymbol{E},\boldsymbol{H},\boldsymbol{J},\boldsymbol{K})||_{C^3([0,T],L^2(\Omega))}\end{aligned} \tag{3.71}$$

Thus we can get

$$\int_{T_i} \epsilon_0 \frac{\boldsymbol{E}_i(t_{n+1}) - \boldsymbol{E}_i(t_n)}{\tau} \cdot \boldsymbol{u}_i = \int_{T_i} \nabla \times \boldsymbol{u}_i \cdot \boldsymbol{H}_i(t_{n+\frac{1}{2}}) - \int_{T_i} \boldsymbol{J}_i(t_{n+\frac{1}{2}}) \cdot \boldsymbol{u}_i$$
$$- \sum_{k \in \nu_i} \int_{a_{ik}} \boldsymbol{u}_i \cdot (\{\boldsymbol{H}_h(t_{n+\frac{1}{2}})\}_{ik} \times \boldsymbol{n}_{ik}) + \int_{T_i} \epsilon_0 \frac{\boldsymbol{E}_i(t_{n+1}) - \tilde{\boldsymbol{E}}_i^{n+1}}{\tau} \cdot \boldsymbol{u}_i$$
$$\int_{T_i} \mu_0 \frac{\boldsymbol{H}_i(t_{n+\frac{3}{2}}) - \boldsymbol{H}_i(t_{n+\frac{1}{2}})}{\tau} \cdot \boldsymbol{v}_i = - \int_{T_i} \nabla \times \boldsymbol{v}_i \cdot \boldsymbol{E}_i(t_{n+1}) - \int_{T_i} \boldsymbol{K}_i(t_{n+1}) \cdot \boldsymbol{v}_i$$
$$+ \sum_{k \in \nu_i} \int_{a_{ik}} \boldsymbol{v}_i \cdot (\{\boldsymbol{E}_h(t_{n+1})\}_{ik} \times \boldsymbol{n}_{ik}) + \int_{T_i} \mu_0 \frac{\boldsymbol{H}_i(t_{n+\frac{3}{2}}) - \tilde{\boldsymbol{H}}_i^{n+\frac{3}{2}}}{\tau} \cdot \boldsymbol{v}_i$$
$$\frac{1}{\epsilon_0 \omega_{pe}^2} \int_{T_i} \frac{\boldsymbol{J}_i(t_{n+\frac{3}{2}}) - \boldsymbol{J}_i(t_{n+\frac{1}{2}})}{\tau} \cdot \boldsymbol{\phi}_i + \frac{\Gamma_e}{\epsilon_0 \omega_{pe}^2} \int_{T_i} \frac{\boldsymbol{J}_i(t_{n+\frac{3}{2}}) + \boldsymbol{J}_i(t_{n+\frac{1}{2}})}{2} \cdot \boldsymbol{\phi}_i$$
$$= \int_{T_i} \boldsymbol{E}_i(t_{n+1}) \cdot \boldsymbol{\phi}_i + \frac{1}{\epsilon_0 \omega_{pe}^2} \int_{T_i} \frac{\boldsymbol{J}_i(t_{n+\frac{3}{2}}) - \tilde{\boldsymbol{J}}_i^{n+\frac{3}{2}}}{\tau} \cdot \boldsymbol{\phi}_i$$
$$\frac{1}{\mu_0 \omega_{pm}^2} \int_{T_i} \frac{\boldsymbol{K}_i(t_{n+1}) - \boldsymbol{K}_i(t_n)}{\tau} \cdot \boldsymbol{\psi}_i + \frac{\Gamma_m}{\mu_0 \omega_{pm}^2} \int_{T_i} \frac{\boldsymbol{K}_i(t_{n+1}) + \boldsymbol{K}_i(t_n)}{2} \cdot \boldsymbol{\psi}_i$$
$$= \int_{T_i} \boldsymbol{H}_i(t_{n+\frac{1}{2}}) \cdot \boldsymbol{\psi}_i + \frac{1}{\mu_0 \omega_{pm}^2} \int_{T_i} \frac{\boldsymbol{K}_i(t_{n+1}) - \tilde{\boldsymbol{K}}_i^{n+1}}{\tau} \cdot \boldsymbol{\psi}_i.$$

Now, if one defines,

$$\xi_i^n(\boldsymbol{u}_i) = \int_{T_i} \epsilon_0 \frac{\boldsymbol{E}_i(t_{n+1}) - \tilde{\boldsymbol{E}}_i^{n+1}}{\tau} \cdot \boldsymbol{u}_i,$$
$$\eta_i^n(\boldsymbol{v}_i) = \int_{T_i} \mu_0 \frac{\boldsymbol{H}_i(t_{n+\frac{3}{2}}) - \tilde{\boldsymbol{H}}_i^{n+\frac{3}{2}}}{\tau} \cdot \boldsymbol{v}_i,$$
$$\zeta_i^n(\boldsymbol{\phi}_i) = \frac{1}{\epsilon_0 \omega_{pe}^2} \int_{T_i} \frac{\boldsymbol{J}_i(t_{n+\frac{3}{2}}) - \tilde{\boldsymbol{J}}_i^{n+\frac{3}{2}}}{\tau} \cdot \boldsymbol{\phi}_i,$$
$$\chi_i^n(\boldsymbol{\psi}_i) = \frac{1}{\mu_0 \omega_{pm}^2} \int_{T_i} \frac{\boldsymbol{K}_i(t_{n+1}) - \tilde{\boldsymbol{K}}_i^{n+1}}{\tau} \cdot \boldsymbol{\psi}_i,$$

then one has:

$$\int_{T_i} \epsilon_0 \frac{\boldsymbol{E}_i(t_{n+1}) - \boldsymbol{E}_i(t_n)}{\tau} \cdot \boldsymbol{u}_i = \int_{T_i} \nabla \times \boldsymbol{u}_i \cdot \boldsymbol{H}_i(t_{n+\frac{1}{2}}) - \int_{T_i} \boldsymbol{J}_i(t_{n+\frac{1}{2}}) \cdot \boldsymbol{u}_i$$
$$- \sum_{k \in \nu_i} \int_{a_{ik}} \boldsymbol{u}_i \cdot (\{\boldsymbol{H}_h(t_{n+\frac{1}{2}})\}_{ik} \times \boldsymbol{n}_{ik}) + \xi_i^n(\boldsymbol{u}_i) \tag{3.72}$$
$$\int_{T_i} \mu_0 \frac{\boldsymbol{H}_i(t_{n+\frac{3}{2}}) - \boldsymbol{H}_i(t_{n+\frac{1}{2}})}{\tau} \cdot \boldsymbol{v}_i = -\int_{T_i} \nabla \times \boldsymbol{v}_i \cdot \boldsymbol{E}_i(t_{n+1}) - \int_{T_i} \boldsymbol{K}_i(t_{n+1}) \cdot \boldsymbol{v}_i$$
$$+ \sum_{k \in \nu_i} \int_{a_{ik}} \boldsymbol{v}_i \cdot (\{\boldsymbol{E}_h(t_{n+1})\}_{ik} \times \boldsymbol{n}_{ik}) + \eta_i^n(\boldsymbol{v}_i) \tag{3.73}$$
$$\frac{1}{\epsilon_0 \omega_{pe}^2} \int_{T_i} \frac{\boldsymbol{J}_i(t_{n+\frac{3}{2}}) - \boldsymbol{J}_i(t_{n+\frac{1}{2}})}{\tau} \cdot \boldsymbol{\phi}_i + \frac{\Gamma_e}{\epsilon_0 \omega_{pe}^2} \int_{T_i} \frac{\boldsymbol{J}_i(t_{n+\frac{3}{2}}) + \boldsymbol{J}_i(t_{n+\frac{1}{2}})}{2} \cdot \boldsymbol{\phi}_i$$
$$= \int_{T_i} \boldsymbol{E}_i(t_{n+1}) \cdot \boldsymbol{\phi}_i + \zeta_i^n(\boldsymbol{\phi}_i) \tag{3.74}$$
$$\frac{1}{\mu_0 \omega_{pm}^2} \int_{T_i} \frac{\boldsymbol{K}_i(t_{n+1}) - \boldsymbol{K}_i(t_n)}{\tau} \cdot \boldsymbol{\psi}_i + \frac{\Gamma_m}{\mu_0 \omega_{pm}^2} \int_{T_i} \frac{\boldsymbol{K}_i(t_{n+1}) + \boldsymbol{K}_i(t_n)}{2} \cdot \boldsymbol{\psi}_i$$
$$= \int_{T_i} \boldsymbol{H}_i(t_{n+\frac{1}{2}}) \cdot \boldsymbol{\psi}_i + \chi_i^n(\boldsymbol{\psi}_i). \tag{3.75}$$

When considering the whole domain, we get

$$\xi_h^n(\boldsymbol{u}_h) = \int_\Omega \epsilon_0 \frac{\boldsymbol{E}_h(t_{n+1}) - \tilde{\boldsymbol{E}}_h^{n+1}}{\tau} \cdot \boldsymbol{u}_h,$$
$$\eta_h^n(\boldsymbol{v}_h) = \int_\Omega \mu_0 \frac{\boldsymbol{H}_h(t_{n+\frac{3}{2}}) - \tilde{\boldsymbol{H}}_h^{n+\frac{3}{2}}}{\tau} \cdot \boldsymbol{v}_h,$$
$$\zeta_h^n(\boldsymbol{\phi}_h) = \frac{1}{\epsilon_0 \omega_{pe}^2} \int_\Omega \frac{\boldsymbol{J}_h(t_{n+\frac{3}{2}}) - \tilde{\boldsymbol{J}}_h^{n+\frac{3}{2}}}{\tau} \cdot \boldsymbol{\phi}_h,$$
$$\chi_h^n(\boldsymbol{\psi}_h) = \frac{1}{\mu_0 \omega_{pm}^2} \int_\Omega \frac{\boldsymbol{K}_h(t_{n+1}) - \tilde{\boldsymbol{K}}_h^{n+1}}{\tau} \cdot \boldsymbol{\psi}_h,$$

and

$$|\xi_h^n(\boldsymbol{u}_h)| \leq \frac{C}{\tau} ||\boldsymbol{E}_h(t_{n+1}) - \tilde{\boldsymbol{E}}_h^{n+1}|| \, ||\boldsymbol{u}_h||,$$
$$|\eta_h^n(\boldsymbol{v}_h)| \leq \frac{C}{\tau} ||\boldsymbol{H}_h(t_{n+\frac{3}{2}}) - \tilde{\boldsymbol{H}}_h^{n+\frac{3}{2}}|| \, ||\boldsymbol{v}_h||,$$
$$|\zeta_h^n(\boldsymbol{\phi}_h)| \leq \frac{C}{\tau} ||\boldsymbol{J}_h(t_{n+\frac{3}{2}}) - \tilde{\boldsymbol{J}}_h^{n+\frac{3}{2}}|| \, ||\boldsymbol{\phi}_h||,$$
$$|\chi_h^n(\boldsymbol{\psi}_h)| \leq \frac{C}{\tau} ||\boldsymbol{K}_h(t_{n+1}) - \tilde{\boldsymbol{K}}_h^{n+1}|| \, ||\boldsymbol{\psi}_h||,$$

By the estimate (3.71),

$$|||\xi_h^n||| + |||\eta_h^n|||| + |\varsigma_h^n||| + |||\chi_h^n||| \tag{3.76}$$

$$\leq C\tau^2 ||(\boldsymbol{E}, \boldsymbol{H}, \boldsymbol{J}, \boldsymbol{K})||_{C^3([0,T],L^2(\Omega))} \tag{3.77}$$

Next define the error terms as:

$$a_h^n = \boldsymbol{E}_h(t_n) - \boldsymbol{E}_h^n, \quad b_h^{n+\frac{1}{2}} = \boldsymbol{H}_h(t_{n+\frac{1}{2}}) - \boldsymbol{H}_h^{n+\frac{1}{2}},$$
$$c_h^{n+\frac{1}{2}} = \boldsymbol{J}_h(t_{n+\frac{1}{2}}) - \boldsymbol{J}_h^{n+\frac{1}{2}}, \quad d_h^n = \boldsymbol{K}_h(t_n) - \boldsymbol{K}_h^n.$$

Subtracting equations(3.54)-(3.57) from equations (3.72)-(3.75), we find:

$$\int_{T_i} \epsilon_0 \frac{a_i^{n+1} - a_i^n}{\tau} \cdot \boldsymbol{u}_i = \int_{T_i} \nabla \times \boldsymbol{u}_i \cdot b_i^{n+\frac{1}{2}} - \int_{T_i} \boldsymbol{c}_i^{n+\frac{1}{2}} \cdot \boldsymbol{u}_i$$
$$- \sum_{k \in \nu_i} \int_{a_{ik}} \boldsymbol{u}_i \cdot (\{b_h^{n+\frac{1}{2}}\}_{ik} \times \boldsymbol{n}_{ik}) + \xi_i^n(\boldsymbol{u}_i)$$
$$\int_{T_i} \mu_0 \frac{b_i^{n+\frac{3}{2}} - b_i^{n+\frac{1}{2}}}{\tau} \cdot \boldsymbol{v}_i = -\int_{T_i} \nabla \times \boldsymbol{v}_i \cdot a_i^{n+1} - \int_{T_i} d_i^{n+1} \cdot \boldsymbol{v}_i$$
$$+ \sum_{k \in \nu_i} \int_{a_{ik}} \boldsymbol{v}_i \cdot (\{a_h^{n+1}\}_{ik} \times \boldsymbol{n}_{ik}) + \eta_i^n(\boldsymbol{v}_i)$$
$$\frac{1}{\epsilon_0 \omega_{pe}^2} \int_{T_i} \frac{c_i^{n+\frac{3}{2}} - c_i^{n+\frac{1}{2}}}{\tau} \cdot \boldsymbol{\phi}_i + \frac{\Gamma_e}{\epsilon_0 \omega_{pe}^2} \int_{T_i} \frac{c_i^{n+\frac{3}{2}} + c_i^{n+\frac{1}{2}}}{2} \cdot \boldsymbol{\phi}_i$$
$$= \int_{T_i} a_i^{n+1} \cdot \boldsymbol{\phi}_i + \zeta_i^n(\boldsymbol{\phi}_i)$$
$$\frac{1}{\mu_0 \omega_{pm}^2} \int_{T_i} \frac{d_i^{n+1} - d_i^n}{\tau} \cdot \boldsymbol{\psi}_i + \frac{\Gamma_m}{\mu_0 \omega_{pm}^2} \int_{T_i} \frac{d_i^{n+1} + d_i^n}{2} \cdot \boldsymbol{\psi}_i$$
$$= \int_{T_i} b_i^{n+\frac{1}{2}} \cdot \boldsymbol{\psi}_i + \chi_i^n(\boldsymbol{\psi}_i).$$

Similar to the proof of stability in the sense of discrete energy (3.3.2), we get:

$$
\begin{aligned}
&\frac{1}{2}\epsilon_0\langle a_i^{n+1}, a_i^{n+1}\rangle + \frac{1}{2}\mu_0\langle b_i^{n+\frac{3}{2}}, b_i^{n+\frac{1}{2}}\rangle + \frac{1}{2\epsilon_0\omega_{pe}^2}\langle c_i^{n+\frac{3}{2}}, c_i^{n+\frac{1}{2}}\rangle \\
&+ \frac{1}{2\mu_0\omega_{pm}}\langle d_i^{n+1}, d_i^{n+1}\rangle + \frac{\tau\Gamma_e}{4\epsilon_0\omega_{pe}^2}\int_{T_i} c_i^{n+\frac{3}{2}}\cdot c_i^{n+\frac{1}{2}} \\
=&\frac{1}{2}\epsilon_0\langle a_i^{n}, a_i^{n}\rangle + \frac{1}{2}\mu_0\langle b_i^{n-\frac{1}{2}}, b_i^{n+\frac{1}{2}}\rangle + \frac{1}{2\epsilon_0\omega_{pe}^2}\langle c_i^{n-\frac{1}{2}}, c_i^{n+\frac{1}{2}}\rangle \\
&+ \frac{1}{2\mu_0\omega_{pm}}\langle d_i^{n}, d_i^{n}\rangle - \frac{\tau\Gamma_e}{4\epsilon_0\omega_{pe}^2}\int_{T_i} c_i^{n+\frac{1}{2}}\cdot c_i^{n-\frac{1}{2}} \\
&-\frac{\tau}{2}\sum_{k\in\nu_i}\int_{a_{ik}} (a_i^{[n+\frac{1}{2}]}\times b_k^{n+\frac{1}{2}} + a_k^{[n+\frac{1}{2}]}\times b_i^{n+\frac{1}{2}})\cdot \boldsymbol{n}_{ik} \\
&-\frac{\tau\Gamma_e}{2\epsilon_0\omega_{pe}^2}\int_{T_i} c_i^{n+\frac{1}{2}}\cdot c_i^{n+\frac{1}{2}} - \frac{\tau\Gamma_m}{\mu_0\omega_{pm}^2}\int_{T_i}\frac{d_i^{n+1}+d_i^n}{2}\cdot d^{[n+\frac{1}{2}]} \\
&+\frac{\tau}{2}(\xi_i^n(a_i^{[n+\frac{1}{2}]}) + \eta_i^n(b_i^{n+\frac{1}{2}}) + \eta_i^{n+1}(b_i^{n+\frac{1}{2}}) + \zeta_i^n(c_i^{n+\frac{1}{2}}) + \zeta_i^{n+1}(c_i^{n+\frac{1}{2}}) + \chi_h^n(d_i^{[n+\frac{1}{2}]})).
\end{aligned}
$$

Again, the term involving a sum over k will vanish due to canceling interface contributions and the metallic boundary condition when adding all elements together, leaving

$$
\begin{aligned}
&\frac{1}{2}\epsilon_0\langle a_h^{n+1}, a_h^{n+1}\rangle + \frac{1}{2}\mu_0\langle b_h^{n+\frac{3}{2}}, b_h^{n+\frac{1}{2}}\rangle + \frac{1}{2\epsilon_0\omega_{pe}^2}\langle c_h^{n+\frac{3}{2}}, c_h^{n+\frac{1}{2}}\rangle + \frac{1}{2\mu_0\omega_{pm}^2}\langle d_h^{n+1}, d_h^{n+1}\rangle \\
=&\frac{1}{2}\epsilon_0\langle a_h^{n}, a_h^{n}\rangle + \frac{1}{2}\mu_0\langle b_h^{n-\frac{1}{2}}, b_h^{n+\frac{1}{2}}\rangle + \frac{1}{2\epsilon_0\omega_{pe}^2}\langle c_h^{n-\frac{1}{2}}, c_h^{n+\frac{1}{2}}\rangle \\
&+ \frac{1}{2\mu_0\omega_{pm}^2}\langle d_h^{n}, d_h^{n}\rangle - \frac{\tau\Gamma_e}{4\epsilon_0\omega_{pe}^2}\sum\int_{T_i} c_i^{n+\frac{1}{2}}\cdot c_i^{n-\frac{1}{2}} \\
&-\frac{\tau\Gamma_e}{4\epsilon_0\omega_{pe}^2}\sum_{T_i}\int_{T_i} c_i^{n+\frac{3}{2}}\cdot c_i^{n+\frac{1}{2}} - \frac{\tau\Gamma_e}{2\epsilon_0\omega_{pe}^2}\sum_{T_i}\int_{T_i} c_i^{n+\frac{1}{2}}\cdot c_i^{n+\frac{1}{2}} - \frac{\tau\Gamma_m}{\mu_0\omega_{pm}^2}\sum_{T_i}\int_{T_i}\frac{d_i^{n+1}+d_i^n}{2}\cdot d_i^{[n+\frac{1}{2}]} \\
&+\frac{\tau}{2}(\xi_h^n(a_h^{[n+\frac{1}{2}]}) + \eta_h^n(b_h^{n+\frac{1}{2}}) + \eta_h^{n+1}(b_h^{n+\frac{1}{2}}) + \zeta_h^n(c_h^{n+\frac{1}{2}}) + \zeta_h^{n+1}(c_h^{n+\frac{1}{2}}) + \chi_h^n(d_i^{[n+\frac{1}{2}]})).
\end{aligned}
$$

Using (3.77) and adding from $n=1$ to $n=m-1$, we get

$$
\begin{aligned}
&(\frac{1}{2}\epsilon_0\langle a_h^m, a_h^m\rangle + \frac{1}{2}\mu_0\langle b_h^{m+\frac{1}{2}}, b_h^{m-\frac{1}{2}}\rangle + \frac{1}{2\epsilon_0\omega_{pe}^2}\langle c_h^{m+\frac{1}{2}}, c_h^{m-\frac{1}{2}}\rangle + \frac{1}{2\mu_0\omega_{pm}^2}\langle d_h^m, d_h^m\rangle)^{\frac{1}{2}} \\
\le&(\frac{1}{2}\epsilon_0\langle a_h^0, a_h^0\rangle + \frac{1}{2}\mu_0\langle b_h^{-\frac{1}{2}}, b_h^{\frac{1}{2}}\rangle + \frac{1}{2\epsilon_0\omega_{pe}^2}\langle c_h^{-\frac{1}{2}}, c_h^{\frac{1}{2}}\rangle + \frac{1}{2\mu_0\omega_{pm}^2}\langle d_h^0, d_h^0\rangle)^{\frac{1}{2}} \\
\le&C\tau^2||(\boldsymbol{E},\boldsymbol{H},\boldsymbol{J},\boldsymbol{K})||_{C^3([0,T],L^2(\Omega))}
\end{aligned}
$$

Therefore,

$$max_{n=0,\dots,N}(||\boldsymbol{E}_h(t_n)-\boldsymbol{E}_h^n||^2+||\boldsymbol{H}_h(t_{n+\frac{1}{2}})-\boldsymbol{H}_h^{n+\frac{1}{2}}||^2+||\boldsymbol{J}_h(t_{n+\frac{1}{2}})-\boldsymbol{J}_h^{n+\frac{1}{2}}||^2+||\boldsymbol{K}_h(t_n)-\boldsymbol{K}_h^n||^2)^{\frac{1}{2}}$$
$$\leq C\tau^2||(\boldsymbol{E},\boldsymbol{H},\boldsymbol{J},\boldsymbol{K})||_{C^3([0,T],L^2(\Omega))}.$$

□

Lemma 3.3.4. *Let P_h denote the standard L^2-projection onto V_h or V_h^0, which is the subspace of V_h with the boundary condition $\boldsymbol{n}\times\boldsymbol{E}=0$ imposed. It is known that the projection error estimate*

$$\|u-P_hu\|_{0,T}\leq Ch_T^{min\{s,k\}+1}\|u\|_{s+1,T}\,, \tag{3.78}$$

holds true for any element T, and that $u\in H^{s+1}(T)$.

Let $(\boldsymbol{E}_h,\boldsymbol{H}_h,\boldsymbol{J},\boldsymbol{K})$ be the weak solution of (3.54)-(3.57), and $(\boldsymbol{E},\boldsymbol{H},\boldsymbol{J},\boldsymbol{K})$ be the solution of (3.1)-(3.4).

$$(\epsilon_0||P_h\boldsymbol{E}-\boldsymbol{E}_h||^2+\mu_0||P_hH-H_h||^2+\frac{1}{\epsilon_0\omega_{pe}^2}||P_h\boldsymbol{J}-\boldsymbol{J}_h||^2+\frac{1}{\mu_0\omega_{pm}^2}||P_h\boldsymbol{K}-\boldsymbol{K}_h||^2)^{\frac{1}{2}}$$
$$\leq Ch^{min\{s,k\}}||(H,E,J,K)||_{C^0([0,T],H^{s+1}(\Omega))}$$

where k is the degree of the basis function.

Proof. We proceed in the same fashion as in Lemma(2.2.4). The semidiscrete scheme for (3.54)-(3.57) is:

$$\begin{aligned}\int_{T_i}\epsilon_0\frac{\partial\boldsymbol{E}_i}{\partial t}\cdot\boldsymbol{u}_i&=\int_{T_i}\nabla\times\boldsymbol{u}_i\cdot\boldsymbol{H}_i-\int_{T_i}\boldsymbol{J}_i\cdot\boldsymbol{u}_i\\&\quad-\sum_{k\in\nu_i}\int_{a_{ik}}\boldsymbol{u}_i\cdot(\{\boldsymbol{H}_h\}_{ik}\times\boldsymbol{n}_{ik})\end{aligned}\tag{3.79}$$

$$\begin{aligned}\int_{T_i}\mu_0\frac{\partial\boldsymbol{H}_i}{\partial t}\cdot\boldsymbol{v}_i&=-\int_{T_i}\nabla\times\boldsymbol{v}_i\cdot\boldsymbol{E}_i-\int_{T_i}\boldsymbol{K}_i\cdot\boldsymbol{v}_i\\&\quad+\sum_{k\in\nu_i}\int_{a_{ik}}\boldsymbol{v}_i\cdot(\{\boldsymbol{E}_h\}_{ik}\times\boldsymbol{n}_{ik})\end{aligned}\tag{3.80}$$

$$\frac{1}{\epsilon_0\omega_{pe}^2}\int_{T_i}\frac{\partial\boldsymbol{J}_i}{\partial t}\cdot\boldsymbol{\phi}_i+\frac{\Gamma_e}{\epsilon_0\omega_{pe}^2}\int_{T_i}\boldsymbol{J}_i\cdot\boldsymbol{\phi}_i=\int_{T_i}\boldsymbol{E}_i\cdot\boldsymbol{\phi}_i \tag{3.81}$$

$$\frac{1}{\mu_0\omega_{pm}^2}\int_{T_i}\frac{\partial\boldsymbol{K}_i}{\partial t}\cdot\boldsymbol{\psi}_i+\frac{\Gamma_m}{\mu_0\omega_{pm}^2}\int_{T_i}\boldsymbol{K}_i\cdot\boldsymbol{\psi}_i=\int_{T_i}\boldsymbol{H}_i\cdot\boldsymbol{\psi}_i. \tag{3.82}$$

Multiplying (3.1) by $\boldsymbol{u}_h \in \mathrm{V}_h$, (3.2) by $\boldsymbol{v}_h \in \mathrm{V}_h$, (3.3) by $\boldsymbol{\phi}_h \in \mathrm{V}_h$, and (3.4) by $\boldsymbol{\psi}_h \in \mathrm{V}_h$, and then integrating each over $\mathcal{T}_i$, we get

$$\begin{aligned}\int_{T_i} \epsilon_0 \frac{\partial \boldsymbol{E}}{\partial t} \cdot \boldsymbol{u}_i &= \int_{T_i} \nabla \times \boldsymbol{H} \cdot \boldsymbol{u}_i - \int_{T_i} \boldsymbol{J} \cdot \boldsymbol{u}_i \\ &= \int_{T_i} \nabla \times \boldsymbol{u}_i \cdot \boldsymbol{H} - \int_{T_i} \boldsymbol{J} \cdot \boldsymbol{u}_i \\ &\quad - \sum_{k \in \nu_i} \int_{a_{ik}} \boldsymbol{u}_i \cdot (\{\boldsymbol{H}\}_{ik} \times \boldsymbol{n}_{ik}) \end{aligned} \tag{3.83}$$

$$\begin{aligned}\int_{T_i} \mu_0 \frac{\partial \boldsymbol{H}}{\partial t} \cdot \boldsymbol{v}_i &= - \int_{T_i} \nabla \times \boldsymbol{E} \cdot \boldsymbol{v}_i - \int_{T_i} \boldsymbol{K} \cdot \boldsymbol{v}_i \\ &= - \int_{T_i} \nabla \times \boldsymbol{v}_i \cdot \boldsymbol{E} - \int_{T_i} \boldsymbol{K} \cdot \boldsymbol{v}_i \\ &\quad + \sum_{k \in \nu_i} \int_{a_{ik}} \boldsymbol{v}_i \cdot (\{\boldsymbol{E}\}_{ik} \times \boldsymbol{n}_{ik}) \end{aligned} \tag{3.84}$$

$$\frac{1}{\epsilon_0 \omega_{pe}^2} \int_{T_i} \frac{\partial \boldsymbol{J}}{\partial t} \cdot \boldsymbol{\phi}_i + \frac{\Gamma_e}{\epsilon_0 \omega_{pe}^2} \int_{T_i} \boldsymbol{J} \cdot \boldsymbol{\phi}_i = \int_{T_i} \boldsymbol{E} \cdot \boldsymbol{\phi}_i \tag{3.85}$$

$$\frac{1}{\mu_0 \omega_{pm}^2} \int_{T_i} \frac{\partial \boldsymbol{K}}{\partial t} \cdot \boldsymbol{\psi}_i + \frac{\Gamma_m}{\mu_0 \omega_{pm}^2} \int_{T_i} \boldsymbol{K} \cdot \boldsymbol{\psi}_i = \int_{T_i} \boldsymbol{H} \cdot \boldsymbol{\psi}_i. \tag{3.86}$$

To simplify matters,Let $\xi_h = P_h \boldsymbol{E} - \boldsymbol{E}_h, \eta_h = P_h \boldsymbol{H} - \boldsymbol{H}_h, \tilde{\xi}_h = P_h \boldsymbol{J} - \boldsymbol{J}_h, \tilde{\eta}_h = P_h \boldsymbol{K} - \boldsymbol{K}_h$. Subtracting(3.79)-(3.82) from (3.83)-(3.86), and adding all elements together, we find

$$\begin{aligned}&\epsilon_0 (\frac{\partial}{\partial t} \xi_h, \boldsymbol{u}_h) - (\eta_h, \nabla \times \boldsymbol{u}_h) + (\tilde{\xi}_h, \boldsymbol{u}_h) + \sum_{T_i} \sum_{k \in \nu_i} \int_{a_{ik}} \boldsymbol{u}_i \cdot (\{\eta_h\}_{ik} \times \boldsymbol{n}_{ik}) \\ =&\epsilon_0 (\frac{\partial}{\partial t} (P_h \boldsymbol{E} - \boldsymbol{E}), \boldsymbol{u}_h) - ((P_h \boldsymbol{H} - \boldsymbol{H}), \nabla \times \boldsymbol{u}_h) \\ &+ (P_h \boldsymbol{J} - \boldsymbol{J}, \boldsymbol{u}_h) + \sum_{T_i} \sum_{k \in \nu_i} \int_{a_{ik}} \boldsymbol{u}_i \cdot (\{P_h \boldsymbol{H} - \boldsymbol{H}\}_{ik} \times \boldsymbol{n}_{ik}) \end{aligned} \tag{3.87}$$

$$\begin{aligned}&\mu_0 (\frac{\partial}{\partial t} \eta_h, \boldsymbol{v}_h) + (\xi_h, \nabla \times \boldsymbol{v}_h) + (\tilde{\eta}_h, \boldsymbol{v}_h) - \sum_{T_i} \sum_{k \in \nu_i} \int_{a_{ik}} \boldsymbol{v}_i \cdot (\{\xi_h\}_{ik} \times \boldsymbol{n}_{ik}) \\ =&\mu_0 (\frac{\partial}{\partial t} (P_h \boldsymbol{H} - \boldsymbol{H}), \boldsymbol{v}_h) + (P_h \boldsymbol{E} - \boldsymbol{E}, \nabla \times \boldsymbol{v}_h) \\ &+ (P_h \boldsymbol{K} - \boldsymbol{K}, \boldsymbol{v}_h) - \sum_{T_i} \sum_{k \in \nu_i} \int_{a_{ik}} \boldsymbol{v}_i \cdot (\{P_h \boldsymbol{E} - \boldsymbol{E}\}_{ik} \times \boldsymbol{n}_{ik}) \end{aligned} \tag{3.88}$$

$$\frac{1}{\epsilon_0\omega_{pe}^2}(\frac{\partial\tilde{\xi}_h}{\partial t},\boldsymbol{\phi}_h)+\frac{\Gamma_e}{\epsilon_0\omega_{pe}^2}(\tilde{\xi}_h,\boldsymbol{\phi}_h)-(\xi_h,\boldsymbol{\phi}_h)$$
$$=\frac{1}{\epsilon_0\omega_{pe}^2})(\frac{\partial}{\partial t}(P_h\boldsymbol{J}-\boldsymbol{J}),\boldsymbol{\phi}_h)+\frac{\Gamma_e}{\epsilon_0\omega_{pe}^2}(P_h\boldsymbol{J}-\boldsymbol{J},\boldsymbol{\phi}_h)-(P_h\boldsymbol{E}-\boldsymbol{E},\boldsymbol{\phi}_h) \tag{3.89}$$

$$\frac{1}{\mu_0\omega_{pm}^2}(\frac{\partial\tilde{\eta}_h}{\partial t},\boldsymbol{\psi}_h)+\frac{\Gamma_m}{\mu_0\omega_{pm}^2}(\tilde{\eta}_h,\boldsymbol{\psi}_h)-(\eta_h,\boldsymbol{\psi}_h)$$
$$=\frac{1}{\epsilon_0\omega_{pm}^2})(\frac{\partial}{\partial t}(P_h\boldsymbol{K}-\boldsymbol{K}),\boldsymbol{\psi}_h)+\frac{\Gamma_m}{\epsilon_0\omega_{pm}^2}(P_h\boldsymbol{K}-\boldsymbol{K},\boldsymbol{\psi}_h)-(P_h\boldsymbol{H}-\boldsymbol{H},\boldsymbol{\psi}_h). \tag{3.90}$$

Letting $\boldsymbol{u}_h=\xi_h$, $\boldsymbol{v}_h=\eta_h$, $\boldsymbol{\phi}_h=\tilde{\xi}_h$ and $\boldsymbol{\psi}_h=\tilde{\eta}_h$, and adding equations (3.87), (3.88), (3.89) and (3.90)together, we can get

$$\begin{aligned}
&\epsilon_0(\frac{\partial}{\partial t}\xi_h,\xi_h)+\mu_0(\frac{\partial}{\partial t}\eta_h,\eta_h)+\frac{1}{\epsilon_0\omega_{pe}^2}(\frac{\partial}{\partial t}\tilde{\xi}_h,\tilde{\xi}_h)+\frac{1}{\mu_0\omega_{pe}^2}(\frac{\partial}{\partial t}\tilde{\eta}_h,\tilde{\eta}_h)\\
=&-\frac{1}{2}\sum_{T_i}\sum_{k\in\nu_i}\int_{a_{ik}}(\xi_i\times\eta_k+\xi_k\times\eta_i)\cdot\boldsymbol{n}_{ik})-\frac{\Gamma_e}{\epsilon_0\omega_{pe}^2}(\tilde{\xi}_h,\tilde{\xi}_h)-\frac{\Gamma_m}{\mu_0\omega_{pm}^2}(\tilde{\eta}_h,\tilde{\eta}_h)\\
&+\epsilon_0(\frac{\partial}{\partial t}(P_h\boldsymbol{E}-\boldsymbol{E}),\xi_h)-(P_h\boldsymbol{H}-\boldsymbol{H},\nabla\times\xi_h)+\sum_{T_i}\sum_{k\in\nu_i}\int_{a_{ik}}\xi_i\cdot\{P_h\boldsymbol{H}-\boldsymbol{H}\}\times\boldsymbol{n}_{ik}\\
&+\mu_0(\frac{\partial}{\partial t}(P_h\boldsymbol{H}-\boldsymbol{H}),\eta_h)+(P_h\boldsymbol{E}-\boldsymbol{E},\nabla\times\eta_h)-\sum_{T_i}\sum_{k\in\nu_i}\int_{a_{ik}}\eta_i\cdot\{P_h\boldsymbol{E}-\boldsymbol{E}\}\times\boldsymbol{n}_{ik}\\
&+\frac{1}{\epsilon_0\omega_{pe}^2}(\frac{\partial}{\partial t}(P_h\boldsymbol{J}-\boldsymbol{J}),\tilde{\xi}_h)-\frac{\Gamma_e}{\epsilon_0\omega_{pe}^2}(\tilde{\xi}_h,\tilde{\xi}_h)+\frac{1}{\mu_0\omega_{pm}^2}(\frac{\partial}{\partial t}(P_h\boldsymbol{K}-\boldsymbol{K}),\tilde{\eta}_h)-\frac{\Gamma_m}{\mu_0\omega_{pm}^2}(\tilde{\eta}_h,\tilde{\eta}_h)\\
\leq&\epsilon_0(\frac{\partial}{\partial t}(P_h\boldsymbol{E}-\boldsymbol{E}),\xi_h)-(P_h\boldsymbol{H}-\boldsymbol{H},\nabla\times\xi_h)+\sum_{T_i}\sum_{k\in\nu_i}\int_{a_{ik}}\xi_i\cdot\{P_h\boldsymbol{H}-\boldsymbol{H}\}\times\boldsymbol{n}_{ik}\\
&+\mu_0(\frac{\partial}{\partial t}(P_h\boldsymbol{H}-\boldsymbol{H}),\eta_h)+(P_h\boldsymbol{E}-\boldsymbol{E},\nabla\times\eta_h)-\sum_{T_i}\sum_{k\in\nu_i}\int_{a_{ik}}\eta_i\cdot\{P_h\boldsymbol{E}-\boldsymbol{E}\}\times\boldsymbol{n}_{ik}\\
&+\frac{1}{\epsilon_0\omega_{pe}^2}(\frac{\partial}{\partial t}(P_h\boldsymbol{J}-\boldsymbol{J}),\tilde{\xi}_h)+\frac{1}{\mu_0\omega_{pm}^2}(\frac{\partial}{\partial t}(P_h\boldsymbol{K}-\boldsymbol{K}),\tilde{\eta}_h) \qquad (3.91)\\
=&\sum_{i=1}^{8}Err_i, \qquad (3.92)
\end{aligned}$$

where $Err_1=0$, $Err_2=0$, $Err_4=0$, $Err_5=0$, $Err_7=0$, $Err_8=0$ by the property of L^2 projection. Further,

$$Err_3\leq\frac{C_{inv}}{h}||\xi_h||\cdot||P_h\boldsymbol{H}-\boldsymbol{H}|| \tag{3.93}$$

and

$$Err_6\leq\frac{C_{inv}}{h}||\eta_h||\cdot||P_h\boldsymbol{E}-\boldsymbol{E}||. \tag{3.94}$$

Thus,

$$\begin{aligned}&\epsilon_0(\frac{\partial}{\partial t}\xi_h,\xi_h)+\mu_0(\frac{\partial}{\partial t}\eta_h,\eta_h)+\frac{1}{\epsilon_0\omega_{pe}^2}(\frac{\partial}{\partial t}\tilde{\xi}_h,\tilde{\xi}_h)+\frac{1}{\mu_0\omega_{pe}^2}(\frac{\partial}{\partial t}\tilde{\eta}_h,\tilde{\eta}_h)\\ \leq&\frac{C_{inv}}{h}(||\xi_h||+||\eta_h||)\cdot(||P_h\boldsymbol{E}-\boldsymbol{E}||+||P_h\boldsymbol{H}-\boldsymbol{H}||).\end{aligned}\tag{3.95}$$

Since

$$\begin{aligned}&\epsilon_0(\xi_h,\xi_h)+\mu_0(\eta_h,\eta_h)+\frac{1}{\epsilon_0\omega_{pe}^2}(\tilde{\xi}_h,\tilde{\xi}_h)+\frac{1}{\mu_0\omega_{pe}^2}(\tilde{\eta}_h,\tilde{\eta}_h)\\ =&\int_0^t(\epsilon_0(\frac{\partial}{\partial s}\xi_h,\xi_h)+\mu_0(\frac{\partial}{\partial s}\eta_h,\eta_h)+\frac{1}{\epsilon_0\omega_{pe}^2}(\frac{\partial}{\partial t}\tilde{\xi}_h,\tilde{\xi}_h)+\frac{1}{\mu_0\omega_{pe}^2}(\frac{\partial}{\partial t}\tilde{\eta}_h,\tilde{\eta}_h))ds\\ &+\epsilon_0(\xi_h^0,\xi_h^0)+\mu_0(\eta_h^0,\eta_h^0)+\frac{1}{\epsilon_0\omega_{pe}^2}(\tilde{\xi}_h^0,\tilde{\xi}_h^0)+\frac{1}{\mu_0\omega_{pe}^2}(\tilde{\eta}_h^0,\tilde{\eta}_h^0),\end{aligned}$$

with inequality (3.95), we obtain

$$\epsilon_0(\xi_h,\xi_h)+\mu_0(\eta_h,\eta_h)+\frac{1}{\epsilon_0\omega_{pe}^2}(\tilde{\xi}_h,\tilde{\xi}_h)+\frac{1}{\mu_0\omega_{pe}^2}(\tilde{\eta}_h,\tilde{\eta}_h)\tag{3.96}$$

$$\begin{aligned}&-(\epsilon_0(\xi_h^0,\xi_h^0)+\mu_0(\eta_h^0,\eta_h^0)+\frac{1}{\epsilon_0\omega_{pe}^2}(\tilde{\xi}_h^0,\tilde{\xi}_h^0)+\frac{1}{\mu_0\omega_{pe}^2}(\tilde{\eta}_h^0,\tilde{\eta}_h^0))\\ &\leq\int_0^t\frac{1}{2\delta}(||\xi_h||^2+||\eta_h||^2)+2\delta\frac{C_{inv}^2}{h^2}(||P_h\boldsymbol{E}-\boldsymbol{E}||^2+||P_h\boldsymbol{H}-\boldsymbol{H}||^2)\end{aligned}\tag{3.97}$$

Let $\lambda=\max_{[0,T]}(||\xi_h(t)||^2+||\eta_h(t)||^2)$.

Since λ is well defined due to the regularity hypotheses on the solution $(\boldsymbol{H},\boldsymbol{E})$ and $(\boldsymbol{H}_h,\boldsymbol{E}_h)$,

$$\begin{aligned}&\epsilon_0(\xi_h,\xi_h)+\mu_0(\eta_h,\eta_h)++\frac{1}{\epsilon_0\omega_{pe}^2}(\tilde{\xi}_h,\tilde{\xi}_h)+\frac{1}{\mu_0\omega_{pe}^2}(\tilde{\eta}_h,\tilde{\eta}_h)\\ \leq&TC_{inv}^2\delta h^{2min\{s,k\}}||(H,E,J,K)||^2_{C^0([0,T],H^{s+1}(\Omega))}+T\lambda\frac{1}{2\delta}\end{aligned}$$

which concludes the proof. □

Theorem 3.3.1. *Let $(\boldsymbol{E},\boldsymbol{H},\boldsymbol{J},\boldsymbol{K})\in C^3([0,T],L(\Omega))\cap C^0([0,T],(\boldsymbol{H}^{s+1}(\Omega))^3)$. Under the CFL condition Lemma(3.3.1), the following error estimate holds:*

$$\begin{aligned}&max_{n=0,\dots,N}(||\boldsymbol{E}(t_n)-\boldsymbol{E}_h^n||^2+||\boldsymbol{H}(t_{n+\frac{1}{2}})-\boldsymbol{H}_h^{n+\frac{1}{2}}||^2+||\boldsymbol{J}(t_{n+\frac{1}{2}})-\boldsymbol{J}_h^{n+\frac{1}{2}}||^2+||\boldsymbol{K}(t_n)-\boldsymbol{K}_h^n||^2)^{\frac{1}{2}})\\ \leq&C(\tau^2||(\boldsymbol{E},\boldsymbol{H},\boldsymbol{J},\boldsymbol{K})||_{C^3([0,T],L^2(\Omega))}+h^{min\{s,k\}}||(\boldsymbol{H},\boldsymbol{E},\boldsymbol{J},\boldsymbol{K})||_{C^0([0,T],H^{s+1}(\Omega))}).\end{aligned}$$

Proof.

Using the triangle inequality and Lemma(3.3.3) and (3.3.4), we can easily get the error estimate. □

3.3.3 EXTENSIONS OF THE DG METHOD TO A PML MODEL

In this section, we extend the above DG method developed for a metamaterial model to a perfectly matched layer (PML) model developed in 1997 [62]. Following the notation of [62], we assume that the PML is a cubical simulation domain, with face regions having absorbing layers with only one normal direction, edge regions being intersection of two face regions, and the corners representing the overlapping parts of three face regions. The complete PML governing equations for the corner region are [62, Eq. (B.4)],

$$\frac{\partial \boldsymbol{E}}{\partial t} + D_1 \boldsymbol{E} = \frac{1}{\epsilon_0} \nabla \times \boldsymbol{H} - \frac{1}{\epsilon_0} \boldsymbol{J} \tag{3.98}$$

$$\frac{\partial \boldsymbol{J}}{\partial t} + D_2 \boldsymbol{J} = \epsilon_0 D_3 \boldsymbol{E} \tag{3.99}$$

$$\frac{\partial \boldsymbol{H}}{\partial t} + D_1 \boldsymbol{H} = -\frac{1}{\epsilon_0} \nabla \times \boldsymbol{E} - \frac{1}{\epsilon_0} \boldsymbol{K} \tag{3.100}$$

$$\frac{\partial \boldsymbol{K}}{\partial t} + D_2 \boldsymbol{K} = \mu_0 D_3 \boldsymbol{H} \tag{3.101}$$

where we denote the 3×3 diagonal matrices $D_1 = diag(\delta_y + \delta_z - \delta_x, \delta_z + \delta_x - \delta_y, \delta_x + \delta_y - \delta_z)$, $D_2 = diag(\delta_x, \delta_y, \delta_z)$, $D_3 = diag((\delta_x - \delta_y)(\delta_x - \delta_z), (\delta_y - \delta_x)(\delta_y - \delta_z), (\delta_z - \delta_x)(\delta_z - \delta_y))$. Here δ_x, δ_y and δ_z are nonnegative functions and represent the damping variations along the x, y and z directions, respectively. Usually, quadratic profiles are chosen for δ_x, δ_y and δ_z [57]. Note that the model (3.98)-(3.101) is the same as (5.12) of Turkel and Yefet [57] (with the assumption that $\epsilon_0 = \mu_0 = 1$) and is well posed mathematically because it is a symmetric hyperbolic system (i.e., the standard Maxwell equations) plus lower order terms [57, p. 545]. Through a simple modification of (3.54), we can obtain the following fully

discontinuous Galerkin scheme for the PML model (3.98)-(3.101):

$$\int_{T_i} \frac{\boldsymbol{E}_i^{n+1} - \boldsymbol{E}_i^n}{\tau} \cdot \boldsymbol{u}_i = \frac{1}{\epsilon_0} \int_{T_i} \nabla \times \boldsymbol{u}_i \cdot \boldsymbol{H}_i^{n+\frac{1}{2}} - \frac{1}{\epsilon_0} \int_{T_i} \boldsymbol{J}_i^{n+\frac{1}{2}} \cdot \boldsymbol{u}_i \tag{3.102}$$

$$- \frac{1}{\epsilon_0} \sum_{k \in \nu_i} \int_{a_{ik}} \boldsymbol{u}_i \cdot (\{\boldsymbol{H}_h^{n+\frac{1}{2}}\}_{ik} \times \boldsymbol{n}_{ik}) - \int_{T_i} D_1 \frac{\boldsymbol{E}_i^{n+1} + \boldsymbol{E}_i^n}{2} \cdot \boldsymbol{u}_i$$

(3.103)

$$\int_{T_i} \frac{\boldsymbol{H}_i^{n+\frac{3}{2}} - \boldsymbol{H}_i^{n+\frac{1}{2}}}{\tau} \cdot \boldsymbol{v}_i = -\frac{1}{\mu_0} \int_{T_i} \nabla \times \boldsymbol{v}_i \cdot \boldsymbol{E}_i^{n+1} - \frac{1}{\mu_0} \int_{T_i} \boldsymbol{K}_i^{n+1} \cdot \boldsymbol{v}_i \tag{3.104}$$

$$+ \frac{1}{\mu_0} \sum_{k \in \nu_i} \int_{a_{ik}} \boldsymbol{v}_i \cdot (\{\boldsymbol{E}_h^{n+1}\}_{ik} \times \boldsymbol{n}_{ik}) - D_1 \int_{T_i} \frac{\boldsymbol{H}_i^{n+\frac{3}{2}} + \boldsymbol{H}_i^{n+\frac{1}{2}}}{2} \cdot \boldsymbol{v}_i$$

(3.105)

$$\int_{T_i} \frac{\boldsymbol{J}_i^{n+\frac{3}{2}} - \boldsymbol{J}_i^{n+\frac{1}{2}}}{\tau} \cdot \boldsymbol{\phi}_i + D_2 \int_{T_i} \frac{\boldsymbol{J}_i^{n+\frac{3}{2}} + \boldsymbol{J}_i^{n+\frac{1}{2}}}{2} \cdot \boldsymbol{\phi}_i = \epsilon_0 D_3 \int_{T_i} \boldsymbol{E}_i^{n+1} \cdot \boldsymbol{\phi}_i \tag{3.106}$$

$$\int_{T_i} \frac{\boldsymbol{K}_i^{n+1} - \boldsymbol{K}_i^n}{\tau} \cdot \boldsymbol{\psi}_i + D_2 \int_{T_i} \frac{\boldsymbol{K}_i^{n+1} + \boldsymbol{K}_i^n}{2} \cdot \boldsymbol{\psi}_i = \mu_0 D_3 \int_{T_i} \boldsymbol{H}_i^{n+\frac{1}{2}} \cdot \boldsymbol{\psi}_i \tag{3.107}$$

(3.108)

3.3.4 NUMERICAL RESULTS

For simplicity, here we only consider the 2D implementation, although the 3D case is quite similar (yet it requires much longer run time). The first two examples reproduce simulations performed in [44] by a different method.

Example 3.3.1. In this example, we will check the convergence rate $O(\tau^2 + h^{min(s,k)})$ of this DGTD method for Maxwell's equations in Metamaterials. We will use the same set up as example(3.2.1). We solved this example with various time step sizes τ and uniformly refined meshes. In our experiments, we tested basis functions of order $N = 1, 2 \; and \; 3$. Selected numerical results are presented in Tables (3.6)-(3.8). Many numerical tests suggest that our scheme has the following error estimate:

$$max_{m \geq 1}(||\boldsymbol{H}^m - \boldsymbol{H}_h^m||_{L^\infty(\Omega)} + ||\boldsymbol{E}^m - \boldsymbol{E}_h^m||_{L^\infty(\Omega)} + ||\boldsymbol{J}^m - \boldsymbol{J}_h^m||_{L^\infty(\Omega)} + ||\boldsymbol{K}^m - \boldsymbol{K}_h^m||_{L^\infty(\Omega)}) \leq Ch^k,$$

where $\boldsymbol{H}^m$ and $\boldsymbol{H}_h$ denote the analytic and numerical solutions at time step m, respectively,

and $k \geq 1$ is the order of the polynomial basis function. Note that in Table 3.8 the convergence rates degenerate when the meshes become finer. We believe that this is caused by the violation of the CFL condition for finer meshes $\frac{1}{\sqrt{\epsilon_0 \mu_0}} \tau \leq Ch$. To confirm this argument and the long time stability of our scheme, we increased the resolution of this example to order $N = 3$ and used the smaller time step $\tau = 10^{-8}$ for 1000 time steps so that we can compare the results obtained in Table 3.8 at the same ending time. Results obtained with order $N = 3$, and $\tau = 10^{-8}$ are shown in Table 3.9.

Table 3.6: The L^2 errors obtained after 10 steps with $\tau = 10^{-6}$ and $k = 1$.

Meshes	$h = \frac{1}{4}$	$h = \frac{1}{8}$	rate	$h = \frac{1}{16}$	rate	$h = \frac{1}{32}$	rate	$h = \frac{1}{64}$	rate
H_x	3.5601e-6	1.7805e-6	0.9996	8.9024e-7	1.0000	4.4512e-7	1.0000	2.2256e-7	1.0000
H_y	3.5601e-6	1.7805e-6	0.9996	8.9024e-7	1.0000	4.4512e-7	1.0000	2.2256e-7	1.0000
E_z	7.1211e-6	3.5614e-6	0.9997	1.7807e-6	1.0000	8.9037e-7	1.0000	4.4518e-7	1.0000
K_x	1.5812e-10	7.9078e-11	0.9997	3.9540e-11	1.0000	1.9770e-11	1.0000	9.8849e-12	1.0000
K_y	1.5812e-10	7.9078e-11	0.9997	3.9540e-11	1.0000	1.9770e-11	1.0000	9.8849e-12	1.0000
J_z	3.8655e-10	1.9332e-10	0.9997	9.6662e-11	1.0000	4.8331e-11	1.0000	2.4165e-11	1.0000

Table 3.7: The L^2 errors obtained after 10 steps with $\tau = 10^{-6}$ and $k = 2$.

Meshes	$h = \frac{1}{4}$	$h = \frac{1}{8}$	rate	$h = \frac{1}{16}$	rate	$h = \frac{1}{32}$	rate	$h = \frac{1}{64}$	rate
H_x	3.5938e-7	9.0173e-8	1.9947	2.2564e-8	1.9987	5.6425e-9	1.9996	1.4115e-9	1.9991
H_y	3.5938e-7	9.0173e-8	1.9947	2.2564e-8	1.9987	5.6425e-9	1.9996	1.4115e-9	1.9991
E_z	7.1869e-7	1.8033e-7	1.9947	4.5122e-8	1.9987	1.1284e-8	1.9996	2.8226e-9	1.9992
K_x	1.5961e-11	4.0048e-12	1.9947	1.0021e-12	1.9987	2.5059e-13	1.9996	6.2685e-14	1.9991
K_y	1.5961e-11	4.0048e-12	1.9947	1.0021e-12	1.9987	2.5059e-13	1.9996	6.2685e-14	1.9991
J_z	3.9013e-11	9.7886e-12	1.9948	2.4494e-12	1.9987	6.1250e-13	1.9996	1.5322e-13	1.9991

Table 3.8: The L^2 errors obtained after 10 steps with $\tau = 10^{-6}$ and $k = 3$.

Meshes	$h = \frac{1}{4}$	$h = \frac{1}{8}$	rate	$h = \frac{1}{16}$	rate	$h = \frac{1}{32}$	rate	$h = \frac{1}{64}$	rate
H_x	2.5657e-8	3.2197e-9	2.9944	4.0580e-10	2.9881	7.0506e-11	2.5250	4.9745e-11	0.5032
H_y	2.5657e-8	3.2197e-9	2.9944	4.0580e-10	2.9881	7.0506e-11	2.5250	4.9745e-11	0.5032
E_z	5.0887e-8	6.3846e-9	2.9946	8.0478e-10	2.9879	1.4040e-10	2.5191	9.9482e-11	0.4970
K_x	1.1396e-12	1.4301e-13	2.9943	1.8017e-14	2.9887	3.0893e-15	2.5440	2.1490e-15	0.5236
K_y	1.1396e-12	1.4301e-13	2.9943	1.8017e-14	2.9887	3.0893e-15	2.5440	2.1490e-15	0.5236
J_z	2.7622e-12	3.4656e-13	2.9946	4.3677e-14	2.9882	7.5786e-15	2.5269	5.3397e-15	0.5052

Comparing Table 3.9 with Table 3.8, we see that the results obtained with the smaller time step $\tau = 10^{-8}$ show $O(h^3)$ convergence rate very well, and the errors are more accurate (about one order of magnitude) than those obtained with $\tau = 10^{-6}$. To check the long

Table 3.9: The L^2 errors obtained after 1000 steps with $\tau = 10^{-8}$ and $k = 3$.

Meshes	$h = \frac{1}{4}$	$h = \frac{1}{8}$	rate	$h = \frac{1}{16}$	rate	$h = \frac{1}{32}$	rate	$h = \frac{1}{64}$	rate
H_x	2.5657e-8	3.2194e-9	2.9945	4.0280e-10	2.9987	5.0365e-11	2.9996	6.3150e-12	2.9956
H_y	2.5657e-8	3.2194e-9	2.9945	4.0280e-10	2.9987	5.0365e-11	2.9996	6.3150e-12	2.9956
E_z	5.0887e-8	6.3839e-9	2.9948	7.9872e-10	2.9987	9.9867e-11	2.9996	1.2522e-11	2.9955
K_x	1.2650e-12	1.5872e-13	2.9946	1.9859e-14	2.9986	2.4831e-15	2.9996	3.1162e-16	2.9943
K_y	1.2650e-12	1.5872e-13	2.9946	1.9859e-14	2.9986	2.4831e-15	2.9996	3.1162e-16	2.9943
J_z	2.5136e-12	3.1534e-13	2.9948	3.9453e-14	2.9987	4.9330e-15	2.9996	6.1881e-16	2.9949
$CPU(s)$	6.357308	8.910876		12.230510		38.56634		140.381352	

Table 3.10: The L^2 errors obtained after 100,000 steps with $\tau = 10^{-8}$ and $k = 3$.

Meshes	$h = \frac{1}{4}$	$h = \frac{1}{8}$	rate	$h = \frac{1}{16}$	rate	$h = \frac{1}{32}$	rate	$h = \frac{1}{64}$	rate
H_x	2.5058e-6	3.1444e-7	2.9944	3.9507e-8	2.9926	5.0192e-9	2.9766	6.5589e-10	2.9359
H_y	2.5058e-6	3.1444e-7	2.9944	3.9507e-8	2.9926	5.0192e-9	2.9766	6.5589e-10	2.9359
E_z	5.1349e-6	6.4365e-7	2.9960	8.0113e-8	3.0063	9.8104e-9	3.0297	1.1392e-9	3.1063
K_x	1.2451e-8	1.5618e-9	2.9950	1.9565e-10	2.9969	2.4595e-11	2.9918	3.1372e-12	2.9708
K_y	1.2451e-8	1.5618e-9	2.9950	1.9565e-10	2.9969	2.4595e-11	2.9918	3.1372e-12	2.9708
J_z	2.5239e-8	3.1651e-9	2.9953	3.9491e-10	3.0027	4.8830e-11	3.0157	5.8722e-12	3.0558

time stability, we run the scheme with order $N = 3$, and $\tau = 10^{-8}$ for 100,000 time steps. The errors obtained are presented in Table 3.10, which still shows $O(h^3)$ convergence rate very well. The comparison between Tables 3.9 and 3.10 shows that the errors of all fields grow linearly in time: $\boldsymbol{H}_x$, $\boldsymbol{H}_y$ and $\boldsymbol{E}_z$ exhibit this property quite clearly, but the induced currents $\boldsymbol{K}_x$ and $\boldsymbol{J}_z$ do not. Still, the latter have to be considered to have solutions proportional to τ. Furthermore, our results show that the algorithm is quite efficient by considering the CPU time (in seconds) recorded in Table 3.9. Exemplary solutions for $\boldsymbol{E}_z$ and the corresponding pointwise errors obtained with order $N = 3$, and $\tau = 10^{-8}$ at the end of 100,000 time steps are presented in Fig(3.13).

Example 3.3.2. Here we consider the 2D transverse magnetic PML model obtained from

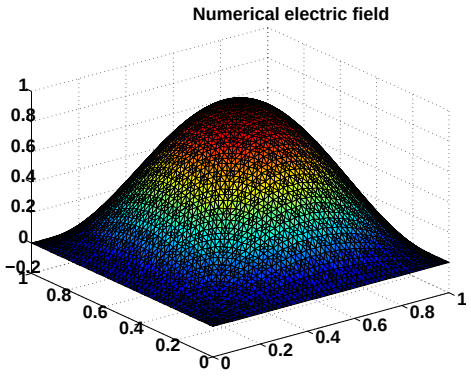

(a) electric field E

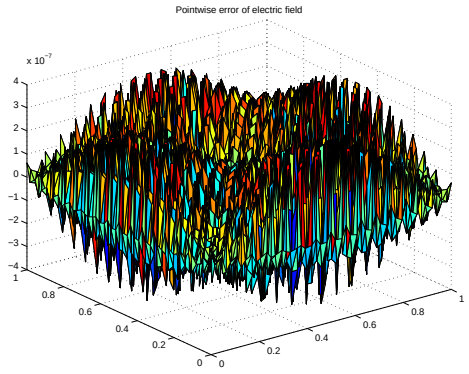

(b) pointwise error of electric field

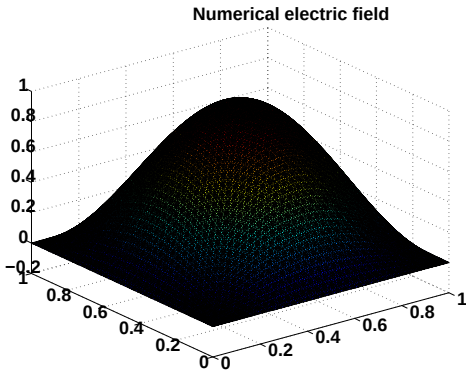

(c) electric field E

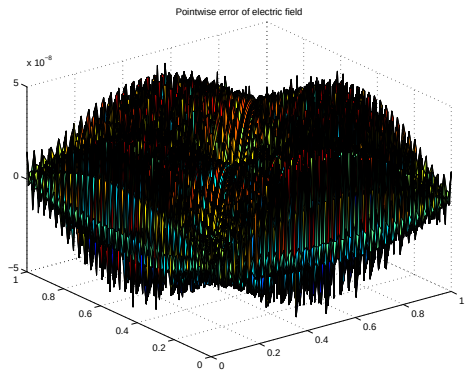

(d) pointwise error of electric field

Figure 3.13: Results obtained with order $N = 3$, and $\tau = 10^{-8}$ after 100,000 time steps. Top row (with $h = \frac{1}{16}$): Ez (left) and its pointwise error (right); bottom row (with $h = \frac{1}{32}$): Ez (left) and its pointwise error (right)

(3.98)-(3.101):

$$
\begin{aligned}
\frac{\partial \boldsymbol{H}_x}{\partial t} &= -\frac{1}{\mu_0}\frac{\partial \boldsymbol{E}_z}{\partial y} - \frac{1}{\mu_0}\boldsymbol{K}_x + (\delta_x - \delta_y)\boldsymbol{H}_x \\
\frac{\partial \boldsymbol{H}_y}{\partial t} &= \frac{1}{\mu_0}\frac{\partial \boldsymbol{E}_z}{\partial x} - \frac{1}{\mu_0}\boldsymbol{K}_y - (\delta_x - \delta_y)\boldsymbol{H}_y \\
\frac{\partial \boldsymbol{E}_z}{\partial t} &= \frac{1}{\epsilon_0}(\frac{\partial \boldsymbol{H}_y}{\partial x} - \frac{\partial \boldsymbol{H}_x}{\partial y}) - \frac{1}{\epsilon_0}\boldsymbol{J}_z - (\delta_x + \delta_y)\boldsymbol{E}_z \\
\frac{\partial J_z}{\partial t} &= \epsilon_0 \delta_x \delta_y \boldsymbol{E}_z \\
\frac{\partial K_x}{\partial t} &= -\delta_x \boldsymbol{K}_x + \mu_0(\delta_x - \delta_y)\delta_x \boldsymbol{H}_x \\
\frac{\partial K_y}{\partial t} &= -\delta_y \boldsymbol{K}_y - \mu_0(\delta_x - \delta_y)\delta_y \boldsymbol{H}_y,
\end{aligned}
$$

where the subscripts x, y and z denote the corresponding components.

For this model, we assume that the physical domain $\Omega = (-0.1, 0.1)^2$ is surrounded by a perfectly matched layer of thickness of 0.05, i.e., the real computational domain is $(-0.15, 0.15)^2$. To test the effectiveness of the PML, we assume that there exists an initial electric source

$$\boldsymbol{E}_z(x, y, 0) = \begin{cases} cos^8(\frac{\pi r}{2r_0}) & \text{if } r \leq r_0; \\ 0 & \text{if } r \geq r_0. \end{cases}$$

where $r_0 = 0.05$, $r = \sqrt{x^2 + y^2}$.

The damping function δ_x is chosen as:

$$\delta_x(x, y) = \begin{cases} \delta_0(x - 0.1)^2 & \text{if } x \geq 0.1; \\ \delta_0(x + 0.1)^2 & \text{if } x \leq -0.1; \\ 0 & \text{elsewhere.} \end{cases}$$

Function δ_y has the same form but varies with respect to the y variable.

In our test, we choose the time step $\frac{1}{6} \times 10^{-12}$, the damping constant $\delta_0 = 1$, the basis function order $N = 2$ on all elements, and the simulation time $\tau \in (0, 3000\tau)$ such that the wave front has reached the simulation boundary. Some snapshots at various time steps are presented in Figs. (3.14) and (3.15), which shows that the PML absorbs the wave reflections at the interfaces very well.

Example 3.3.3. In [61], simulations are performed for double negative (DNG) metamaterial for two cases: (1) when the index of refraction $n \approx -1$ and (2) when $n \approx -6$. The general index of refraction, n_i, where i stands for the index tracking the medium the wave is propagating through, is given by the expression

$$n_i = \sqrt{\frac{\epsilon_i}{\epsilon_0}}\sqrt{\frac{\mu_i}{\mu_0}} = \sqrt{\epsilon_r}\sqrt{\mu_r}.$$

Since both ϵ_r and μ_r are negative, n_i is negative as well. Also, [61] adopted two lossy

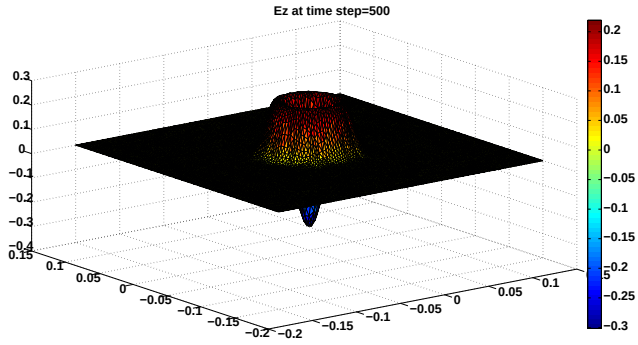

(a) electric field E

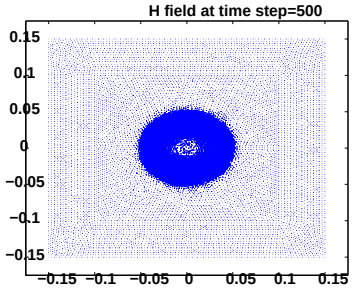

(b) magnetic field Hx,Hy

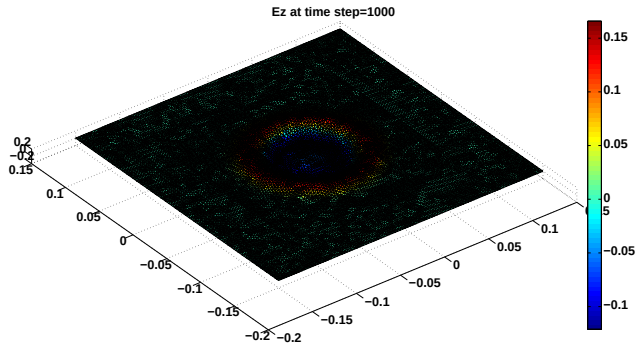

(c) electric field E

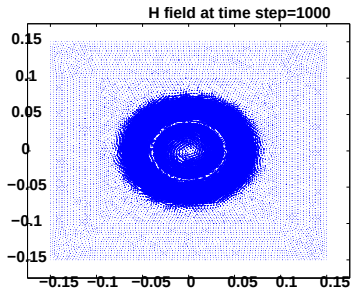

(d) magnetic field Hx,Hy

Figure 3.14: Top row: contour plot of Ez (left) and $\boldsymbol{H}$ field (right) at time step 500 in metamaterials with PML boundary conditions; bottom row: the same plots at time step 1000.

Drude polarization and magnetization models:

$$\epsilon(\omega) = \epsilon_0(1 - \frac{\omega_{pe}^2}{\omega(\omega - j\gamma_e)}) \tag{3.109}$$

$$\mu(\omega) = \mu_0(1 - \frac{\omega_{pm}^2}{\omega(\omega - j\gamma_m)}). \tag{3.110}$$

In our simulations, we chose a TE wave which consists of the field components $\boldsymbol{H}_x$, $\boldsymbol{H}_y$, and $\boldsymbol{E}_z$. Wave impedance is given by $\eta_i = \frac{\sqrt{\mu_i}}{\sqrt{\epsilon_i}}$. If we let 'trans' mean transmitted and 'inc' means incident, a matched slab is defined by $\eta_{trans} = \eta_{inc}$. For simulations of both cases,$n \approx -1$ and $n \approx -6$, matched slabs are considered, in which case $\omega_{pe} = \omega_{pm} = \omega_p$

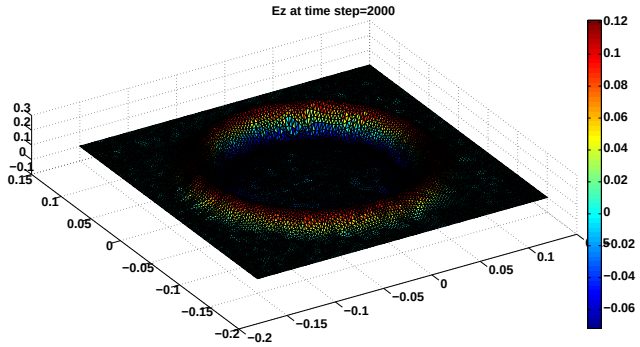

(a) electric field E

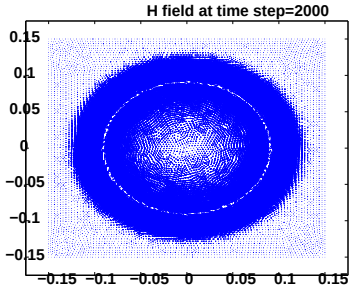

(b) magnetic field Hx,Hy

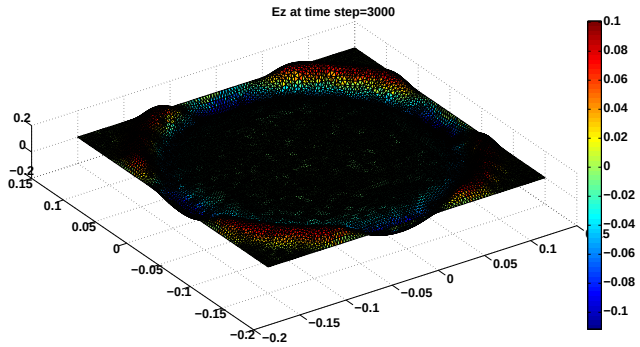

(c) electric field E

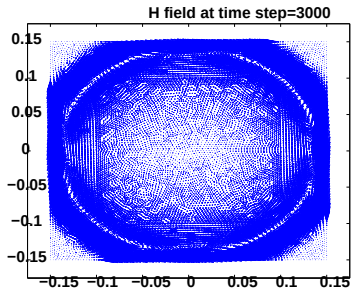

(d) magnetic field Hx,Hy

Figure 3.15: Top row: contour plot of Ez (left) and $\boldsymbol{H}$ field (right) at time step 2000 in metamaterials with PML boundary conditions; bottom row: the same plots at time step 3000.

and $\Gamma_e = \Gamma_m = \Gamma$. In all cases, $\Gamma = 10^8\ s^{-1}$, frequency is $f_0 = 30GHz$, the time step, $\Delta t = \frac{1}{6} \times 10^{-12}$ s, and the simulation domain is $[0, 0.083] \times [0, 0.06]$. The boundary is a PML with a thickness of 0.0008. Also, for both cases, multiple cycle $m-n-m$ pulses were used to generate the smooth source, thereby producing minimal noise.

These pulses are given by

$$f(t) = \begin{cases} 0 & \text{for } t < 0 \\ g_{on}(t)sin(\omega t) & \text{for } 0 < t < mT_p \\ sin(\omega t) & \text{for } mT_p < t < (m+n)T_p \\ g_{off}(t)sin(\omega t) & \text{for } (m+n)T_p < t < (m+n+m)T_p \\ 0 & \text{for } (m+n+m)T_p < t \end{cases}$$

where $x_{on}(t) = \frac{t}{mT_p}$, $x_{off} = \frac{t-(m+n)T_p}{mT_p}$, and the continuous functions in C^2 are

$$g_{on} = 10x_{on}^3(t) - 15x_{on}^4(t) + 6x_{on}^5(t)$$
$$g_{off} = 1 - [10x_{off}^3(t) - 15x_{off}^4(t) + 6x_{off}^5(t)].$$

For the case when $n \approx -1$, $\omega_p = 2\pi\sqrt{2}f_0 \approx 2.66573 \times 10^{11}$ rad/s, so $\Gamma = 3.75 \times 10^{-4}$. One can easily see that given this value of ω_p, the real part of both ϵ_r and μ_r is -1, and thus $n \approx -1$ since $n = \sqrt{\epsilon_r}\sqrt{\mu_r}$. Similarly, when $n \approx -6$, $\omega_p = 2\pi\sqrt{7}f_0 \approx 4.98712 \times 10^{11}$ rad/s, so $\Gamma = 2.01 \times 10^{-4}\omega_p$. The Gaussian beam varies spatially as $exp(-x^2/\omega_0^2)$, where ω_0 is the "waist". The single slab has a dimension of $[0.024, 0.044] \times [0.006, 0.058]$. The source is placed at $x = 0.004$.

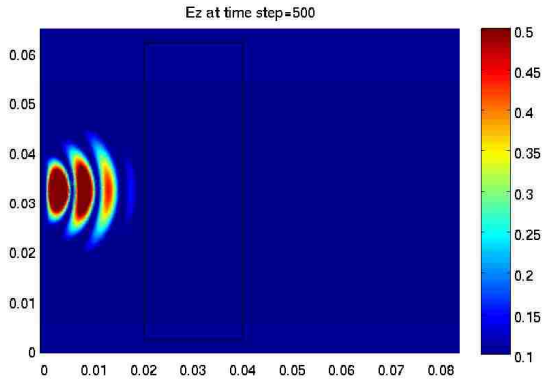

(a) Ez at time step=500

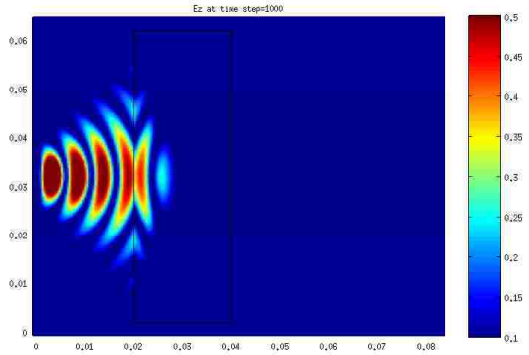

(b) Ez at time step=1000

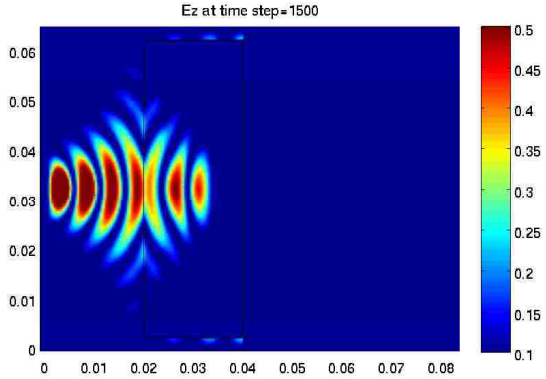

(c) Ez at time step=1500

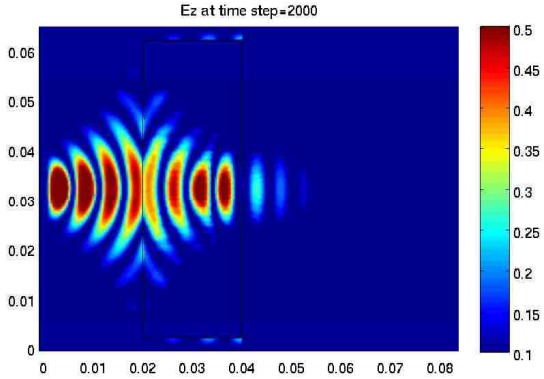

(d) Ez at time step=2000

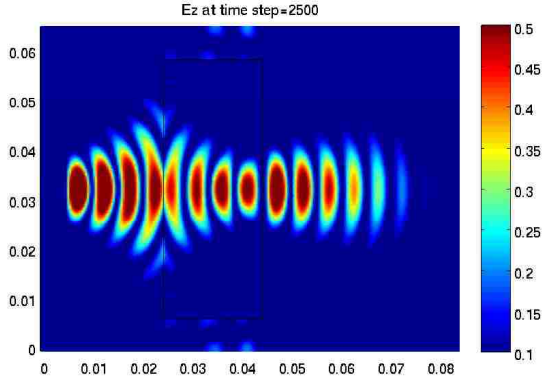

(e) Ez at time step=2500

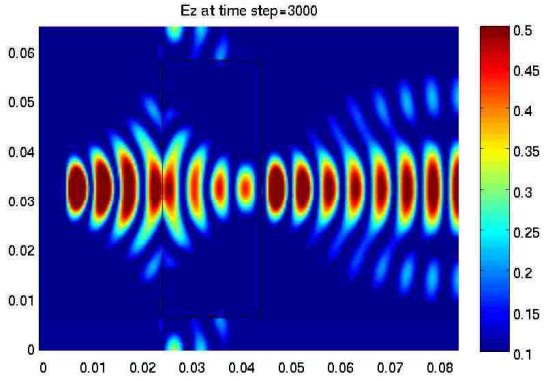

(f) Ez at time step=3000

Figure 3.16: Single slab metamaterial with $n \approx -1$

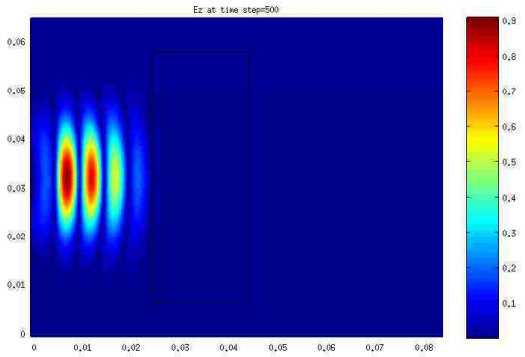

(a) Ez at time step=500

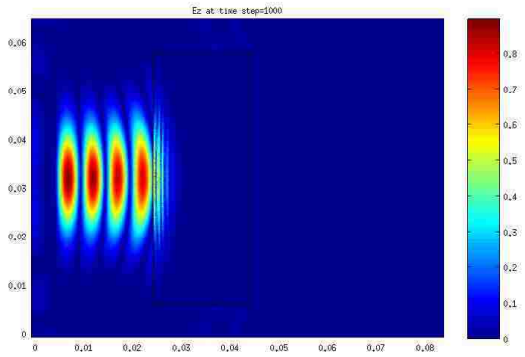

(b) Ez at time step=1000

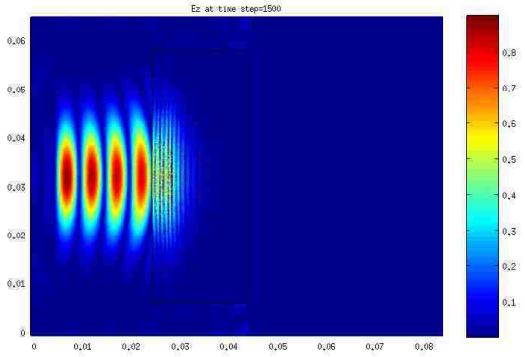

(c) Ez at time step=1500

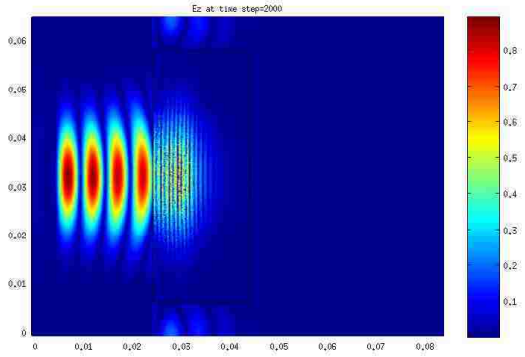

(d) Ez at time step=2000

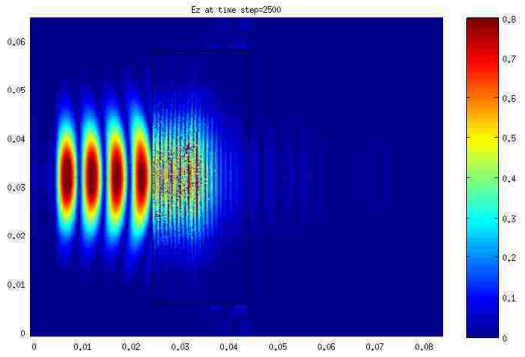

(e) Ez at time step=2500

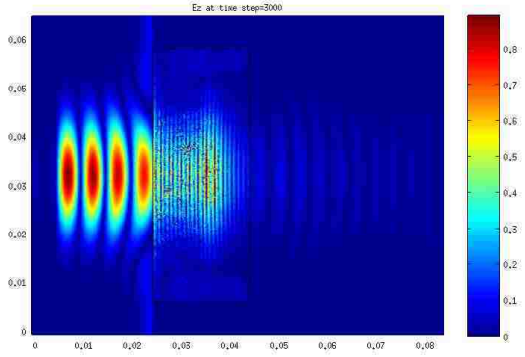

(f) Ez at time step=3000

Figure 3.17: Single slab metamaterial with $n \approx -6$

Chapter 4

HOMOGENIZATION OF MAXWELL'S EQUATIONS IN DISPERSIVE MEDIA BY DG

In this dissertation, we talk about the homogenization of Periodically varying coefficients for Maxwell's equations in dispersive media by the Discontinuous Galerkin Method. This section is based on our work [46]. Several techniques have appeared for solving the time-dependent Maxwell's equations with periodically varying coefficients. For the first time, we apply the discontinuous Galerkin (DG) method to this homogenization problem in dispersive media. For simplicity, our focus is obtaining a solution in two-dimensions (2D) using 2D corrector equations. Our numerical results show the DG method to be both convergent and efficient. Furthermore, our solution is consistent with previous treatments and theoretical expectations.

We study the periodic homogenization of Maxwell's equations for dispersive media in the time domain, in a material presenting heterogeneous micro structures (composite materials). We shall first note that the study of the DG method for Maxwell's equations in dispersive media(whose physical parameters such as permitivity and/or permeability are wavelength dependent) is limited. It just has been developed recently[34, 35, 37, 49, 58]. In [35], a fully implicit DG method for solving dispersive media and its convergence rate are given, but the governing function doesn't have a rapidly oscillating coefficient. This is the first work to combine both of these properties using DG-FEM.

When the period of the structure is small compared to the wavelength, the coefficients in Maxwell's equations oscillate rapidly. These oscillating coefficients are difficult to treat numerically in simulations. Homogenization is a process in which the composite material having a microscopic structure is replaced with an equivalent material having macroscopic, homogeneous properties. The fields are computed only in the unit cell and then generalized over the whole domain. Therefore, given a large finite lattice of heterogeneous composites, the time of computation and the memory requirement can be greatly reduced without the

loss of accuracy.

Bensoussan, Lions, and Papanicolaou [8] studied the homogenization method applied to Maxwell's type equations with rapidly oscillating coefficients early on and derived convergence results. The mathematical literature on electromagnetics in complex media is not, as yet, very extensive. The bigger part deals with the study of time-harmonic waves in chiral media or elliptic problems. See [5, 15, 30, 38, 54]for a comprehensive account of research activities in this direction. The literature in the time domain is even more restricted. We refer to [7, 25] and references therein. In [7], Barbatis and Stratis studied the periodic homogenization of Maxwell's equations for dissipative bianisotropic media in the time domain, both in R3 and in a bounded domain with the perfect conductor boundary condition, but they did not show any numerical results to support their analysis. Furthermore, Bossavit, Griso, and Miara [11] studied the behavior of the electromagnetic field of a medium presenting periodic microstructures made of a bianisotropic material by the periodic unfolding method introduced by D. Cioranescu, A. Damlamian and G. Griso in the abstract framework of stationary elliptic equations [17]. They talked about the treatment of time-dependent coefficients (nonstationary) which yields a limit constitutive law different from the original one, in particular the convolution operator that accounts for memory effects. Wellander [59] used the two-scale convergence method (see, [3]) to obtain convergence results for the homogenization method for the time-dependent Maxwell's equations with linear constitutive relations in a heterogeneous medium. He further expanded them to treat cases in which the material possesses a nonlinear conductivity, or is possibly nonperiodic. Banks et al. [6] used the periodic unfolding method presented in [17, 18] in the abstract framework of stationary elliptic equations to simulate the electromagnetic field in a composite material exhibiting heterogeneous microstructures. In [15], they discussed the multiscale analysis of Maxwell's equations in composite materials with a periodic microstructure, and they showed that higher-order correctors are essential for solving Maxwell's equations in composite materials when ϵ is not sufficiently small. However, they only dealt with a time-harmonic problem by the edge element method. The engineering literature is dominated by the simple mixture formulae, which are derived using physical arguments. For an excellent overview and history of the mixture formulae, see [54, 55].

Our effort here is motivated by the homogenization of time-harmonic Maxwell's equations or boundary value problems. This topic has not been studied when the time domain and the dispersive media are involved in the Maxwell's equations in a heterogeneous material. we thus need to consider two factors: one is the homogenization of rapidly oscillating coefficients, and one is the fully DG scheme to solve the corrector function in the unit cell and the homogenized Maxwell's equations in the whole domain. Our method is based on homogenization of equations of maxwell's type from [8, 15] to simulate the periodic homogenization of Maxwell's equations for dispersive media in the time domain, in a material presenting heterogeneous microstructures by DG finite element method. We use the first order corrector because we assume ϵ is small enough. Refer to [15] for a comparison between the first order and the second order corrector functions. To our best knowledge, this is the first time using DG finite element method to solve the homogenization of periodically varying coefficients for Maxwell's equations in dispersive media in time domain. We are able to obtain the convergence rate for the fully DG scheme of the Homogenization method. We could not test the convergence rate numerically due to the difficulties of finding the exact solution to the Maxwell's equations in heterogeneous materials, and multiple factors of the convergence rate. However, we can test the schemes stability and convergence. Also a comparison is made between the effective coefficients obtained by the homogenization method presented here and those computed by the traditional Maxwell Garnett mixture formula in different shapes of inclusions while [6] only compares them in the circular inclusion. A comparison between the asymptotic homogenization approach and the M-G formula for 3-D periodic lattices featuring complex-media inclusions with bianisotropic properties is given in [54].

4.1 THE HOMOGENIZATION BY DG METHOD

4.1.1 THE GOVERNING EQUATIONS

The governing equations for the isotropic homogeneous microstructures [35] are

$$\boldsymbol{E}_{tt} + \nabla \times (c_v^2 \nabla \times \boldsymbol{E}) + \omega_p^2 \boldsymbol{E} - \boldsymbol{J}(\boldsymbol{E}) = \mathbf{f} \quad \text{in} \quad \Omega \times (0, T), \tag{4.1}$$

where $\boldsymbol{E}$ is the electric field, c_v is the speed of light, ω_p is the plasma frequency, $\mathbf{f}$ is an added source term, and $\boldsymbol{J}$ is the polarization current density represented as

$$\boldsymbol{J}(\boldsymbol{E}) \equiv \boldsymbol{J}(\boldsymbol{x}, t; \boldsymbol{E}) = \nu\omega_p^2 \int_0^t e^{-\nu(t-s)} \boldsymbol{E}(\boldsymbol{x}, s) ds. \tag{4.2}$$

Here $\nu \geq 0$ is the electron-neutron collision frequency. It is to be emphasized that c_v is constant in (4.1). In this paper we examine the case that $c_v = 1/\sqrt{\varepsilon\mu}$ is a periodic function of position, where ε and μ are the permitivity and permeability of the composite material. Specifically, we consider $c_v = c_v(\frac{\boldsymbol{x}}{\epsilon})$ to be rapidly oscillating spatial functions, where $\epsilon > 0$ denotes the relative size of a periodic microstructure of the composite material. Our governing equations now model isotropic *heterogeneous* microstructures (composite materials):

$$\boldsymbol{E}_{tt} + \nabla \times (c_v^2(\frac{\boldsymbol{x}}{\epsilon}) \nabla \times \boldsymbol{E}) + \omega_p^2 \boldsymbol{E} - \boldsymbol{J}(\boldsymbol{E}) = \mathbf{f} \quad \text{in} \quad \Omega \times (0, T), \tag{4.3}$$

Here Ω is a bounded Lipschitz polyhedron in $R^d (d = 2, 3)$. Moreover, we assume that the boundary $\partial\Omega$ of Ω is a prefect conductor so that

$$\boldsymbol{n} \times \boldsymbol{E} = 0 \text{ on } \partial\Omega \times (0, T)$$

Where $\boldsymbol{n}$ denotes the unit outward normal of $\partial\Omega$. Furthermore, we assume the initial conditions for (4.3) are given as

$$\boldsymbol{E}(\boldsymbol{x}, 0) = \boldsymbol{E}_0(\boldsymbol{x}) \text{ and } \boldsymbol{E}_t(\boldsymbol{x}, 0) = \boldsymbol{E}_1(\boldsymbol{x}),$$

where $\boldsymbol{E}_0(\boldsymbol{x})$ and $\boldsymbol{E}_1(\boldsymbol{x})$ are some given functions.

4.1.2 THE HOMOGENIZED PROBLEM

Before we homogenize the governing equations, we treat a simpler problem for the purpose of introducing the homogenization technique. Consider the following equations

with rapidly oscillating coefficients (from [15]):

$$\begin{aligned} &\nabla \times (A^\epsilon \nabla \times \boldsymbol{u}_\epsilon) - \omega^2 u_\epsilon = f(\boldsymbol{x}), \quad \boldsymbol{x} \in \Omega, \\ &\nabla \cdot \boldsymbol{u}_\epsilon = 0, \quad \boldsymbol{x} \in \Omega, \\ &\boldsymbol{u}_\epsilon \times \boldsymbol{n} = 0, \quad \boldsymbol{x} \in \partial\Omega \end{aligned} \tag{4.4}$$

where $A^\epsilon(\boldsymbol{x}) = (a^\epsilon_{ij}(\boldsymbol{x})) = (a_{ij}(\frac{\boldsymbol{x}}{\epsilon}))$ for the 1-periodic functions $a_{ij}(\frac{\boldsymbol{x}}{\epsilon})$, and $\Omega \in R^3$ is a bounded Lipschitz polygonal convex domain or a smooth domain with a microstructure. For the requirements and properties of a coefficient matrix A^ϵ, refer to [15]. Letting $\xi = \frac{\boldsymbol{x}}{\epsilon}$, the reference periodic cell Q is, without loss of generality, defined as $Q = \{\xi = \{\xi_1, \xi_2, \xi_3\} : 0 < \xi_i < 1, i = 1, 2, 3\}$. The construction of the homogenized problem requires solving for the matrix valued function $\boldsymbol{\theta}(\xi) = \{\boldsymbol{\theta}^1, \boldsymbol{\theta}^2, \boldsymbol{\theta}^3\}$. The corrector subterms $\boldsymbol{\theta}^p$ are solutions to the corrector equations

$$\begin{aligned} &\nabla_\xi \times (A(\xi)\nabla_\xi \times \boldsymbol{\theta}^p(\xi)) = -\nabla_\xi \times (A(\xi)\mathbf{e}_p), \quad \xi \in Q, \\ &\nabla_\xi \cdot \boldsymbol{\theta}^p(\xi) = 0, \quad \xi \in Q, \\ &\boldsymbol{\theta}^p(\xi) \times \boldsymbol{n} = 0, \quad \xi \in \partial Q, \end{aligned} \tag{4.5}$$

where e_p denotes any of $e_1 = \{1, 0, 0\}$, $e_2 = \{0, 1, 0\}$, $e_3 = \{0, 0, 1\}$.
There are two methods for obtaining the homogenized coefficients matrix $\widehat{A}$:

1. The first method is to solve for the components $\boldsymbol{\chi}^j(\xi)$ of the matrix-valued function $\boldsymbol{\chi}(\xi) = (\boldsymbol{\chi}^1(\xi), \boldsymbol{\chi}^2(\xi), \boldsymbol{\chi}^3(\xi))$ from the equation

$$\nabla_\xi \cdot (A^{-1}(\xi)\nabla_\xi \boldsymbol{\chi}^j(\xi)) = -\nabla_\xi \cdot (A^{-1}(\xi)\mathbf{e}_j), \tag{4.6}$$

   We then define

$$\widehat{A} = (\mathcal{M}(A^{-1}(\xi)(I_3 + \nabla_\xi \boldsymbol{\chi}(\xi)))^{-1},$$

   where $\mathcal{M}v = \int_Q v(\xi)\, d\xi$.

2. The second method is to set

$$\widehat{A} = \mathcal{M}(A(\xi) + A(\xi)\nabla_\xi \times \boldsymbol{\theta}(\xi)). \tag{4.7}$$

Now we can define the solution $\boldsymbol{u}^0(\boldsymbol{x})$ of the homogenized equations for (4.4) as

$$\begin{aligned} &\nabla \times (\widehat{A}\nabla \times \boldsymbol{u}^0) - \omega^2 u^0 = f(\boldsymbol{x}), \quad \boldsymbol{x} \in \Omega, \\ &\nabla \cdot \boldsymbol{u}^0 = 0, \quad \boldsymbol{x} \in \Omega, \\ &\boldsymbol{u}^0 \times \boldsymbol{n} = 0, \quad \boldsymbol{x} \in \partial\Omega. \end{aligned} \tag{4.8}$$

The first order multiscale asymptotic expansion for problem (4.4):

$$\boldsymbol{u}_\epsilon(\boldsymbol{x}) = \boldsymbol{u}^0(\boldsymbol{x}) + \epsilon\boldsymbol{\theta}(\xi)\nabla \times \boldsymbol{u}^0(\boldsymbol{x}), \tag{4.9}$$

4.1.3 REDUCTION TO TWO SPATIAL DIMENSIONS

When dealing with 2D problems, some changes need to be made to the corrector function.

In a similar manner to the three-dimensional case, we may construct the corrector function for 2D, which involves solving for the corrector $\boldsymbol{W}(\xi)$, a vector function in 2D.

$$\begin{aligned} &\nabla_\xi \times (a(\xi)\nabla_\xi \times \boldsymbol{W}(\xi)) = -\nabla_\xi \times a(\xi), \quad \xi \in Q, \\ &\nabla_\xi \cdot \boldsymbol{W}(\xi) = 0, \quad \xi \in Q, \\ &\boldsymbol{W}(\xi) \times \boldsymbol{n} = 0, \quad \xi \in \partial Q, \end{aligned} \tag{4.10}$$

Here, $a(\xi)$ is the coefficient, a scalar function, and Q is the reference cell of the periodic structure that occupies $\Omega \in R^2$. Then the homogenized coefficient $\widehat{a}$ is

$$\widehat{a} = \int_Q a(\xi) + a(\xi)\nabla_\xi \times \boldsymbol{W}(\xi)d\xi \tag{4.11}$$

and the corresponding homogenized equations are:

$$\begin{aligned}
&\nabla \times (\widehat{a}\nabla \times \boldsymbol{u}^0) - \omega^2 u^0 = f(\boldsymbol{x}), \quad \boldsymbol{x} \in \Omega, \\
&\nabla \cdot \boldsymbol{u}^0 = 0, \quad \boldsymbol{x} \in \Omega, \\
&\boldsymbol{u}^0 \times \boldsymbol{n} = 0, \quad \boldsymbol{x} \in \partial\Omega.
\end{aligned} \tag{4.12}$$

The first order multiscale asymptotic expansion for problem (4.4) in 2D is

$$\boldsymbol{u}_\epsilon(\boldsymbol{x}) = \boldsymbol{u}^0(\boldsymbol{x}) + \epsilon \boldsymbol{W}(\xi)\nabla \times \boldsymbol{u}^0(\boldsymbol{x}). \tag{4.13}$$

For proofs of the above homogenization, refer to [8].

4.2 A FULLY DISCRETE DG SCHEME

Now we can proceed to construct the DG finite element scheme for this homogenization method. Notice that there are two types of equations to solve for. One is the corrector function in the unit cell, and the other is the homogenized Maxwell's equation over the whole domain.

1. A DG finite element of scheme for the corrector functions in unit cell Q.

   We consider a shape-regular mesh T_{h_0} that partitions the unit cell Q into disjoint tetrahedral (or other types, e.g., triangular) elements {K}, such that $\overline{Q} = \bigcup_{K \in T_{h_0}} K$. We denote the diameter of K by h_K, and the mesh size h_0 by $h_0 = max_{K \in T_{h_0}} h_K$. Furthermore, we denote the set of all interior faces by $F_{h_0}^I$, the set of all boundary faces by $F_{h_0}^B$, and the set of all faces by $F_{h_0} = F_{h_0}^I \bigcup F_{h_0}^B$.

   We assume that the finite element space $\boldsymbol{V}_{h_0}$ is given by

$$\boldsymbol{V}_{h_0} = \{\boldsymbol{v} \in \boldsymbol{L}^2(\Omega) : \boldsymbol{v}|_K \in (P_l(K))^d, K \in T_{h_0}\}, \quad d = 2, 3, \quad l \geq 1,$$

   where $P_l(K)$ denotes the space of polynomials of total degree at most l on K. To

construct the DG scheme, we need a bilinear form a_{h_0} defined on $\boldsymbol{V}_{h_0} \times \boldsymbol{V}_{h_0}$ as follows:

$$a_{h_0}(\boldsymbol{u}, \boldsymbol{v}) = \sum_{K \in T_{h_0}} \int_K A(\xi) \nabla \times \boldsymbol{u} \cdot \nabla \times \boldsymbol{v} d\boldsymbol{x} - \sum_{f \in F_{h_0}} \int_f [[\boldsymbol{u}]]_T \cdot \{\{A(\xi) \nabla \times \boldsymbol{v}\}\} dA$$
$$- \sum_{f \in F_{h_0}} \int_f [[\boldsymbol{v}]]_T \cdot \{\{A(\xi) \nabla \times \boldsymbol{u}\}\} dA + \sum_{f \in F_{h_0}} \int_f a [[\boldsymbol{u}]]_T \cdot [[\boldsymbol{v}]]_T dA.$$

Here $[[\boldsymbol{v}]]_T$ and $\{\{\boldsymbol{v}\}\}$ are the standard notation for the tangential jumps and averages of $\boldsymbol{v}$ across an interior face $f = \partial K^+ \bigcap \partial K^-$ between two neighboring elements K^+ and K^-:

$$[[\boldsymbol{v}]]_T = \boldsymbol{n}^+ \times \boldsymbol{v}^+ + \boldsymbol{n}^- \times \boldsymbol{v}^-, \quad \{\{\boldsymbol{v}\}\} = (\boldsymbol{v}^+ + \boldsymbol{v}^-)/2,$$

where $\boldsymbol{v}^\pm$ denotes the traces of $\boldsymbol{v}$ from within $K^\pm$, and $\boldsymbol{n}^\pm$ denote the unit outward normal vectors on the boundaries $\partial K^\pm$, respectively. While on a boundary face $f = \partial K \bigcap \partial \Omega$, we define $[[\boldsymbol{v}]]_T = \boldsymbol{n} \times \boldsymbol{v}$ and $\{\{\boldsymbol{v}\}\} = \boldsymbol{v}$. Finally, a is a penalty function, which is defined on each face $f \in F_{h_0}$ as:

$$a|_f = \gamma A(\xi) h_0^{-1}$$

where $h_0|_f = min\{h_{K^+}, h_{K^-}\}$ for an interior face $f = \partial K^+ \bigcap \partial K^-$, and $h_0|_f = h_k$ for a boundary face $f = \partial K \bigcap \partial Q$. The penalty parameter γ is a positive constant and has to be chosen sufficiently large to guarantee the coercivity of $a_{h_0}(\cdot, \cdot)$.
For the corrector equation:

$$\begin{aligned} &\nabla_\xi \times (A(\xi) \nabla_\xi \times \boldsymbol{\theta}^p(\xi)) = -\nabla_\xi \times (A(\xi) \mathbf{e}_p), \quad \xi \in Q, \\ &\nabla_\xi \cdot \boldsymbol{\theta}^p(\xi) = 0, \quad \xi \in Q, \\ &\boldsymbol{\theta}^p(\xi) \times \boldsymbol{n} = 0, \quad \xi \in \partial Q, \end{aligned} \tag{4.14}$$

Multiplying both sides of the above equation by $\boldsymbol{v} \in \boldsymbol{V}_{h_0}$ and integrating over Q leads

to the discrete DG scheme for the corrector equation:

$$\begin{aligned}
&\sum_{K\in T_{h_0}}\int_K A(\xi)\nabla_\xi\times\boldsymbol{\theta}^p_{h_0}(\xi)\cdot\nabla_\xi\times\boldsymbol{v}d\xi-\sum_{f\in F_{h_0}}\int_f[[\boldsymbol{\theta}^p_{h_0}(\xi)]]_T\cdot\{\{A(\xi)\nabla_\xi\times\boldsymbol{v}\}\}dA\\
&-\sum_{f\in F_{h_0}}\int_f[[\boldsymbol{v}]]_T\cdot\{\{A)(\xi)\nabla_\xi\times\boldsymbol{\theta}^p_{h_0}(\xi)\}\}dA+\sum_{f\in F_{h_0}}\int_f a[[\boldsymbol{\theta}^p_{h_0}(\xi)]]_T\cdot[[\boldsymbol{v}]]dA \qquad (4.15)\\
&=-\sum_{K\in T_{h_0}}\int_K(A(\xi)\mathbf{e}_p)\cdot\nabla_\xi\times\boldsymbol{v}.
\end{aligned}$$

Similarly, we get the discrete DG scheme for the corrector equation for 2D:

$$\begin{aligned}
&\sum_{K\in T_{h_0}}\int_K A(\xi)\nabla_\xi\times\boldsymbol{W}^p_{h_0}(\xi)\cdot\nabla_\xi\times\boldsymbol{v}d\xi-\sum_{f\in F_{h_0}}\int_f[[\boldsymbol{W}^p_{h_0}(\xi)]]_T\cdot\{\{A(\xi)\nabla_\xi\times\boldsymbol{v}\}\}dA\\
&-\sum_{f\in F_{h_0}}\int_f[[\boldsymbol{v}]]_T\cdot\{\{A)(\xi)\nabla_\xi\times\boldsymbol{\theta}^p_{h_0}(\xi)\}\}dA+\sum_{f\in F_{h_0}}\int_f a[[\boldsymbol{W}^p_{h_0}(\xi)]]_T\cdot[[\boldsymbol{v}]]dA \qquad (4.16)\\
&=-\sum_{K\in T_{h_0}}\int_K(A(\xi)\mathbf{e}_p)\cdot\nabla_\xi\times\boldsymbol{v}.
\end{aligned}$$

2. DG finite element for the homogenized Maxwell's equations.

We consider a shape-regular mesh T_h that partitions the domain Ω into disjoint tetrahedral (or other types, e.g., triangular) elements {K}, such that $\overline{\Omega}=\bigcup_{K\in T_h}K$. We denote the diameter of K by h_K, and the mesh size h by $h=max_{K\in T_h}h_K$. Furthermore, we denote the set of all interior faces by F_h^I, the set of all boundary faces by F_h^B, and the set of all faces by $F_h=F_h^I\bigcup F_h^B$.

We assume that the finite element space $\boldsymbol{V}_h$ is given by

$$\boldsymbol{V}_h=\{\boldsymbol{v}\in\boldsymbol{L}^2(\Omega):\boldsymbol{v}|_K\in(P_l(K))^d,K\in T_h\},\quad d=2,3,\quad l\geq 1,$$

As usual, we can define the solution $\boldsymbol{E}^0$ of the homogenized Maxwell equation for (4.3) as

$$\begin{aligned}
&\boldsymbol{E}^0_{tt}+\nabla\times(\widehat{A}\nabla\times\boldsymbol{E}^0)+\omega_p^2\boldsymbol{E}^0-\boldsymbol{J}(\boldsymbol{E}^0)=\mathbf{f}\quad\text{in}\quad\Omega\times(0,T), \qquad (4.17)\\
&\boldsymbol{n}\times\boldsymbol{E}=0\quad on\quad\partial\Omega\times(0,T)
\end{aligned}$$

Here, $\widehat{A}$ is the homogenized coefficient matrix of $c_v^2(\frac{\boldsymbol{x}}{\epsilon})$ (for 2D, we use the scalar $\widehat{a}$ instead).

Using the above homogenization method, we get the numerical homogenized coefficient $\widehat{A}_{h_0}$ or $\widehat{a}_{h_0}$ of $c_v^2(\frac{\boldsymbol{x}}{\epsilon})$ for 3D and 2D respectively,

$$\begin{aligned}\widehat{A}_{h_0} &= \int_Q [A(\xi) + A(\xi)\nabla_\xi \times \boldsymbol{\theta}_{h_0}(\xi)]d\xi \\ \widehat{a}_{h_0} &= \int_Q [a(\xi) + a(\xi)\nabla_\xi \times \boldsymbol{W}_{h_0}(\xi)]d\xi.\end{aligned} \tag{4.18}$$

To define a fully discrete scheme of the homogenized Maxwell equation, we divide the time interval $(0,T)$ into M uniform subintervals by points $0 = t_0 < t_1 < t_2 < ... < t_M = T$, where $t_k = k\tau$, and denote $I^k = [t_{k-1}, t_{k+1}]$. Moreover, we define $\boldsymbol{u}^k = \boldsymbol{u}(., t_k)$ for $0 \le k \le M$, and denote the difference operators:

$$\overline{\boldsymbol{u}}^k = (\boldsymbol{u}^{k+1} + \boldsymbol{u}^{k-1})/2 \quad \delta_\tau^2 \boldsymbol{u}^k = (\boldsymbol{u}^{k+1} - 2\boldsymbol{u}^k + \boldsymbol{u}^{k-1})/\tau^2.$$

Now we can formulate an implicit scheme for (4.17): for any $1 \le k \le M-1$, find $\boldsymbol{E}_h^{0,k+1} \in \boldsymbol{V}_h$ such that

$$(\delta_\tau^2 \boldsymbol{E}_h^{0,k}, \boldsymbol{v}) + a_h(\overline{\boldsymbol{E}}_h^{0,k}, \boldsymbol{v}) + \omega_p^2(\overline{\boldsymbol{E}}_h^{0,k}, \boldsymbol{v}) - (\boldsymbol{J}_h^{0,k}, \boldsymbol{v}) = (\overline{f}^k, \boldsymbol{v}), \quad \forall \boldsymbol{v} \in \boldsymbol{V}_h. \tag{4.19}$$

Similarly, we define the bilinear form a_h on $\boldsymbol{V}_h \times \boldsymbol{V}_h$ as follows (use $\widehat{a}_{h_0}$ for 2D):

$$\begin{aligned}a_h(\boldsymbol{u}, \boldsymbol{v}) = &\sum_{K \in T_h} \int_K \widehat{A}_{h_0} \nabla \times \boldsymbol{u} \cdot \nabla \times \boldsymbol{v} d\boldsymbol{x} - \sum_{f \in F_h} \int_f [[\boldsymbol{u}]]_T \cdot \{\{\widehat{A}_{h_0} \nabla \times \boldsymbol{v}\}\} dA \\ &- \sum_{f \in F_h} \int_f [[\boldsymbol{v}]]_T \cdot \{\{\widehat{A}_{h_0} \nabla \times \boldsymbol{u}\}\} dA + \sum_{f \in F_h} \int_f a[[\boldsymbol{u}]]_T \cdot [[\boldsymbol{v}]] dA.\end{aligned}$$

Here a is a penalty function, which is defined on each face $f \in F_h$ as

$$a|_f = \gamma \widehat{A}_{h_0} h^{-1},$$

where $h|_f = min\{h_{K^+}, h_{K^-}\}$ for an interior face $f = \partial K^+ \bigcap \partial K^-$, and $h|_f = h_k$ for a boundary face $f = \partial K \bigcap \partial\Omega$. The penalty parameter γ is a positive constant and has to be chosen sufficiently large to guarantee the coercivity of $a_h(\cdot, \cdot)$.

The initial approximation is

$$\boldsymbol{E}_h^{0,0} = \prod_h \boldsymbol{E}_0^0, \quad \boldsymbol{E}_h^{0,1} = \prod_h (\boldsymbol{E}_0^0 + \tau \boldsymbol{E}_1^0 + \frac{\tau^2}{2} \boldsymbol{E}_{tt}^0(0)), \tag{4.20}$$

where $\boldsymbol{J}_h^{0,k}$ is defined by the recursive formula:

$$\boldsymbol{J}_h^{0,0} = 0, \quad \boldsymbol{J}_h^{0,k} = e^{-\nu\tau}\boldsymbol{J}_h^{0,k-1} + \frac{\nu\omega_p^2}{2}\tau(e^{-\nu\tau}\boldsymbol{E}_h^{0,k-1} + \boldsymbol{E}_h^{0,k}), \quad k \geq 1. \tag{4.21}$$

In (4.20), $\boldsymbol{E}_{tt}^0(0)$ can be obtained by setting $t = 0$ in (4.17). With the corrector $\boldsymbol{\theta}_{h_0}$ and the homogenized solution $\boldsymbol{E}_h^{0,k+1}$, we can use the multiscale asymptotic expansions to get $\boldsymbol{E}_h^{k+1}$:

$$\boldsymbol{E}_{h,h_0}^{k+1}(\boldsymbol{x}) = \boldsymbol{E}_h^{0,k+1}(\boldsymbol{x}) + \epsilon\boldsymbol{\theta}_{h_0}(\xi)\nabla \times \boldsymbol{E}_h^{0,k+1}(\boldsymbol{x}) + ... \tag{4.22}$$

For 2D, we use $\boldsymbol{W}_{h_0}(\xi)$ instead of $\boldsymbol{\theta}_{h_0}(\xi)$ in (4.22).

We now provide some numerical results to support our DG finite element homogenization method. The first and second examples are used to test the homogenization method. In the first example, we used the time-harmonic Maxwell's equations with rapidly oscillating coefficients to test if our DG finite element homogenization is convergent and stable. The second example is to compare our method to the theoretical M-G method in different kinds of inclusions, in which we will see the similarities and differences between our method and the M-G method. Example 3 is focused on solving our governing equations in a periodic heterogeneous medium. For simplicity, all of our problems are based on 2D ($\Omega = (0,1) \times (0,1)$). The basis function for all problems is composed of a discontinuous linear finite element, and the mesh is uniformly refined triangular elements.

The implementation of the Multiscale DG finite element method for solving the Maxwell's equations (4.3) in composite materials consists of the following parts,

- Part I. Compute the cell functions (4.15) ((4.16) for 2D) for the corrector θ_{h_0} ($\boldsymbol{W}_{h_0}$ for 2D) on a reference cell $Q = (0,1)^2$.
- Part II. After solving (4.18) for the homogenized coefficient $\widehat{A}_{h_0}$ ($\widehat{a}_{h_0}$ for 2D), solve the implicit DG finite scheme for modified homogenized Maxwell's equations (4.19)-(4.21) over the whole domain Ω.
- Part III. Calculate numerically the multiscale asymptotic expansions (4.22).

4.3 NUMERICAL RESULTS

Example 4.3.1. To validate the homogenization method, we first test on the homogenized problem. Comparing to [[15] example 5.1], we use the DG method to test the stability of the DG homogenization method. We consider the same time-harmonic Maxwell's equations with rapidly oscillating coefficients given by

$$\begin{aligned} &\nabla \times (a(\frac{\boldsymbol{x}}{\epsilon})\nabla \times \boldsymbol{u}^\epsilon) - \omega^2 \boldsymbol{u}^\epsilon = \boldsymbol{f}(\boldsymbol{x}), \quad \boldsymbol{x} \in \Omega, \\ &\nabla \cdot \boldsymbol{u}^\epsilon = 0, \quad \boldsymbol{x} \in \Omega, \\ &\boldsymbol{u}^\epsilon \times \boldsymbol{n} = 0, \quad \boldsymbol{x} \in \partial\Omega. \end{aligned} \tag{4.23}$$

We assume that $\Omega = (0,1)^2$ is a periodic structure, where $\epsilon = \frac{1}{100}$, $\omega^2 = 1$. The coefficient $a(\frac{\boldsymbol{x}}{\epsilon})$ is a continuous and rapidly oscillating periodic function, as in the following:

$$a(\frac{\boldsymbol{x}}{\epsilon}) = \frac{20}{(2 + 1.5sin(2\pi(\frac{x}{\epsilon}) + 0.75))(2 + 1.5sin(2\pi(\frac{y}{\epsilon}) + 0.75))}$$

Let $\boldsymbol{x} = (x, y)$, and $\boldsymbol{E}_1$ be the multiscale DG finite element solution based on (4.13), with $\boldsymbol{f} = (30, 30)^T$.

These figures ((4.1)-(4.3)) clearly show that our DG finite element homogenization method is stable and convergent for time-harmonic Maxwell's equations with rapidly oscillating coefficients as the mesh size becomes smaller.

Example 4.3.2. The second example is to verify our method of finding homogenized coefficients. We will compare our numerical DG finite element method discussed here to the theoretical mixture models, the Maxwell-Garnett formula. Here we will only show the result from method 2 ((4.7) for 3D, (4.11) for 2D).

In Figure (4.5), we present a comparison of the homogenized coefficients in differently shaped inclusions. We find that for a square or circle inclusion, our numerical method produces almost the same coefficient as M-G formulas, which is best suited for smooth canonical shapes(i.e., ellipses). When the shape is not smooth, the result produced by our

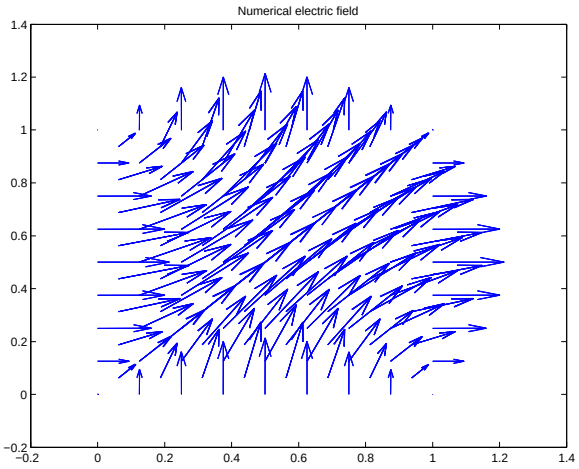

(a) the multiscale electric field $\boldsymbol{E}^1$,

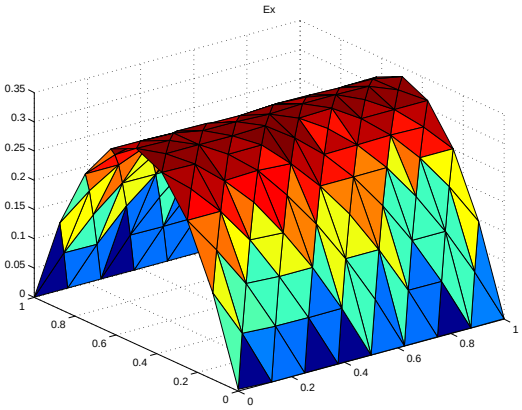

(b) $\boldsymbol{E}^1_x$, the x component of $\boldsymbol{E}^1$

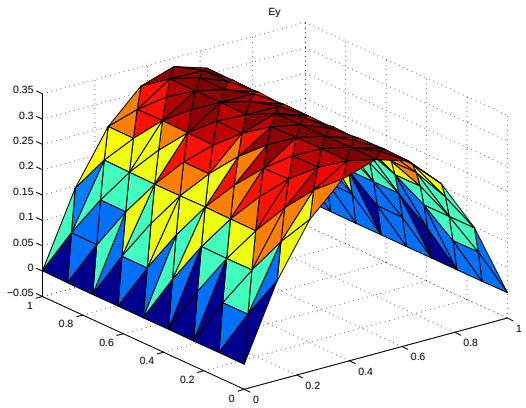

(c) $\boldsymbol{E}^1_y$, the y component of $\boldsymbol{E}^1$

Figure 4.1: unit cell mesh size $1/2^7$, domain mesh size $1/2^3$ for example (4.3.1)

method is bigger than the M-G result. In general, if you want to have a higher effective coefficient, complex shaped inclusions should be used.

Example 4.3.3. In this problem we choose the material parameters $\epsilon = 2$, $\mu = 1$ inside the inclusion. So $c_v^2 = 0.5$ here inside the inclusion. The host medium is free space, and the volume fraction is 0.4, with $\omega_p = \nu = 1$. The source term $f = 0$ in Ω. We solve a

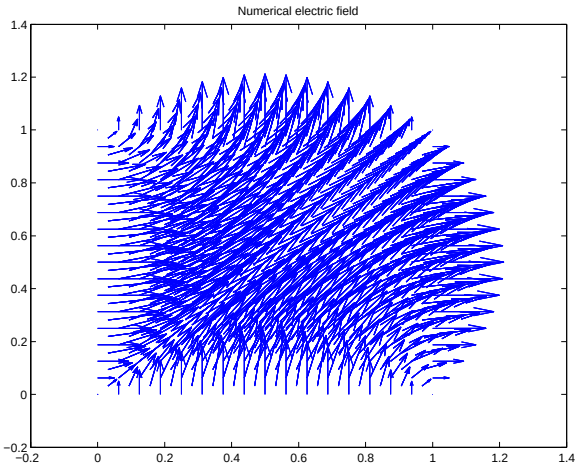

(a) the multiscale electric field $\boldsymbol{E}^1$,

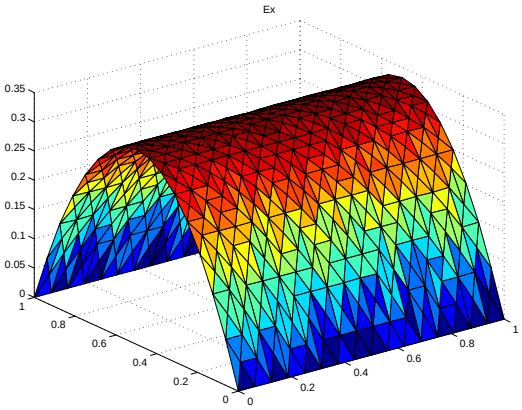

(b) $\boldsymbol{E}^1_x$, the x component of $\boldsymbol{E}^1$

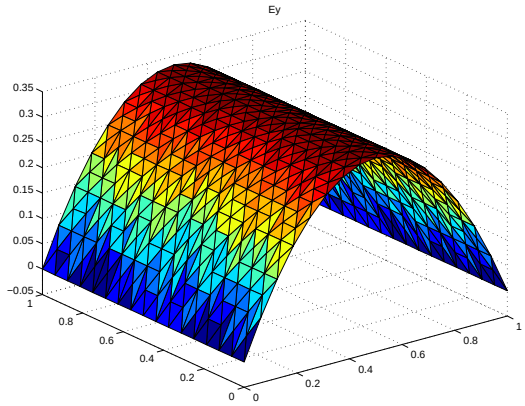

(c) $\boldsymbol{E}^1_y$, the y component of $\boldsymbol{E}^1$

Figure 4.2: unit cell mesh size $1/2^7$, domain mesh size $1/2^4$ for example (4.3.1)

two-dimensional version of (4.1) with initial conditions

$$\boldsymbol{E}^0 = \boldsymbol{E}(x, y, 0) = (cos(\pi x)sin(\pi y), sin(\pi x)cos(\pi y))^T$$

$$\boldsymbol{E}^1 = \boldsymbol{E}_t(x, y, 0) = e^{-\tau}(cos(\pi x)sin(\pi y), sin(\pi x)cos(\pi y))^T$$

Note that $\nabla \cdot \boldsymbol{E}^i = 0$ in Ω and $\boldsymbol{n} \times \boldsymbol{E}^i = 0$ on $\partial\Omega$, $i = 0, 1$. The time step size is chosen as $\tau = 0.02$. Since the exact solution is unknown, we just plot the numerical solution $\boldsymbol{E}$ at the final time $T = 1$ obtained with $h = \frac{1}{8}, \frac{1}{16}, \frac{1}{32}$, $\epsilon = 10^{-5}$ and the unit cell mesh size $h_0 = \frac{1}{2^7}$.

From these figures (4.6), we can clearly say that the numerical solution is convergent to

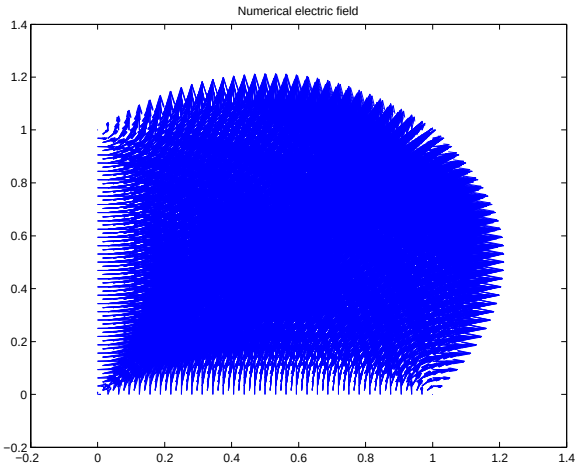

(a) the multiscale electric field $\boldsymbol{E}^1$,

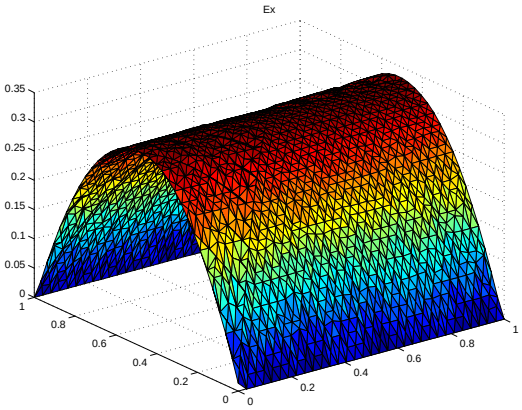

(b) $\boldsymbol{E}^1_x$, the x component of $\boldsymbol{E}^1$

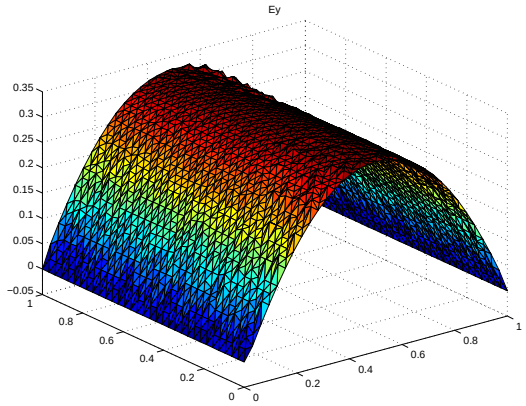

(c) $\boldsymbol{E}^1_y$, the y component of $\boldsymbol{E}^1$,

Figure 4.3: unit cell mesh size $1/2^7$, domain mesh size $1/2^5$ for example (4.3.1)

the same solution for different meshes. This example illustrates that our DG homogenization scheme is quite effective for heterogeneous periodic materials.

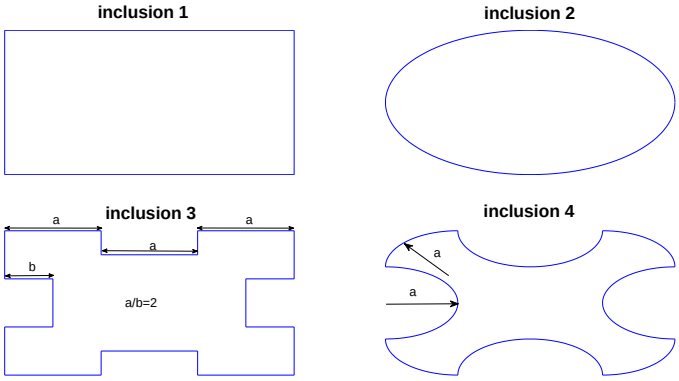

Figure 4.4: Geometry of the studied two-dimensional inclusions

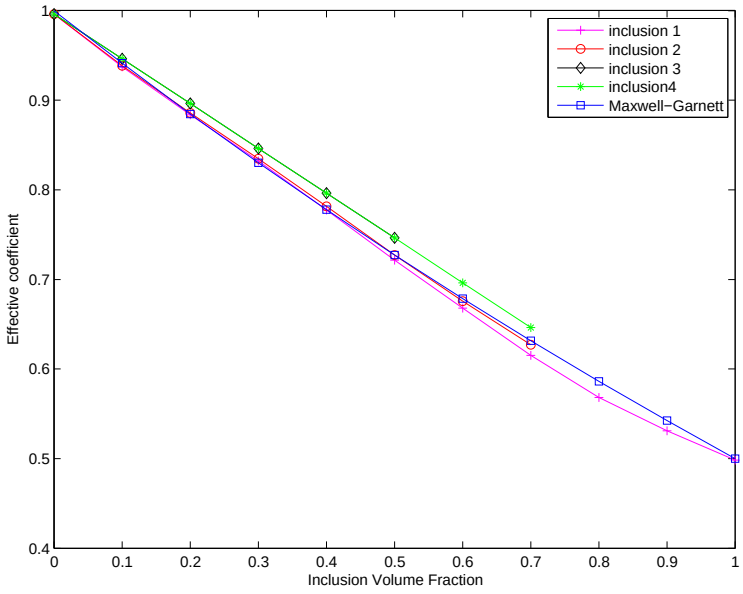

Figure 4.5: for problem (4.3.2), computed homogenized $\widehat{a}_{h_0}$ for the governing equation for $c_v(\frac{\boldsymbol{x}}{\epsilon})$ with $\epsilon = 2$, $\mu = 1$ inside the inclusion (figure (4.4)). So $c_v^2 = 0.5$ inside the inclusion.The host medium is free space. The mesh size is $h_0 = 1/2^7$

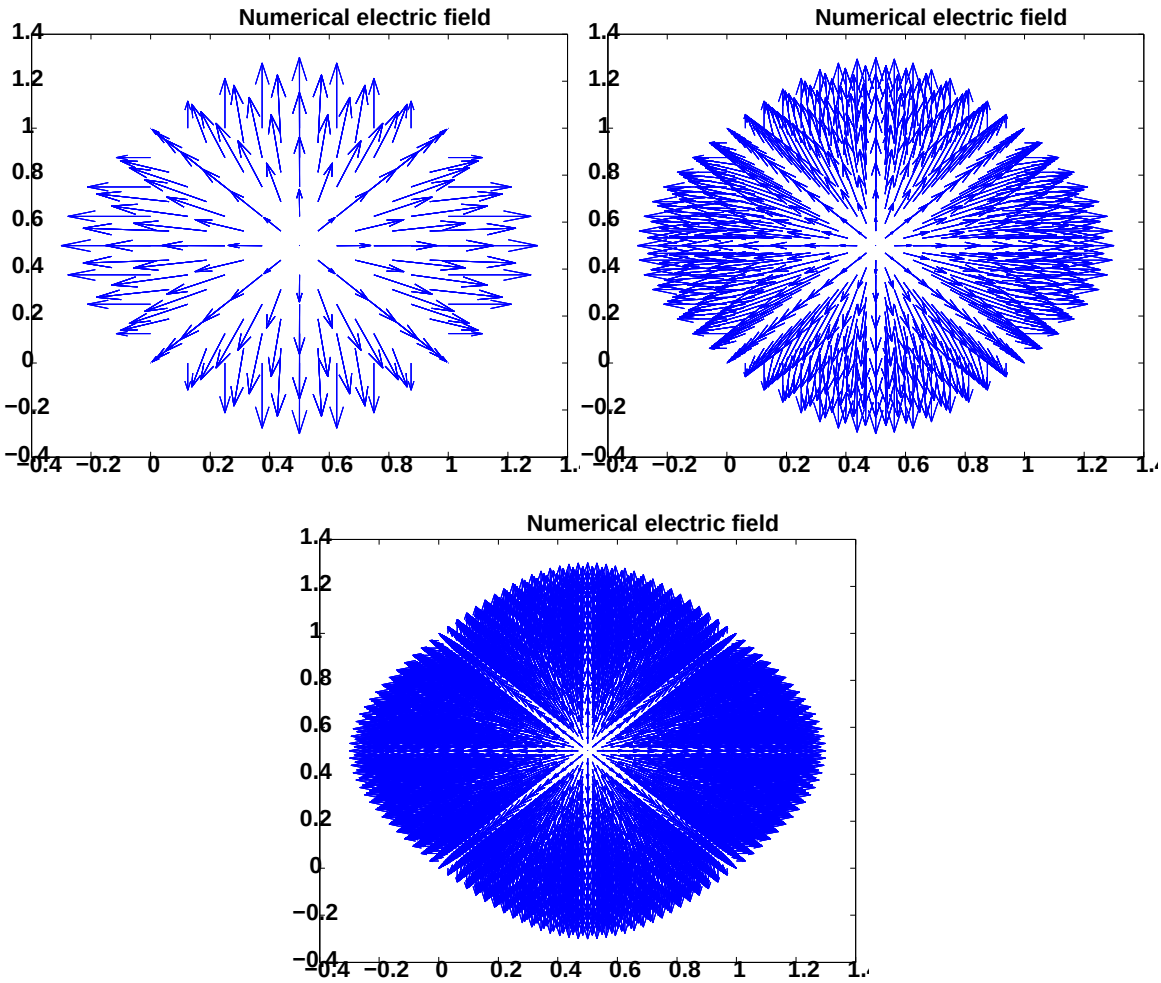

Figure 4.6: The numerical electric fields $\boldsymbol{E}$ at time $T = 1$ obtained with $\tau = 0.02$ and different meshes: $h = \frac{1}{8}$, $h = \frac{1}{16}$, $h = \frac{1}{32}$

Chapter 5

CONCLUSION AND FUTURE WORK

5.1 SUMMARY

This dissertation further developed DG-FEM for solving Maxwell's equations based on the nodal discontinuous Galerkin method introduced by Hesthaven and Warburton in ([28, 29]). Prior to the present work, DG-FEM combined with RK schemes was used to solve time difference problems, but a rigorous proof establishing the stability and convergence rate of the fully discrete DG-FEM RK scheme was lacking. In chapter 3, such a proof was presented. The analytic error estimate, $O(h^{min\{s,k\}} + \tau^2)$, is consistent with the numerical results previously found by J. Li [44]. It was further pointed out that this method of proof works for any order RK scheme, which has important implications in any engineering context that makes use of similar schemes. For example, the explicit low-storage version of RK (LSERK) methods are widely used by engineers because of the significant reduction in memory demands. These engineers typically solve PDEs in the element-wise semi-discrete form using LSERK and DG-FEM without having established that their methods are actually stable and convergent. In the case of Maxwell's equations, this dissertation has justified the use of these methods by providing a versatile way to prove that these schemes are convergent.

In chapter 4, the DG-FEM was applied to solve Maxwell's equations in metamaterials. A new DG scheme was developed that uses a leap-frog time step in order to solve the time domain Maxwell's equations in metamaterials, as given in ([48]). A rigorous stability proof and error estimates were provided. Although this scheme is implicit and is more computationally expensive than RK-FEM, the numerical results show that its convergence rate is CTh^{k+1} due to the upwind flux, which is one order higher than the convergence rate of RK-FEM. This is consistent with the results in other published works.

Chapter 4 also presented a second DG time difference DG-FEM for solving Maxwell's

equation in metamaterials. This method has an error estimate of $O(h^{min\{s,k\}} + \tau^2)$ with the use of a central flux and numerical results were provided to support the analytic error estimate. Numerical simulations of wave propagation in double negative (DNG) metamaterials supplemented with PML boundary conditions were carried out using this method. The simulations were designed to model the exotic phenomenon of backward wave propagation, as discovered by previous investigators, and are the first to model this phenomenon using DG-FEM.

In chapter 5, the homogenization multi-scale DG-FEM was developed for the first time. Specifically, a solution to the time-dependent Maxwell's equations with periodically varying coefficients in dispersive media is found by the DG method. We carried out the fully DG scheme for the homogenization method and were able to obtain its convergence rate. The latter could not be tested numerically due to the lack of a known exact solution to Maxwell's equations in heterogeneous materials, as well as to the presence of multiple factors affecting the convergence rate. However, we did show that our solution is convergent in (4.3.1) and in (4.3.3). The comparison we made for the effective coefficients obtained by the homogenization method versus those computed by the MG mixture formula both affirms the correctness of our code and shows that we can solve Maxwell's equations in arbitrarily complicated shapes of inclusions. There are several follow-up works planned, including more detailed simulations dealing with non-stationary coefficients as well as adding varying coefficients in the convolution term of our governing equations.

5.2 FUTURE WORK

Since metamaterials are an extremely rich and exciting area for applying the DG-FEM, with notable applications including invisibility cloaks, sub-wavelength imaging, and novel antenna designs, most of the examples given in this dissertation can be considered a starting point mainly aimed at reproducing simulation results already obtained using simpler methods. The real power of DG-FEM will reveal itself when simulating realistic phenomena with complicated geometries and material properties. For example, the DG homogenization method can be used to simulate wave propagation in metamaterials constructed from peri-

odic microstructures [12, 39], which could be used to both help build and understand actual metamaterial devices. Experience has shown that applications such as this are computationally expensive, taking many days to run, especially if performed in 3D. The algorithms underlying the implementation of DG-FEM are highly parallelizable, so another line of future work involves writing a parallel version of my code to allow it to run on graphics processing units.

BIBLIOGRAPHY

[1] Y. Ould Agha A. Nicolet, F. Zolla and S. Guenneau. Geometrical transformations and equivalent materials in computational electromagnetism. *COMPEL: The International Journal for Computation and Mathematics in Electrical and Electronic Engineering*, 27:806 – 819, 2008.

[2] S. Adjerid, K. D. Devine, J. E. Flaherty, and L. Krivodonova. A posteriori error estimation for discontinuous galerkin solutions of hyperbolic problems. *Computer Methods in Applied Mechanics and Engineering*, 191(11-12):1097–1112, 2002.

[3] G. Allaire. Homogenization and two-scale convergence. *SIAM Journal on Mathematical Analysis*, 23(6):1482–1518, 1992.

[4] D. N. Arnold, F. Brezzi, B. Cockburn, and L. D. Marini. Unified analysis of discontinuous galerkin methods for elliptic problems. *SIAM Journal on Numerical Analysis*, 39(5):1749–1779, 2002.

[5] C. Athanasiadis, G. Costakis, and IG Stratis. Electromagnetic scattering by a homogeneous chiral obstacle in a chiral environment. *IMA Journal of Applied Mathematics*, 64(3):245–258, 2000.

[6] H. Banks, V. Bokil, D. Cioranescu, N. Gibson, G. Griso, and B. Miara. Homogenization of periodically varying coefficients in electromagnetic materials. *Journal of Scientific Computing*, 28(2):191–221, 2006.

[7] G. Barbatis and I. G. Stratis. Homogenization of maxwell's equations in dissipative bianisotropic media. *Mathematical Methods in the Applied Sciences*, 26(14):1241–1253, 2003.

[8] A. Bensoussan, J. L. Lions, and G. Papanicolaou. *Asymptotic analysis for periodic structures*, volume 5. North-Holland Pub. Co., Amsterdam; New York, 1978.

[9] J. P. Berenger. A perfectly matched layer for the absorption of electromagnetic waves. *Journal of Computational Physics*, 114(2):185–200, 1994.

[10] A. Bossavit. Solving maxwell equations in a closed cavity, and the question of 'spurious modes'. *Magnetics, IEEE Transactions on*, 26(2):702–705, 1990.

[11] A. Bossavit, G. Griso, and B. Miara. Modelling of periodic electromagnetic structures bianisotropic materials with memory effects. *Journal de mathematiques pures et appliquees*, 84(7):819–850, 2005.

[12] G. Bouchitte and B. Schweizer. Homogenization of maxwell's equations in a split ring geometry*. *Multiscale Modeling & Simulation*, 8(3):717–750, 2010.

[13] A. Bouquet, C. Dedeban, and S. Piperno. Discontinuous galerkin time-domain solution of maxwell's equations on locally refined grids with fictitious domains. *COMPEL - The International Journal for Computation and Mathematics in Electrical and Electronic Engineering*, 29(3):578–601, 2010.

[14] S. C. Brenner and L. R. Scott. *The mathematical theory of finite element methods*, volume 15. Springer-Verlag, New York, 1994.

[15] L. Cao, Y. Zhang, W. Allegretto, and Y. Lin. Multiscale asymptptoc method for maxwell's equations in composite materials. *SIAM Journal on Numerical Analysis*, 47(6):4257–4289, 2009.

[16] Weng Cho Chew and William H. Weedon. A 3d perfectly matched medium from modified maxwell's equations with stretched coordinates. *Microwave and Optical Technology Letters*, 7(13):599–604, 1994.

[17] D. Cioranescu, A. Damlamian, and G. Griso. Periodic unfolding and homogenization. *Comptes Rendus Mathematique*, 335(1):99–104, 2002.

[18] D. Cioranescu and Patrizia Donato. *An introduction to homogenization*, volume 17. Oxford University Press, Oxford, Great Britain; New York, 1999.

[19] B. Cockburn, G. Karniadakis, and C. Shu. *Discontinuous Galerkin methods :theory, computation, and applications*, volume 11. Springer, Berlin; New York, 2000.

[20] B. Cockburn, F. Li, and C. Shu. Locally divergence-free discontinuous galerkin methods for the maxwell equations. *Journal of Computational Physics*, 194(2):588–610, 2004.

[21] S. A. Cummer. Dynamics of causal beam refraction in negative refractive index materials. *Applied Physics Letters*, 82(13):2008–2010, 2003.

[22] C. Dawson and J. Proft. Discontinuous and coupled continuous/discontinuous galerkin methods for the shallow water equations. *Computer Methods in Applied Mechanics and Engineering*, 191(41-42):4721–4746, 2002.

[23] V. Dolean, H. Fahs, L. Fezoui, and S. Lanteri. Locally implicit discontinuous galerkin method for time domain electromagnetics. *Journal of Computational Physics*, 229(2):512–526, 2010.

[24] L. Fezoui, S. Lanteri, S. Lohrengel, and S. Piperno. Convergence and stability of a discontinuous galerkin time-domain method for the 3d heterogeneous maxwell equations on unstructured meshes. *ESAIM: Mathematical Modelling and Numerical Analysis*, 39(06):1149, 2005.

[25] L. Fezoui, S. Lanteri, S. Lohrengel, and S. Piperno. Convergence and stability of a discontinuous galerkin time-domain method for the 3d heterogeneous maxwell equations on unstructured meshes. *ESAIM.Mathematical Modelling and Numerical Analysis*, 39(6):1149–1176, 2005.

[26] M. J. Grote, A. Schneebeli, and D. Schotzau. Interior penalty discontinuous galerkin method for maxwell's equations: Energy norm error estimates. *Journal of Computational and Applied Mathematics*, 204(2):375–386, 2007.

[27] Y. Hao, R. Mittra, and Inc ebrary. *FDTD modeling of metamaterials*. Artech House, Norwood, Mass., 2009.

[28] J. S. Hesthaven and T. Warburton. Nodal high-order methods on unstructured grids: I. time-domain solution of maxwell's equations. *Journal of Computational Physics*, 181(1):186–221, 2002.

[29] J. S. Hesthaven and T. Warburton. *Nodal discontinuous Galerkin methods :algorithms, analysis, and applications*. Springer, New York, 2008.

[30] T. Y. Hou, X. Wu, and Z. Cai. Convergence of a multiscale finite element method for elliptic problems with rapidly oscillating coefficients. *Mathematics of Computation*, 68(227):pp. 913–943, 1999.

[31] Paul Houston, Ilaria Perugia, Anna Schneebeli, and Dominik Schotzau. Interior penalty method for the indefinite time-harmonic maxwell equations. *Numerische Mathematik*, 100:485–518, 2005.

[32] F. Q. Hu, M. Y. Hussaini, and P. Rasetarinera. An analysis of the discontinuous galerkin method for wave propagation problems. *Journal of Computational Physics*, 151(2):921–946, 1999.

[33] J. Huang, X. Huang, and W. Han. A new discontinuous galerkin method for kirchhoff plates. *Computer Methods in Applied Mechanics and Engineering*, 199(23-24):1446–1454, 2010.

[34] Y. Huang and J. Li. Interior penalty discontinuous galerkin method for maxwell's equations in coldplasma. *Journal of Scientific Computing*, 41(3):321–340, 2009.

[35] Y. Huang, J. Li, and W. Yang. Interior penalty dg methods for maxwell's equations in dispersive media. *Journal of Computational Physics*, 230(12):4559–4570, 2011.

[36] T. J. R. Hughes, G. Scovazzi, P. B. Bochev, and A. Buffa. A multiscale discontinuous galerkin method with the computational structure of a continuous galerkin method. *Computer Methods in Applied Mechanics and Engineering*, 195(19-22):2761–2787, 2006.

[37] D. Jiao and J. Jin. Time-domain finite-element modeling of dispersive media. *Microwave and Wireless Components Letters, IEEE*, 11(5):220–222, 2001.

[38] C. Kenig and Z. Shen. Homogenization of elliptic boundary value problems in lipschitz domains. *Mathematische Annalen*, 350(4):867–917, 2011.

[39] R. V. Kohn and S. P. Shipman. Magnetism and homogenization of microresonators. *Multiscale Modeling & Simulation*, 7(1):62–31, 2008.

[40] S. Lanteri and C. Scheid. Convergence of a discontinuous galerkin scheme for the mixed time-domain maxwell's equations in dispersive media. *IMA Journal of Numerical Analysis*, 2012.

[41] D. Levy, C. Shu, and J. Yan. Local discontinuous galerkin methods for nonlinear dispersive equations. *Journal of Computational Physics*, 196(2):751–772, 2004.

[42] D. Levy and E. Tadmor. From semidiscrete to fully discrete: Stability of runge-kutta schemes by the energy method. *SIAM Review*, 40(1):40–73, 1998.

[43] J. Li. Numerical convergence and physical fidelity analysis for maxwell's equations in metamaterials. *Computer Methods in Applied Mechanics and Engineering*, 198(37-40):3161–3172, 2009.

[44] J. Li. Development of discontinuous galerkin methods for maxwell's equations in metamaterials and perfectly matched layers. *Journal of Computational and Applied Mathematics*, 236(5):950–961, 2011.

[45] J. Li. Optimal l-2 error estimates for the interior penalty dg method for maxwell's equations in cold plasma. *Communications in Computational Physics*, 11(2):319–334, 2012.

[46] J. Li and J. Waters. Homogenized discontinuous galerkin method for maxwells equations in periodic structured dispersive media. *Contemporary Mathematics*, 586:247–256, 2013.

[47] J. Li, J. Waters, and E. A. Machorro. An implicit leap-frog discontinuous galerkin method for the time-domain maxwell's equations in metamaterials. *Computer Methods in Applied Mechanics and Engineering*, 223-224(0):43–54, 2012.

[48] Jichun Li and Aihua Wood. Finite element analysis for wave propagation in double negative metamaterials. *Journal of Scientific Computing*, 32:263–286, 2007.

[49] T. Lu, P. Zhang, and W. Cai. Discontinuous galerkin methods for dispersive and lossy maxwell's equations and pml boundary conditions. *Journal of Computational Physics*, 200(2):549–580, 2004.

[50] E. Machorro. Discontinuous galerkin finite element method applied to the 1-d spherical neutron transport equation. *Journal of Computational Physics*, 223(1):67–81, 2007.

[51] E. Montseny, S. Pernet, X. Ferrieres, and G. Cohen. Dissipative terms and local time-stepping improvements in a spatial high order discontinuous galerkin scheme for the time-domain maxwell's equations. *Journal of Computational Physics*, 227(14):6795–6820, 2008.

[52] J.C. Nedelec. Mixed finite elements in r3. *Numerische Mathematik*, 35:315–341, 1980.

[53] J. Tinsley O., I. Babuska, and C. E. Baumann. A discontinuoushpfinite element method for diffusion problems. *Journal of Computational Physics*, 146(2):491–519, 1998.

[54] O. Ouchetto, S. Zouhdi, A. Bossavit, G. Griso, B. Miara, and A. Razek. Homogenization of structured electromagnetic materials and metamaterials. *Journal of Materials Processing Technology*, 181(1-3):225–229, 2007.

[55] A. H. Sihvola and Institution of Electrical Engineers. *Electromagnetic mixing formulas and applications*, volume 47. Institution of Electrical Engineers, London, 1999.

[56] F. L. Teixeira and W. C. Chew. General closed-form pml constitutive tensors to match arbitrary bianisotropic and dispersive linear media. *Microwave and Guided Wave Letters, IEEE*, 8(6):223–225, 1998.

[57] E. Turkel and A. Yefet. Absorbing pml boundary layers for wave-like equations. *Applied Numerical Mathematics*, 27(4):533–557, 1998.

[58] B. Wang, Z. Xie, and Z. Zhang. Error analysis of a discontinuous galerkin method for maxwell equations in dispersive media. *Journal of Computational Physics*, 229(22):8552–8563, 2010.

[59] Niklas Wellander. Homogenization of the maxwell equations: Case i. linear theory. *Applications of Mathematics*, 46:29–51, 2001.

[60] A. Nicolet Y. Ould Agha, F. Zolla and S. Guenneau. On the use of pml for the computation of leaky modes: An application to microstructured optical fibres. *COMPEL: The International Journal for Computation and Mathematics in Electrical and Electronic Engineering*, 27:95 – 109, 2008.

[61] R. Ziolkowski. Pulsed and cw gaussian beam interactions with double negative metamaterial slabs. *Opt. Express*, 11(7):662–681, 2003.

[62] R. W. Ziolkowski. Maxwellian material based absorbing boundary conditions. *Computer Methods in Applied Mechanics and Engineering*, 169(3-4):237–262, 1999.

[63] J. Zitelli, I. Muga, L. Demkowicz, J. Gopalakrishnan, D. Pardo, and V. M. Calo. A class of discontinuous petrov-galerkin methods. part iv: The optimal test norm and time-harmonic wave propagation in 1d. *Journal of Computational Physics*, 230(7):2406–2432, 2011.

Jiajia Waters
5920 Mt. Flora Ct., Las Vegas, NV 89156
wangj16@unlv.nevada.edu, 702.445.1430

- EDUCATION
  PhD, Computational Mathematics
  UNLV, Spring 2013
  GPA: 3.956 /4.0
  Advisor, Dr. Jichun Li.

  BS, Department of Computer Science and Technology, July 2007
  Chongqing University of Posts and Telecommunications, Chongqing China

- WORK EXPERIENCE
  Graduate Assistant — Fall 2008 - Present
  Math Department, University of Nevada, Las Vegas

  - Course instructor: Taught almost all first and second year math courses.
  - Course breakout instructor: The only student in recent years selected to oversee the lab and problem solving workshops for computational linear algebra (at the level of Golub & Van Loan) and vector calculus.

  Managerial Assistant — 2007 - 2008
  Xuankun Animation Company, Shanghai, China

  Undergraduate Research Assistant — 2005 - 2007
  High Performance Computing Laboratory of Professor Tian Youxian

  - Responsible for writing benchmark speed tests for solving systems of linear equations in parallel using C and MPI.

- TECHNICAL EXPERTISE
  Scientific computing, high level programming, numerically solving nonlinear partial differential equations (expert in Finite Element methods)

- COMPUTING SKILLS
  Languages & Software: C++, C, Fortran, MATLAB, FreeFem++, Microsoft Office products
  Operating Systems: Unix, Mac, Windows
  Typesetting: LaTeX

- SPOKEN LANGUAGES
  Fluent in Mandarin Chinese and English.

- HONORS & AWARDS

  - Awarded a travel grant to give a research talk at the October 2011 American Mathematical Society (AMS) Meeting in Salt Lake City, Utah
  - Outstanding Graduate of Chongqing University of Posts and Telecommunications

- Outstanding Student Scholarship Recipient, Chongqing University of Posts and Telecommunications, 2004-2007
- National Computer Rank Examination Certificate (Rank III - Database), 2005

- PUBLICATIONS

  J. Li & J. Waters, An implicit leap-frog discontinuous Galerkin method for the time-domain Maxwell's equations in metamaterials, Computer Methods in Applied Mechanics and Engineering, Volumes 223-224, 1 June 2012, Pages 43-54.

  J. Li & J. Waters, Homogenized discontinuous Galerkin method for Maxwell's equations in periodic structured dispersive media, Recent Advances in Scientific Computing and Applications, AMS Contemporary Mathematics, in press

  M. Neda, F. Pahlevani, & J. Waters, Sensitivity computations of the Leray-α model, Recent Advances in Scientific Computing and Applications, AMS Contemporary Mathematics, in press

Jiajia Waters

waters.jiajia@gmail.com, 702.445.1430

OBJECTIVE

To apply my expertise using the discontinuous Galerkin finite element method for solving Maxwell's Equations in metamaterials to related or unrelated real world problems.

EDUCATION

PhD, Computational Mathematics
UNLV, Expected May 2013
Advisor, Jichun Li
GPA: 3.96/4.0

BS, Information and Computing Science
Department of Computer Science and Technology, July 2007
Chongqing University of Posts and Telecommunications, Chongqing China

EXPERIENCE IN SCIENTIFIC COMPUTING

3+ years experience: C, C++, FreeFem++, MATLAB, Python
Scientific Libraries: The GSL and Boost libraries were both utilized when I wrote my own three-dimensional DG code using C++.
Linux kung-fu: Intermediate– writing makefiles and simple scripts to automate tasks.
High Performance Computing: Used UNLV's cluster remotely in order to compute the results presented in my publications.
GPU Parallel Programming: Currently learning CUDA in online courses offered through Coursera and Udacity.

WORK EXPERIENCE

Graduate Assistant Fall 2008 - Present
Math Department, University of Nevada, Las Vegas

- *Course instructor:* Taught almost all first and second year math courses.
- *Course breakout instructor:* The only student in recent years selected to oversee the lab and problem solving workshops for computational linear algebra (at the level of Golub & Van Loan) and vector calculus.

Managerial Assistant 2007 - 2008
Xuankun Animation Company, Shanghai, China

Undergraduate Research Assistant 2005 - 2007
High Performance Computing Laboratory of Professor Tian Youxian

- Responsible for writing benchmark speed tests for solving systems of linear equations in parallel using C and MPI.

HONORS & AWARDS

- Selected and granted funding to attend a 2-week workshop on homogenization methods for Maxwell's equations at the University of Chicago, Summer 2012
- Awarded a travel grant to give a research talk at the October 2011 American Mathematical Society (AMS) Meeting in Salt Lake City, Utah
- Outstanding Graduate of Chongqing University of Posts and Telecommunications
- Outstanding Student Scholarship Recipient, Chongqing University of Posts and Telecommunications, 2004-2007
- National Computer Rank Examination Certificate (Rank III - Database), 2005

LANGUAGES

Fluent in Mandarin Chinese and English

PUBLICATIONS J. Li & J. Waters, An implicit leap-frog discontinuous Galerkin method for the time-domain Maxwells equations in metamaterials, Computer Methods in Applied Mechanics and Engineering, Volumes 223-224, 1 June 2012, Pages 43-54.

J. Li & J. Waters, Homogenized discontinuous Galerkin method for Maxwell's equations in periodic structured dispersive media, Recent Advances in Scientific Computing and Applications, AMS Contemporary Mathematics, in press

M. Neda, F. Pahlevani, & J. Waters, Sensitivity computations of the Leray-α model, Recent Advances in Scientific Computing and Applications, AMS Contemporary Mathematics, in press